

https://dspace.org/

The measurement of the slurry rheology from the discharge of a rotary grinding mill

Bailie, Darrell Stephen

2016-06-08
http://hdl.handle.net/10539/20442

Downloaded from a DSpace repository. https://dspace.org/

The Measurement of the Slurry Rheology from the discharge of a Rotary grinding mill

Darrell Stephen Bailie
BSc (Eng) Chem

A dissertation submitted to the faculty of Engineering
in partial fulfillment of the requirements
for the Degree of Master of Science in Engineering

The University of the Witwatersrand
Department of Chemical Engineering
Johannesburg
South Africa
1995

DECLARATION

I Darrell Stephen Bailie declare that this dissertation is my own unaided work, except where acknowledgement is made in the text to other authors. This work has not been submitted, in whole or in part, for a degree at this or any other University. It is being submitted for the degree of Master of Science in Engineering at the University of the Witwatersrand, Johannesburg, South Africa.

Signed: .....

Darrell Bailie

Date: 21 August 1995

ABSTRACT

In South Africa mineral processing is a very important activity and with declining ore grades and increased need for foreign revenue it is necessary to develop methods which will keep ore processing costs as low as possible. Milling is an example of a capital intensive unit operation which has much scope for more efficient operation.

Better control of the viscosity of the slurry discharged from a rotary grinding mill will result in improved milling efficiency and hence a saving in electricity and steel costs will be experienced. More effective and consistent grinding in the mill will also result in an improved mineral recovery.

Slurry rheology is the variable of interest in monitoring and controlling a wet grinding mill rather than other measures of slurry composition presently used (eg percent solids). Up to this point in time however this variable has not been successfully used due to the fact that a sufficiently reliable and robust device for measuring the viscosities of slurries on an on-line basis has not been available.

This project was undertaken to develop just such a device (which is in the process of being patented by Professor M H Moys). The flow rate of a fluid down a vertical tube is a function if its viscosity as well as other quantifiable variables. This is the basis of the operation of the measurement device. Useful features of this device include the fact that it has no moving parts, is inexpensive and robust and is subject to little wear. The measurement can be

performed directly on the stream in question and it is unlikely to be blocked up by fibres/particles. A self cleaning facility may also be included.

Based on the experimental results the technique shows much promise and it is anticipated that the basic design could easily evolve into a useful, practical device for the measurement of the apparent viscosity of settling slurries as well as other fluids. If a differential pressure cell is also connected to the device it may be used to obtain the density of the fluid being sampled.

A model based on the principles of conservation of momentum was developed and solved numerically using MATLAB (which uses 5th order Runge Kutta) as well as a Turbo Pascal program using 4th order Runge Kutta. The model was also simplified slightly by neglecting acceleration of the fluid (a simplification which was shown experimentally to hold) and solved analytically. The results predicted by the model differ only slightly from the experimentally determined results.

The device has been tested on pilot mills at MINTEK's research facility as well as the Anglo American Research labs, with varying degrees of success.

ACKNOWLEDGEMENTS

I would like to express my gratitude and appreciation to:

- Professor M.H.Moys, my Academic supervisor, for the guidance and encouragement he has given me as well as for his valuable insight.
- MINTEK and the FRD for providing the necessary funding for the project.
- Peter Cockcroft and Theo Prassinos from the workshop, for their help in constructing my equipment.
- The administrational staff in department, especially Sonja Reid and Ann Vos for taking care of the important things like office space, money and other requirements.
- The Students in the Department of Chemical Engineering for providing valuable insight into much more than just my MSc Project.
- My family for providing much encouragement. A special thanks to my parents Joan and Stephen Bailie for putting up with the disarray which arises during the writing up of a dissertation and my brother Grant for his help in manufacturing the electronic equipment required.

- Elizabeth Martin for some size analysis data on mineral slurries used.
- Craig Dyer for his ongoing encouragement and patience and for helping me with the graphing routines in my Turbo Pascal program.
- Tristin Hahn and Sean Fox for taking care of the network.
- Fellow post graduate students including Theo Chronis, Paul Harvey, Paul Holmes, Martin Van Nierop, Greg Visser, Paul Sauthoff, Arno Steinmüller and Elias Xanthoulis for many hours of interesting conversations and fun experiences.
- Willie Nicol and Craig McGregor for their assistance in the use of MATLAB.

Please note that this list is in no particular order. If I have forgotten anyone, please accept my apologies. I would like to thank everyone who contributed in any way to make this dissertation possible.

TABLE OF CONTENTS

DECLARATION i
ABSTRACT ii
ACKNOWLEDGEMENTS iv
TABLE OF CONTENTS vi
LIST OF FIGURES x

Chapter 1 INTRODUCTION 1

1.1 Motivation of the project 2
1.2 Objectives of this dissertation 3
1.3 Structure of this dissertation 4

Chapter 2 LITERATURE SURVEY 6

2.1 Introduction 7
2.2 The importance of viscosity in mineral processing 7
2.3 The rheology of mineral slurries 11
2.4 Techniques for viscosity measurement 15
2.4.1 Roto-viscometers 15
2.4.2 Capillary tube viscometers 18
2.4.3 Other techniques 21
2.5 The theoretical approach 22
2.6 The significance of conductivity measurements 23
2.7 Techniques used to overcome sampling problems 26
2.8 Conclusion 28

Chapter 3 EQUIPMENT USED AND EXPERIMENTAL PROCEDURE 29
3.1 Introduction 30
3.2 Design and construction of equipment 31
3.3 Operation of the equipment 36
3.4 Software development 36
3.5 Preparation for experiments 40
3.5.1 Viscosity measurement with the haake viscometer 40
3.5.2 Preparation of standards for calibration 41
3.5.3 Preparation of slurries 42
3.5.4 Techniques used to prevent settling of slurries 43
3.6 Experimental procedure 46
3.6.1 Measurement of drainage velocity 47
3.6.2 Measurement of pressure 48
3.7 Conclusions 48

Chapter 4 THEORETICAL CONSIDERATIONS 49
4.1 Introduction 50
4.2 The microscopic momentum balance 50
4.2.1 The rigorous form of the momentum balance 50
4.2.2 Evaluation of this approach 51
4.3 The macroscopic momentum balance 52
4.3.1 The generalised form of the macroscopic momentum balance 52
4.3.2 Using the newtonian model 54
4.4 Numerical solution of the differential equation 56
4.5 Simplified analytical solution 57

Chapter 5 EXPERIMENTAL RESULTS AND DISCUSSION ... 60

5.1 Introduction ... 61
5.2 Experiments using glycerol solutions ... 61
5.2.1 The rheology of glycerol solutions ... 62
5.2.2 Drainage data using glycerol solutions ... 63
5.3 Experiments using carboxy-methyl-cellulose solutions ... 65
5.3.1 The rheology of carboxy-methyl-cellulose solutions ... 65
5.3.2 Drainage data from cmc solutions ... 66
5.4 Experiments using slurries ... 67
5.4.1 The rheology of mineral slurries ... 68
5.4.2. Drainage data for mine dump sand ... 70
5.4.3 Density measurement using the new "viscometer" ... 74
5.4.4 Drainage data from western deeps mine slurry ... 75
5.5 Conclusions ... 75

Chapter 6 PILOT MILL WORK ... 76

6.1 Introduction ... 77
6.2 Work conducted at mintek ... 77
7.2.1 Description of tests conducted on pilot mill ... 77
7.2.2 Discussion of results ... 78
7.3 Work conducted at the anglo pilot mill ... 80
7.4 Conclusions ... 80

Chapter 7 CONCLUSIONS ... 81

7.1 Benefits of this research ... 82
7.2 Interesting points to note ... 82
7.3 Concluding comments ... 83

REFERENCES ... 84

APPENDICES 88

Appendix A Listing of main elements of computer program 89
Appendix B Table of viscosities of glycerol solutions 103
Appendix C Size distribution data for mine dump sand used in most experiments 104
Appendix D Selected rheograms 105
Appendix E Unprocessed data 115
Appendix F MCAD Program for simplified analytical solution 116
Appendix G Overview of previous work 120
Appendix H Matlab and Pascal routines for the mumerical solution of the model 127

List Of Figures

Chapter 2

Figure 2.1 A fluid between two parallel plates, subject to a shear force 12
Figure 2.2 Different models for the rheology of fluids 13
Figure 2.3 (a) A cup and bob viscometer, (b) A cone viscometer 16
Figure 2.4 A schematic representation of gravity flow type capillary viscometer .. 19
Figure 2.5 Apparent viscosity of a mineral slurry as inferred from its flow down a vertical tube using a Newtonian model - Baillie and Stewart (1992) .. 20
Figure 2.6 The Nametre vibrational viscometer (Kawatra 1988) 22
Figure 2.7 An example of a conductivity probe (Montani 1988) 24
Figure 2.8 Response of a probe for 2 rotations of a grinding mill (Moys 1987) ... 25
Figure 2.9 Average probe response at different concentrations (Montani 1988) .. 25
Figure 2.10 Sectional view of system used by clarke (1967) 27
Figure 2.11 Sampling system used by Valentyk (1970) 27

Chapter 3

Figure 3.1 Diagram of early viscometer design 31
Figure 3.2 New 'viscometer' developed by Prof M.H.Moys 32
Figure 3.3 Conductivity probes 33
Figure 3.4 Circuit diagram of one channel of the conductivity circuit 34
Figure 3.5 A simplified schematic of the wiring diagram for the system 35
Figure 3.6 An algorithm of the computer program 37
Figure 3.7 Step changes in voltage with time obtained by adding the 5 voltage signals to get the single voltage shown above 38
Figure 3.8 The MV II sensor system 40
Figure 3.9 The Haake viscometer 41
Figure 3.10 Diagram of a draft tube mixing tank 43
Figure 3.11 The ideal profile of the base of a draft tube mixer 45
Figure 3.12 The fillet and cone approximation of the ideal tank bottom 45
Figure 3.13 One way of mounting the Haake viscometer 46
Figure 3.14 Final mounting arrangement of the Haake viscometer 47

Chapter 4

Figure 4.1 Details of the nomenclature used 53
Figure 4.2 Numerical solution of the differential equation describing the system .. 57

Chapter 5

Figure 5.1 Viscosity of glycerol solutions (from the CRC Handbook) 61
Figure 5.2 Rheograms of glycerol solutions 62
Figure 5.3 Drainage lines for glycerol solutions in a 12 mm tube 63
Figure 5.4 A plot of velocity^{-1} as a function of viscosity using glycerol solutions .. 64
Figure 5.5 Typical rheograms for CMC solutions 65
Figure 5.6 Typical drainage lines for CMC solutions 66
Figure 5.7 Rheograms from slurry made from mine dump sand 68
Figure 5.8 The relationship between %solids and viscosity for mine dump sand .. 69
Figure 5.9 Rheograms for slurry obtained from the Western Deeps gold mine 70
Figure 5.10 Drainage velocity as a function of percent solids for mine dump sand . 71
Figure 5.11 Drainage velocity as a function of percent solids for a mind dump slurry 72
Figure 5.12 Drainage velocity as a function of percent solids for Western Deeps slurry 73
Figure 5.13 Density as measured using the new 'viscometer' verses % solids by mass 74
Figure 5.14 Drainage data from a Western Deeps slurry sample 75

Chapter 6

Figure 6.1 The arrangement of the viscosity sampling system used at MINTEK .. 78
Figure 6.2 Changes in apparent viscosity of the mill discharge and feed water flow with the progress of time 79
Figure 6.3 Response of the density of the mill discharge to changes in feed water flow rate 79

CHAPTER 1

INTRODUCTION

1.1 Motivation of the project

Existing techniques used for the measurement of the viscosities of fluids are not well suited for use with settling slurries. The discharge stream from a rotary grinding mill is a good example of such a fluid.

It is only in the recent past that the performance of comminution operations has been the subject of investigation and hence this field has not been fully explored in all its complexities. Research has shown that improved control of slurry viscosities in milling circuits would result in substantial savings. At present however a reliable device which could be used to measure slurry viscosity in the harsh environment of a milling circuit is not available.

Much benefit will be gained if a device could be developed to reliably measure the viscosities of slurries in an industrial environment. Professor M.H.Moys recently proposed a technique which could potentially be used to measure the viscosity of such fluids. The concepts developed by Professor Moys deserved further investigation. A slurry viscometer could be developed, using these fundamental and creative ideas. As with most good inventions the proposed device would be simple having few moving parts, it would be inexpensive to manufacture and reliable.

The Author of this report decided that the he would like to investigate the concept in more depth, and develop the ideas further, in order to determine the operability of the concept.

1.2 Objectives of this dissertation

The objectives of this dissertation are as follows:

i) Gain a broad understanding of the importance of the measurement of slurry viscosity in an industrial environment as well as the underlying techniques involved in the characterization of the rheological properties of slurries.

ii) Develop and produce a simple, robust device which, while operating in an industrial environment will provide an on-line measurement of slurry viscosity.

iii) Produce analytical models to describe the operation of the measuring instrument described in (ii) above.

iv) Test the device on an operational grinding mill, and perform some experimental work, including step changes in feed water flow rate while the device is on-line.

1.3 Structure of the dissertation

This report is structured is the following way:

Chapter 1 forms a general introduction by providing the motivation for the project as well as the objectives and aims of the author of the thesis. Included in chapter 1 is the layout of the thesis.

In **Chapter 2** the reader is provided with some background information on the different ways in which slurry rheology can be characterised. A literature survey is also included, in which the work of some previous research work in this field is highlighted.

Chapter 3 include a description of the equipment used as well as the experimental procedure. We examine the way in which the equipment works and look at related topics such as the development of software and the preparations required for experimental work.

In **Chapter 4** some theoretical concepts are examined, including a model of the dynamic response of the system derived from the fundamental momentum balance. The model is solved numerically using MATLAB (which uses 5th order Runge Kutta as well as using a Turbo Pascal program written (using 4th order Runge Kutta). The slightly simplified model of the system (in which acceleration is neglected) is solved analytically.

In **Chapter 5** we look at the results obtained and discuss some interesting effects which are observed when using slurries.

Chapter 6 deals with the pilot mill work conducted at MINTEK's pilot mill in Randburg as well at the Anglo research labs.

Then finally we get to **Chapter 7** where the concluding comments and discussion are given.

CHAPTER 2

LITERATURE SURVEY

Despite the profusion of work done in recent years on topics related to the characterization of the rheological properties of slurries, a reliable device for the measurement of even an apparent viscosity of a slurry in the industrial environment has not been developed.

The literature presented here is intended to give the reader a broad overview of some underlying issues related to the measurement of the rheological properties of slurries as well as the reasoning as to why such a measurement should and would be of interest in an industrial environment. The difficulties experienced by previous researches are also examined. Short summaries of some selected publications are included in appendix G for the reader's convenience.

2.1 Introduction

In recent years there has been much research done in the field of slurry rheology with the result that a profusion of work has been published on this subject. In this chapter it has been my objective to summarize the most important findings of this research and to reveal some of the problems researches have been faced with in measuring the rheological properties of slurries. A selection of published articles are briefly summarized in appendix G in order to give the reader a feeling for the type of literature available.

The results of my literature survey confirm the belief that information on slurry rheology would be useful in improving the efficiency of milling circuits. I also show that the main reason for the fact that this variable is not utilized for the control of milling circuits is due to the lack of a reliable, robust instrument which could be used to measure the rheological properties of slurries in the industrial environment.

2.2 The importance of viscosity in mineral processing

Pulp viscosity is an important parameter in all minerals processing operations and effects the efficiency of operation of mills, cyclones, flotation circuits, classification operations, heavy medium separation, dewatering systems, slurry pipeline transportation, tailing clarification (Laapas 1982) and the CIP process (Thomas et al 1989). In this section, however the focus is on the importance of viscosity in the operation of milling circuits. Until recently knowledge of the importance of slurry rheology in mill performance has been limited (Kimpel 1979).

The viscosity of slurry in milling circuits has been largely neglected due to a number of factors, including the following :

(1) The role of slurry viscosity in comminution operations has only come under close scrutiny during the last 15 years or so.

(2) The magnitude of the potential savings has not been fully recognized.

(3) Comminution is not considered as a separate field of research and is interdisciplinary by nature (Herbst 1990).

(4) Implementation of new untested technology involves some risk which mines are often not willing to assume.

(5) The significance of slurry viscosity has not been fully appreciated in industry (Moys 1989).

(6) The difficulty of making on-line measurements of the viscosity of dense mineral slurries (Moys 1989, Kawatra and Eisele 1988).

Despite the fact that this matter has been the subject of many investigations in recent years a robust, reliable and effective device to measure slurry viscosity has not been developed. The lack of suitable, reliable equipment to measure slurry viscosity is a problem.

Potential benefits of better control of viscosity in milling operations.

Milling is one of the most energy-intensive operations in the minerals processing industry and consumes as much as 25% of the power used in minerals processing (Kawatra and Eisele 1988). In some industries, for example the processing of metalliferous ores, energy used in comminution operations constitutes 50% or more of the total energy requirements for raw minerals processing (Herbst 1990). Milling is an inherently inefficient process with typical efficiencies of less then 5% (Herbst 1990) and the efficiency of

a wet grinding mill can be improved by better control of slurry rheology (Kawatra and Eisele 1988)

Even a small increase in efficiency will result in a substantial saving (Kawatra 1988, Hemmings and Boyes 1977). Not only would there be a savings in electricity but also a saving on steel costs. An improvement in mineral recovery would also follow from better control of rheology in milling circuits (Hemmings and Boyes 1977, Moys 1989).

The potential economic benefits of better control of milling circuits have been estimated by Herbst (1990) who showed that energy savings could amount to between 10 and 20 percent from better control of grinding circuits alone. Saving in steel costs as a result of reduced wear of the media and mill lining would result in savings of at least the same order of magnitude.

According to Kawatra and Eisele (1988) the grinding efficiency of the entire grinding circuit in a tumbling media mill may be improved by better control of mill slurry rheology, since the rheology not only effects the rate of fines production but also the functioning of the hydrocyclones. Suitable on-stream sensors are 'essential for more effective control of mineral processing operations, particularly grinding circuits' (Hemmings and Boyes 1977)

Atkins and Hinde (1975) have shown that under manual control a typical grinding circuit is subject to unnecessarily large fluctuations resulting in inefficient utilization of grinding capacity. Increasing automation may thus result in improved recoveries and more efficient operation of the plant. By implementing control over mill water addition on the basis of mill discharge viscosity measurements, both a production benefit and reduced grinding media

wear are indicated (Boyes 1978).

The main difficulties associated with manual control include large lag times, difficulties in coping with disturbances and human limitations eg fatigue; on the other hand automation has advantages of sensitivity to process disturbances, reduced response time, consistent response to disturbances and reliability without human limitations (Hemmings and Boyes 1977).

The development of a suitable device which will measure the slurry viscosity will increase the scope for automation in the mineral processing industry resulting in the above-mentioned benefits. The accuracy of the measuring device is however not critical because of the very strong relationship between percent solids and slurry viscosity in the region of efficient mill behaviour - a 1% change in percent solids results in on average a 35% change in viscosity in the range of percent solids typical of the mill discharge of an average gold mine (Moys 1989).

The role of slurry viscosity in milling

As we can see from the foregoing paragraphs, the viscosity of the slurry directly effects mill behaviour. The slurry should be viscous enough so as to be homogeneous thus thinly coating the grinding media and yet it should not be so viscous so as to adhere to the mill wall throughout the rotation of the mill. It should also be thin enough to flow 'fairly rapidly' through the mill under a relatively low hydraulic gradient (Hemmings and Boyes 1977).

If the viscosity is too high the efficiency of the mill is reduced due to the fact that the thick pulp restricts the movement of the grinding media and cushions their impact, thereby reducing grinding activity (Hemmings and Boyes 1977,

Taggart 1954, Cross 1967). The grinding behaviour deviates from first order when the slurry inside the mill develops a significant yield value and this leads to lower breakage rates (Klimpel 1979, Kawatra and Eisele 1987). The effective diameter of the mill may also be reduced and premature centrifuging can occur (Moys 1989, Tangsathitkulchai 1989). At higher viscosities the risk of choking the mill also increases.

If the viscosity is too low there will be incomplete coverage of the media by the pulp resulting in increased wear rates of the media and liners. The grinding media make direct contact with each other and with the mill lining as a result of the much thinner layer of slurry covering the media and the mill lining. Reduced mill holdup with thin pulps also unnecessarily reduces the capacity of the mill (Hemmings and Boyes 1977). From an economic viewpoint, high wear rates impose a minimum operating viscosity in a mill. Power is also 'wasted in tumbling the excess water' (Moys 1988).

It is interesting to note that the residence time is also an important factor affected by pulp consistency. At high pulp viscosities, the larger residence times and longer exposure to grinding forces may compensate for reduced grinding efficiencies. Conversely, at lower pulp viscosities where grinding may be more effective, lower residence times may reduce overall performance. An optimum slurry viscosity exists and it has been suggested that the optimum lies around 150 cP (Hemmings and Boyes 1977 and Boyes 1978).

2.3 The rheology of mineral slurries

In order to familiarise the reader with the underlying principles of fluid rheology, some background information is given and underlying ideas briefly examined. We will first look at a definition of rheology and then examine

some typical fluids.

The study of rheology of fluids covers the techniques used to describe the flow characteristics of fluids, in particular their shearing characteristics. To illustrate the concept we will refer to a fluid between two parallel plates, one plate being stationary, while the other is free to move (see figure 2.1).

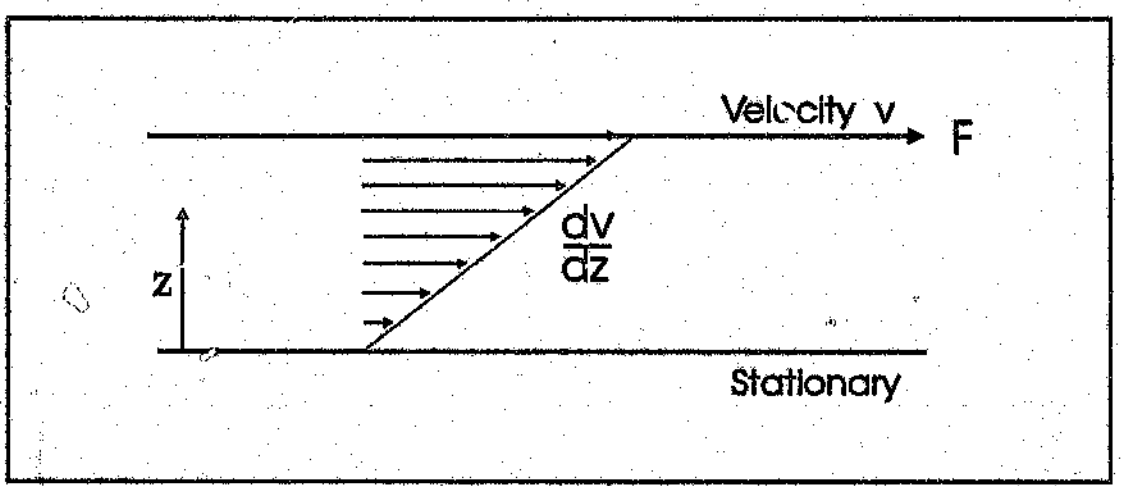


Figure 2.1 - A fluid between two parallel plates, subject to a shear force.

A velocity gradient is set up in the fluid. As the velocity gradient or shear rate is increased, so the shearing force required also increases. One of the goals of rheological studies is to describe how the shear stress applied is related to the shear rate (velocity gradient). Fluids are classed into different categories, depending on which model most closely describes their behaviour under shearing conditions. Many different models exists, the most simple being the Newtonian model, where there is a linear relationship between shear stress (τ) and shear rate, the proportionality constant being the Newtonian viscosity. A few different models are illustrated in figure 2.2.

Mineral slurries are difficult to characterize partially as a result of their non-Newtonian behaviour, especially at high percent solids. Another difficulty

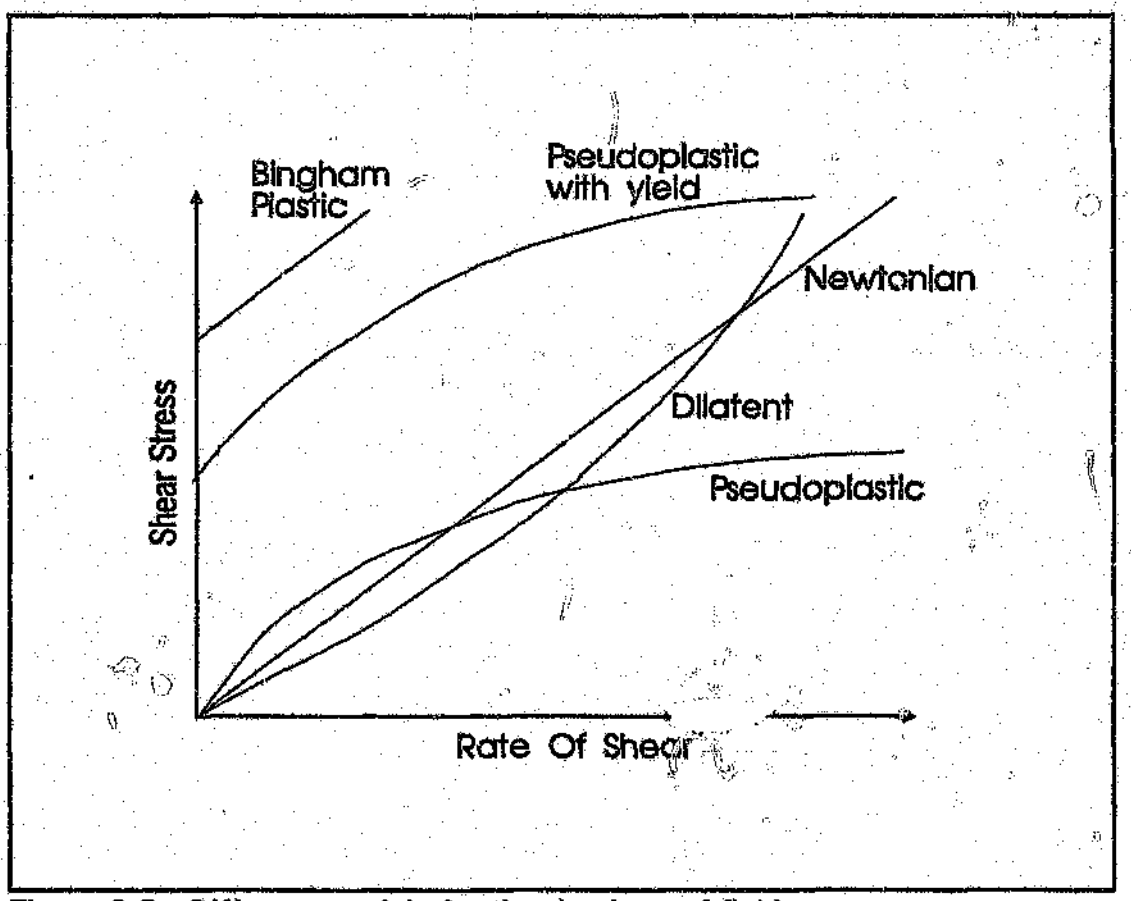


Figure 2.2 - Different models for the rheology of fluids.

relates to the settling nature of slurries (Hansford et al 1976). Shear stress is generally a non-linear function of shear rate especially for highly concentrated slurries. Thus if the shear stress is measured at a fixed shear rate this provides only one point on the shear stress/shear rate curve. This single point can provide the apparent viscosity which is the ratio of the shear stress to shear rate.

There are a large number of variables which influence the way slurries behave under shearing forces and this further complicates attempts to model the behaviour of mineral slurries. Factors effecting slurry rheology include particle

size distribution, average particle size, shape of particles, particle concentration, surface properties of the solid, pH as well as temperature. Volume fraction on its own is not adequate to characterize the rheological properties of a slurry (Jeffrey and Acrivos 1976). A linear relationship exists between the apparent viscosity of a slurry and temperature (mainly as a result of its effect on the viscosity of the carrier fluid). An exponential relationship exists between slurry viscosity and concentration. There is a direct relationship between the size of particles and the viscosity in mineral slurries (Hansford et al 1976, Clarke 1967)

Dilute slurries behave approximately as Newtonian fluids but their behaviour deviates substantially from Newtonian with increasing percent solids. Typical mineral slurries display dilatant behaviour up to 50% solids by volume (Clarke 1967). Increasing the concentration changes the behaviour progressively to pseudo plastic with higher concentrations displaying a yield value (Kawatra and Eisele 1987, Austin et al 1984)

Abbas and Crowe (1987) reported that the slurry they used fitted neither the Bingham plastic nor power law models and suggested use should be made of a turbulent mixing model analogous to Prandtl's mixing-length concept. Cheng (1984) even suggested that there is no unique viscosity curve for a fixed solids concentration, rather a distribution function of curves. Various models have been used to describe the rheology of suspensions including the Ostwald-de Waele equation, the Rabinowitch equation, the Ellis equation, the Prandtl-Eyring equation, the Reiner-Philippoff equation, the Williamson equation, the Cross equation, the Oldroyd equation, the Van Wazer equation, the power law and many more with varied success (Jinescu 1974).

2.4 Techniques for viscosity measurement

Various techniques exist for the measurement of the viscosity index of fluids but few can successfully be used to characterize the rheology of slurries. Many difficulties arise when attempting to characterize the behaviour of slurries. Illustrations of some sampling systems tried by various authors can be found in section 2.7 as well as appendix G.

Problems encountered include settling of the slurry during measurement, wall slippage due to the presence of pure liquids at the solid-liquid interface, turbulence effects and difficulties in obtaining a representative sample.

2.4.1 Roto-viscometers

There are various types of roto-viscometers available, but the most common commercially available laboratory viscometer is the bob-and-cup viscometer.

The underlying principle of operation of the rotational type viscometer is as follows (see figure 2.3) : a rotating body (commonly cylindrical in shape, but use is also made of conical shapes) is immersed in the fluid and is subject to a viscous drag or retarding force. This drag force is the result of the shearing forces set up in the velocity gradient formed and the amount of drag is a function of the geometry of the system, the nature of the fluid and the shear rate. A common form of roto-viscometer is the bob-and-cup viscometer which employs two concentric cylinders. There are two possible arrangements, namely the Searle system and the Couette system (Skubnik 1972). The Searle system has a stationary outer cylinder and an inner cylinder which is free to rotate while the Couette system the outer cylinder rotates about the inner stationary cylinder. A velocity gradient is established in the liquid between the cylinders when the inner/outer cylinder is rotated. Typical examples of this

type of viscometer include the Haake and the Brookfield viscometers.

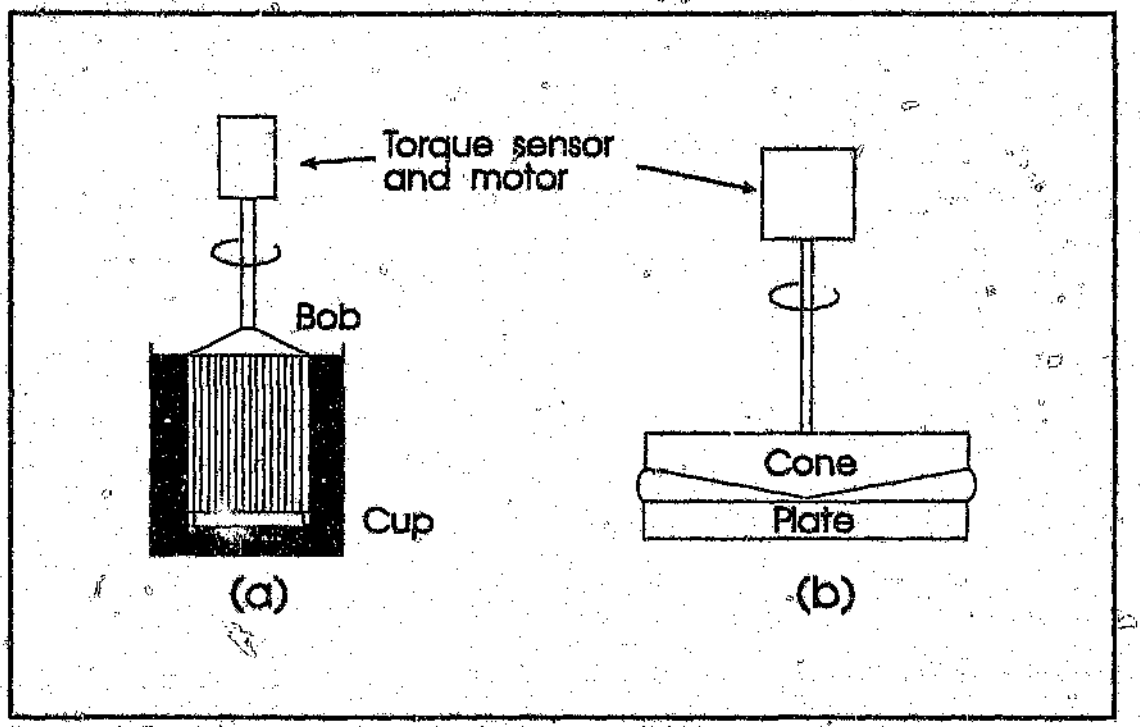


Figure 2.3 - (a) A cup and bob viscometer, (b) A cone viscometer.

The Brookfield viscometer operates at a fixed shear rate and provides an apparent viscosity at that shear rate. For non-Newtonian fluids the relevance of this data is not well established, although such data is of some value.

The Haake viscometer is capable of operating at a variable shear rate and can be used to plot the entire shear stress/shear rate curve thereby fully characterizing the fluid.

The use of the roto-viscometer for the measurement of slurry rheology has been examined by many different authors including Hansford et al (1976), Hemmings and Boyes (1977), Kimpel (1979), Moys (1987), Blazezyk and Petela (1986), Reeves (1985) as well as Tangsathitkulchai and Austin (1988).

Disadvantages of a Roto-viscometer :

(1) Roto type viscometers are subject to Vand wall effects (Whiten et al 1992) - a layer of pure liquid forms between the slurry and the cylinder, causing slip and unreliable viscosity measurements. This effect may be reduced by etching grooves in the bobbin perpendicular to the direction of rotation.

(2) The formation of Taylor vortices at higher rotational speeds may occur (Whiten et al 1992)

(3) Turbulence may occur at higher rotational speeds and its effect on the viscosity is difficult to quantify.

(4) Roto-viscometers are usually not robust enough to use in an industrial environment.

(5) In flow-through models, the passage of fluid through the shearing gap during sampling will have some effect on the calibration (Dealy 1984). A degree of turbulence may be introduced which may introduce some form of error (Downward et al 1987).

(6) Unless sufficient turbulence is maintained, coarse solids will settle and the viscosity reading will not be representative. However the presence of turbulence in the measuring system introduces scatter in the data due to torque fluctuations on the rotating mechanism (Hemmings and Boyes 1977).

(7) The gap between the two surfaces is usually quite small, and when dealing with suspensions it is important that the largest particle diameter is small enough not to lodge between the two surfaces.

(8) There are problems associated with sampling difficulties and problems in obtaining representative samples for measurement

Advantages of Roto-viscometers :

(1) The Haake viscometer can be used to generate an entire shear stress/shear rate curve.

(2) The Contraves and Haake viscometers are available in models which have a magnetic torque coupling to avoid the use of rotary seals and are available in both flow through and immersion models.

2.4.2 Capillary tube viscometers

The capillary tube viscometer uses a relationship between the flow rate of a liquid down a capillary tube and the pressure drop to give an apparent viscosity (Downard et al 1987) The reader is referred to figure 2.4 for a schematic representation of a gravity flow type capillary viscometer. Capillary tube viscometers have been examined by Laapas (1987) and Whiten et al (1992). Cohen and Metzner (1986) examine apparent slip flow of polymer solutions in a capillary viscometer.

De Vancey and Shelton (1986) used a device they called a consistometer. This piece of equipment was capable of determining the viscosity under only one flow condition, namely free fall through a small bore tube (Marsden 1962). This is not a true capillary tube but the principle of operation is similar. As can be seen from figure 2.5 there is a relationship between the flow rate of slurry down a narrow bore vertical tube (12 mm) and its viscosity.

Disadvantages of the capillary tube viscometer :

(1) The capillary tube is subject to Vand wall effects (Whiten et al 1982, Downward et al 1987) resulting in a layer of very dilute slurry forming at the wall of the tube. Plug flow can thus occur in the tube hence giving unreliable results (Downard et al 1987 and Whiten et al 1992). This phenomena is well documented (Jinescu 1974). This problem may

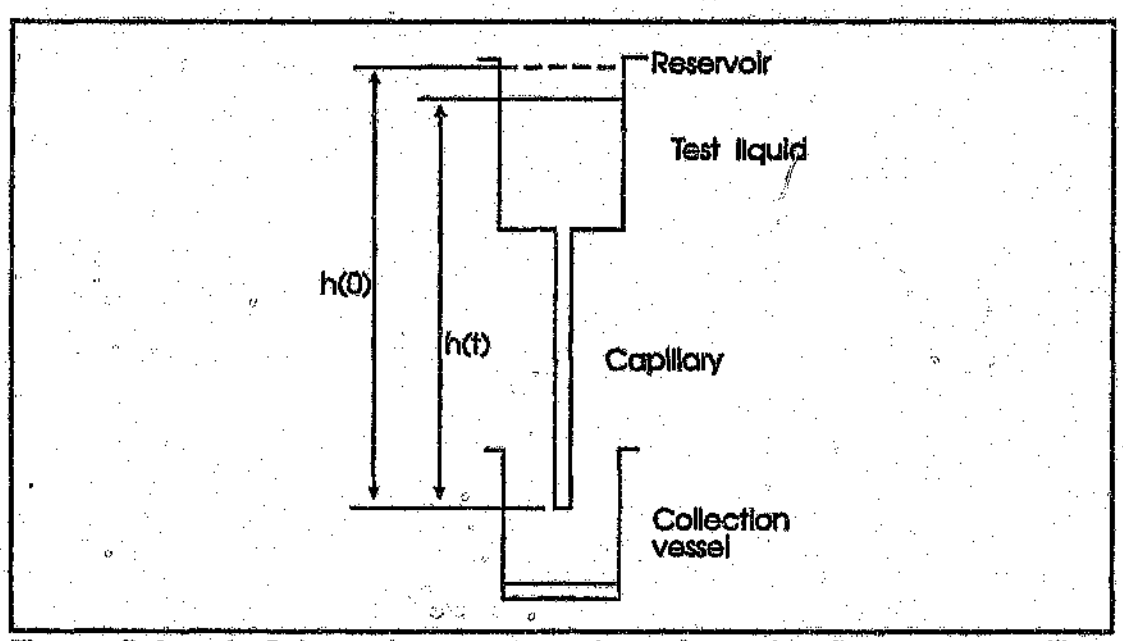


Figure 2.4 - A Schematic representation of gravity flow type capillary viscometer

be partially solved by using roughened tubing (Bailie and Stewart 1992, Skubnik 1972).

(2) The effects of turbulence are difficult to quantify although for more concentrated slurries there seems to be less of a marked transition from laminar to turbulent flow and this transition appears to occur more slowly (Whiten et al 1992). Turbulence may therefore not be a problem of significance and the effects of high Reynolds numbers in capillary tubes requires further investigation.

(3) These units are usually not calibrated directly and are most often calibrated using fluids of known viscosity.

(4) They give an apparent viscosity at a particular shear rate determined by the physical dimensions of the tube. This is known as the Fahraeus-Lindqvist effect (Downward et al 1987)

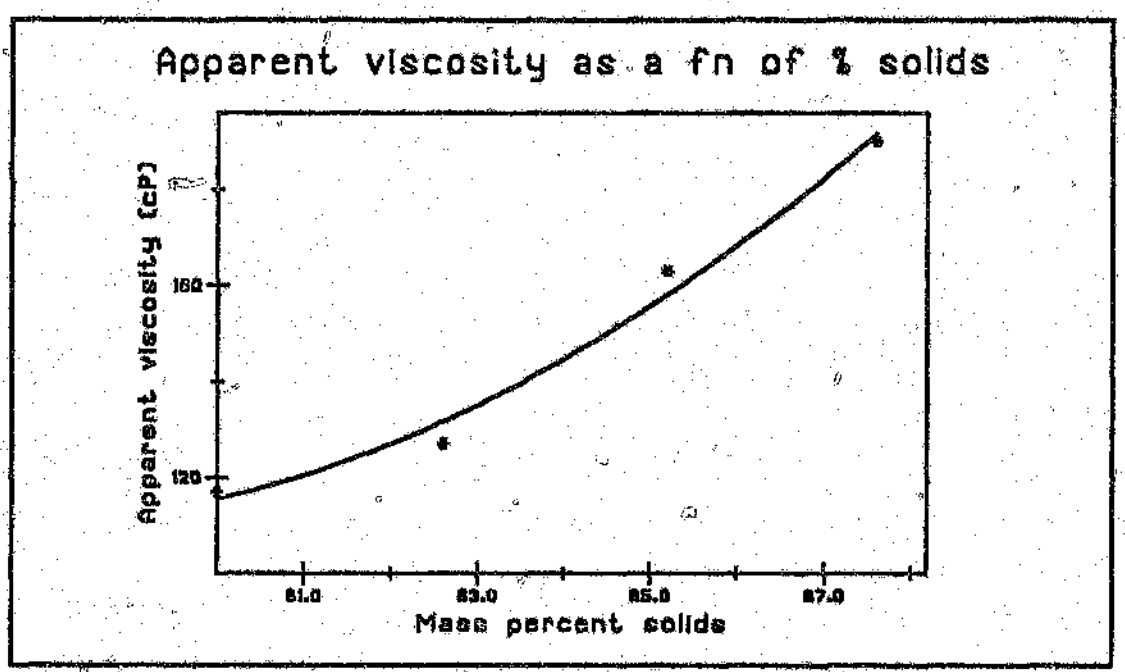


Figure 2.5 - Apparent Viscosity of a mineral slurry as inferred from its flow down a vertical tube using a Newtonian Model - Bailie and Stewart (1992)

(5) The effect of swirl on viscosity is not known (Hansford et al 1976), although this effect may be reduced by careful design of the tube entrance.

(6) The tube may become blocked, but this problem may be overcome by using a larger diameter tube or a more elaborate sampling system; however laminar flow should be maintained (by for example imposing a relatively low pressure drop across the tube).

(7) In the unsteady state system start-up flow may be a factor (the initially stationary fluid has to accelerate to a terminal velocity), although this is usually negligible (Dutta 1986). This is confirmed by the author's work which indicates that the fluid quickly accelerates to a terminal velocity.

Advantages of the Capillary tube viscometer

(1) It is simple to construct and maintain and can be made from readily available materials.

(2) If designed correctly it should be robust enough for industrial use.

(3) It has no moving parts.

(4) They are particularly suitable for the measurement of low viscosities such as those of light hydrocarbons and aqueous solutions as well as highly viscous materials such as asphalts and molten plastics (Dealy 1984).

2.4.3 Other techniques

Various other techniques have been used with mixed results.

Vibrational viscometers work on the principle that a fluid has a tendency to dampen the vibration of a probe which is a function of the product of the viscosity and density of the fluid (Dealey 1984). Installation is relatively simple as there are no pumps or motors involved, and the response time is low, in the order of a few seconds. Kawatra et al (1988) tried using a Nametre vibrating sphere viscometer (see figure 2.5), but they experienced numerous problems with drift and dependencies of the measured viscosity on the flow rate. After several modifications most of the problems were solved to a certain extent and some relative success was obtained.

Some vibrational viscometers use ultrasonic pulses (notably the Bendix and Unipan models) and may be more suitable than the Nametre viscometer used by Kawatra.

Falling-cylinder viscometers are covered by a Czech patent and the only

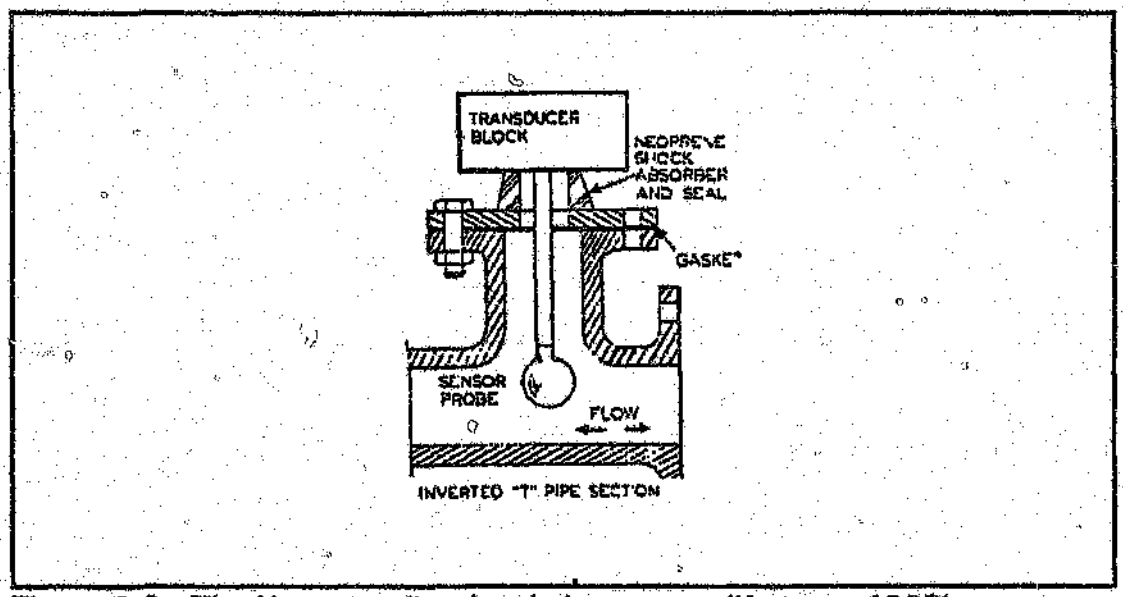


Figure 2.6 - The Nametre vibrational viscometer. (Kawatra 1988)

commercial model available is made by Norcross. They are not suitable for use with slurries.

Another novel device used for the measurement of pulp viscosity is the "drag blade", a metal plate mounted on the side of a pipe carrying the suspension, in such a way that the total force exerted on it by the flowing fluid can be measured.

2.5 The theoretical approach

The purely theoretical approach has been adopted by some authors to quantify the behaviour of slurries. However many assumptions are required, the primary one being that of spherical particles. Theoretical models based on the interaction of spheres have failed to describe the rheology of real suspensions over the full concentration range (Mandersloot 1979).

This approach does have some merit for dilute suspensions of spherical

particles and provides quite satisfactory predictions under certain circumstances (Dabak and Yucel 1986).

Einstein did work on the rheology of suspensions and his work is quite frequently referred to, and forms the basis of early research work done in this field. Einstein considered a suspension of rigid spherical particles with the hydrodynamics being governed by Stokes law.

The theoretical approach is complicated by the fact that there are so many factors affecting the rheology of suspensions. Fundamental forces acting in suspensions include thermal forces, electrical forces arising from charges on particles and many others. This has lead some researches to investigate double layer charge theory and charge formation in suspensions, leading to complicated theoretical relationships which are often of little practical value, but are of interest never the less (Jeffrey and Acrivos 1976).

2.6 The significance of conductivity measurements

From the results of investigations carried out (Moys 1988, Vermeulen et al 1984, Montini and Moys 1988) in the use of a conductivity probe bolted to the shell of the grinding mill it appears that potential exists that much useful information can be gleaned from the use of a conductivity probe. Possible useful information includes locating the toe and shoulder of the load, indicating whether the load is centrifuging or not, and providing a fairly accurate index of the viscosity of the load. Figure 2.7 shows one possible way of mounting the conductivity probe (Montini 1988), figure 2.8 shows the response of a conductivity probe with two rotations of the mill (Moys 1987) and figure 2.9 shows how the response of the probe changed with different concentrations of slurry (Montani 1988).

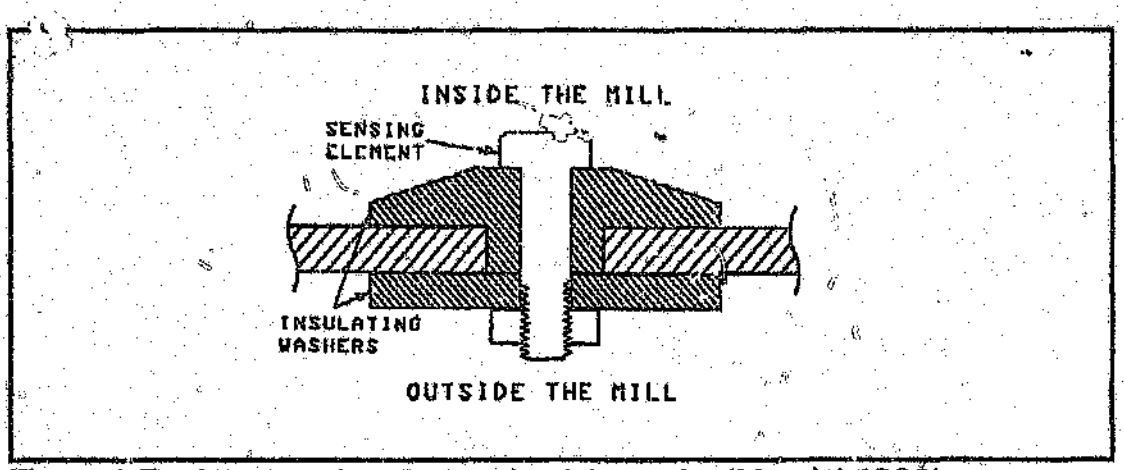


Figure 2.7 - An example of a conductivity probe (Montini 1988)

As the conductivity probe enters the load, the conductivity increases giving an indication of the location and size of the load in the mill (see figure 2.8). However the most interesting area in the conductivity signal centres around the type of drainage that takes place as the probe leaves the load (see figure 2.9). The rate of drainage is a measure of the slurry viscosity. If the slurry has a high viscosity the drainage would be incomplete and the probe would still be coated with slurry when entering the load again. Therefore by analyzing the nature of the drainage one can obtain an indication of the slurry viscosity.

Advantages of the conductivity probe include the fact that it does not suffer from the large lag times associated with techniques which are based on measurements from the mill discharge making it easier to tune the controller. The conductivity probe is also of low cost and installation procedures are simple.

Disadvantages include the fact that the probe must withstand the harsh conditions in the mill and may need regular replacement. There are certainly potential benefits to be gained from the use of conductivity probes in a mill

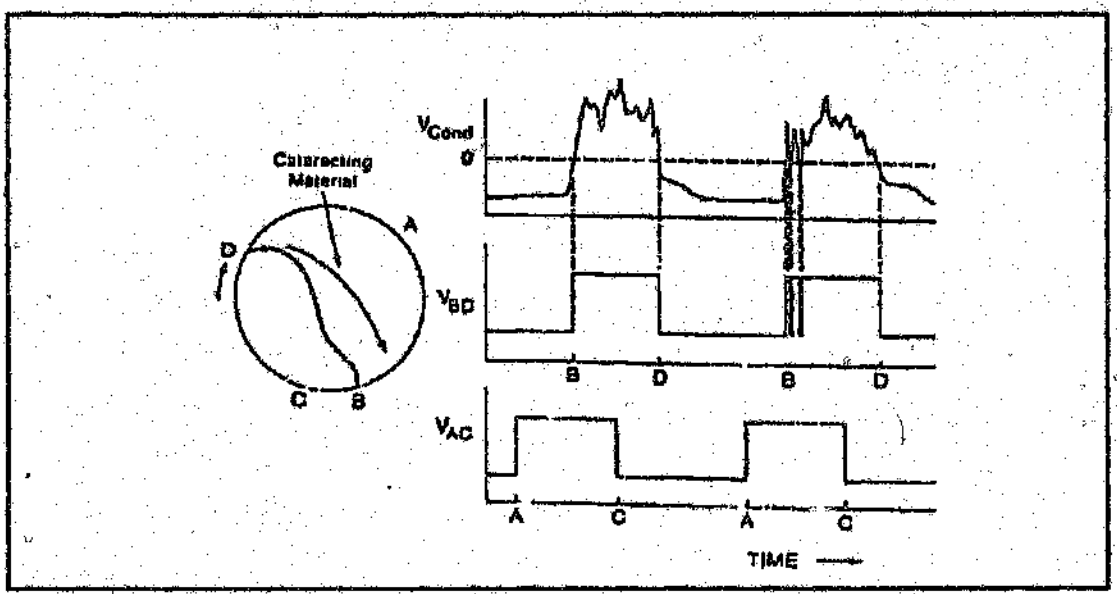


Figure 2.8 - Response of a probe for 2 rotations of a grinding mill (Moys 1987)

shell alone or in conjunction with other measurements and their use deserves further investigation. One problem is the interpretation on the signals from

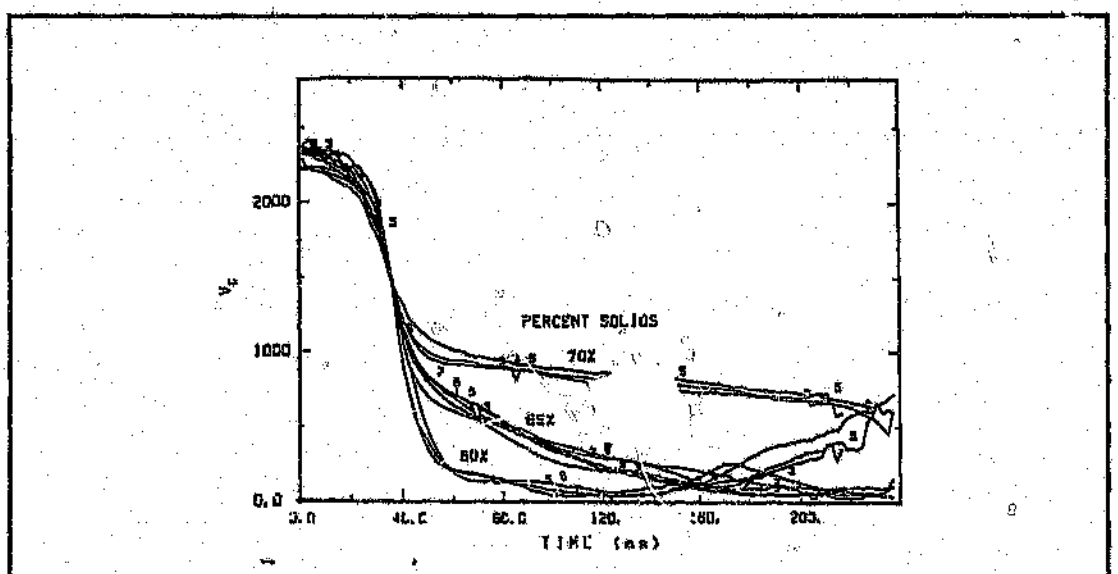


Figure 2.9 - Average probe response at different concentrations (Montani 1988)

such probes to gain as much useful information as possible. Suitable electronic processing would 'clean up' the signals and make the data so obtained more useful (Vermeulen et al 1984).

2.7 Techniques used to overcome sampling problems.

Sampling problems are difficult to overcome. The discharge from a wet mill includes fibres, wire and large particles, which easily choke up the viscosity measuring device. On line measurements are also made more difficult by the settling nature of slurry. Even in batch systems settling is a problem. Various attempts have been made to overcome these problems and some interesting devices have been designed. In this section we will examine some of these ideas.

Batch systems have to be fitted with some sort of circulation or agitation system. An example of such a system was that used by Clarke (1967) as illustrated in figure 2.10. Clarke used a draft tube type mixer, with the impeller mounted in the base of the container. This results in a uniform flow of slurry around the bobbin. It is also possible to circulate the slurry in a batch system at a sufficiently high rate to maintain the suspension thus eliminating the need for a stirrer.

Continuous systems have to handle the larger particles, fibres and wires discharged from a mill. These systems usually require some sort of screening first. Valentyk (1970) used a rotating screen for this purpose as illustrated in figure 2.11.

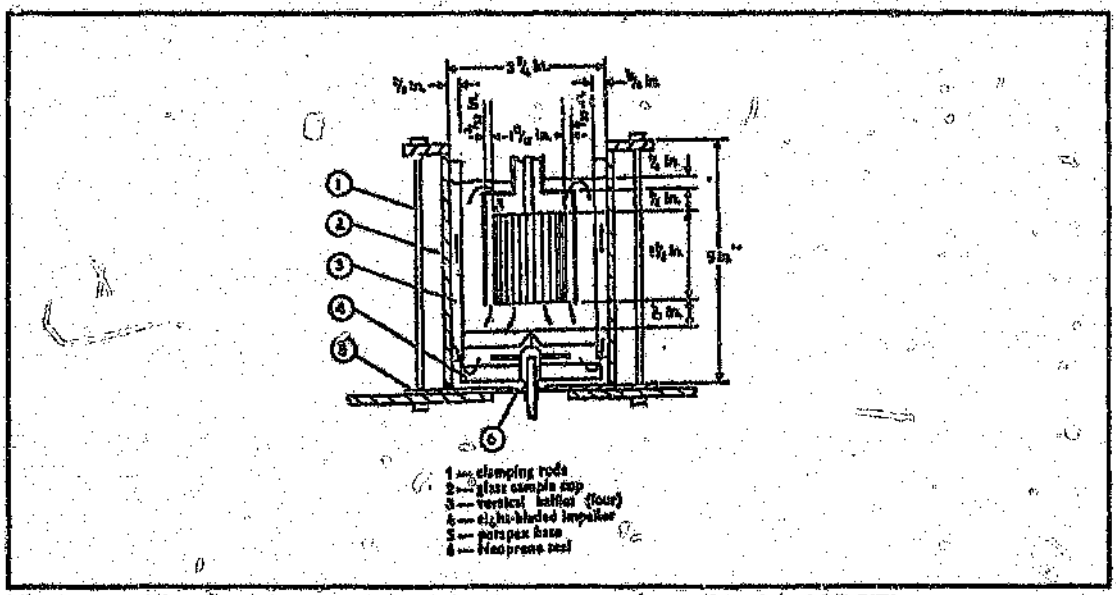


Figure 2.10 - Sectional view of system used by Clarke (1967)

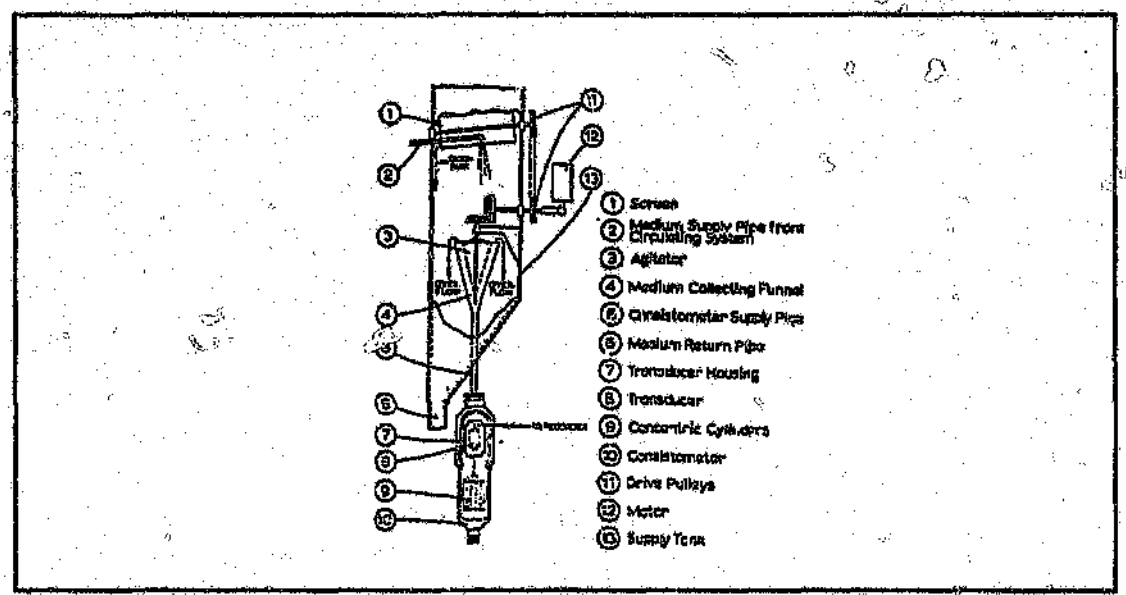


Figure 2.11 - Sampling system used by Valentyk (1970)

2.8 Conclusion

From the literature survey it is clear that slurry rheology is a very important parameter in the efficient operation of many mineral processing operations, milling in particular. We can see that the measurement of the rheological properties of slurries is problematic, due to many factors including the settling nature of slurries as well as the harsh environment in which such devices are required to operate. We see however that there is a large potential savings to be gained from improvements in the efficiency of operation of milling circuits and that an online viscometer capable of operating in the industrial environment would prove to be very useful.

CHAPTER 3

EXPERIMENTAL SECTION

The human spirit of discovery is unmatched by any other creation, and it is this spirit which drives us to discover new territories and expand the envelope of human understanding. With this spirit in mind we enthusiastically tackle the problem of the measurement of slurry rheology. We examine the evolution of ideas into possible solutions, from the initial concept to the final design.

The preparation for experimental work is also examined, including factors such as the use of viscosity standards, preparation of slurries, and actual experimental procedure. Finally some conclusions are made with respect to this work.

3.1 Introduction

Let us start with some kind of objective in mind as we begin to explore the possibilities of discovery. Our objective: the development of a simple, reliable, robust viscometer or consistometer for use in the industrial environment. The device should preferably have no moving parts (or only a few moving parts) and should provide a reliable indication of the consistency or apparent viscosity of a slurry.

In the literature survey we looked at the two most useful approaches to this problem, namely the roto-viscometer and capillary viscometer. We saw that the use of roto-viscometers had been well tried by numerous authors and that blockage of the relatively narrow gap between the stationary and moving surfaces was a big problem, and that the rotary type viscometer was inherently not very robust due to the requirement that the torque on the rotating shaft be accurately measured. For these reasons we did not pursue this concept any further. We did however use a slightly modified Haake bobbin viscometer during the experimental phase to obtain rheograms for the slurries used.

The capillary viscometer has also been tried by some researchers and also had problems with choking as noted from the literature survey. But what if we were to use a conventional tube of slightly larger diameter in a similar way to that in which a capillary viscometer operates? If the tube were large enough it would be unlikely to choke up with slurry. We saw in the literature survey that under conditions of fixed pressure drop the velocity of a fluid flowing in a pipe is a function of the fluid properties, including its viscosity. This principle could be used to obtain a value for the apparent viscosity of a liquid, but how?

Early research focused on the use of a tube open to the atmosphere, through which slurry is allowed to flow on a continuous basis (see figure 3.1). This technique had some drawbacks, however, since it required that a side stream of slurry be pumped to an open trough at the top of the tube. This slurry then flows down the tube under the influence of gravity and is allowed to rejoin the main stream. This is not very convenient.

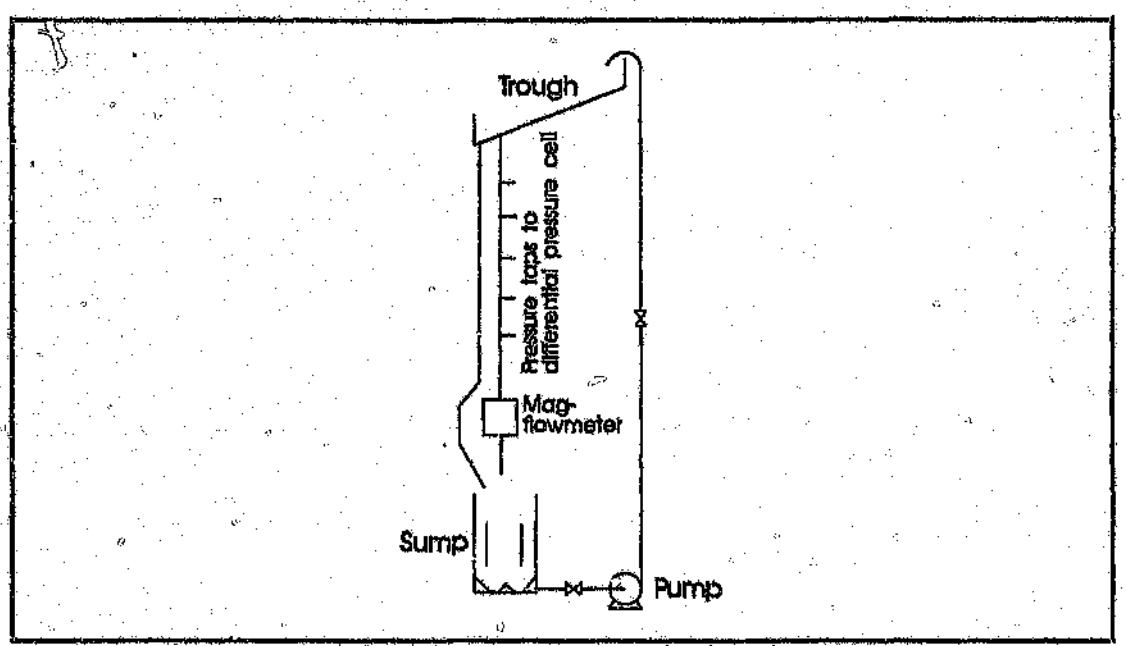


Figure 3.1 - Diagram of early viscometer design

Professor M.H. Moys suggested using an idea he had developed, which uses a similar principle, except it operates in a cyclical, batch mode, as will be explained in the next section. This is the approach that was adopted.

3.2 Design and construction of equipment

A diagram of the equipment used appears in figure 3.2. The equipment used consists of a vertical tube fitted with five pairs of conductivity probes. The bottom end of the tube is immersed in the slurry or fluid of interest, contained in a draught tube mixing tank to prevent the slurry from settling. The upper

end of the tube is connected to a DP cell to measure the pressure, and via solenoid valves to a venturi vacuum pump and to the atmosphere. The conductivity probes and solenoids are linked to a computer, which takes measurements and controls the viscometer.

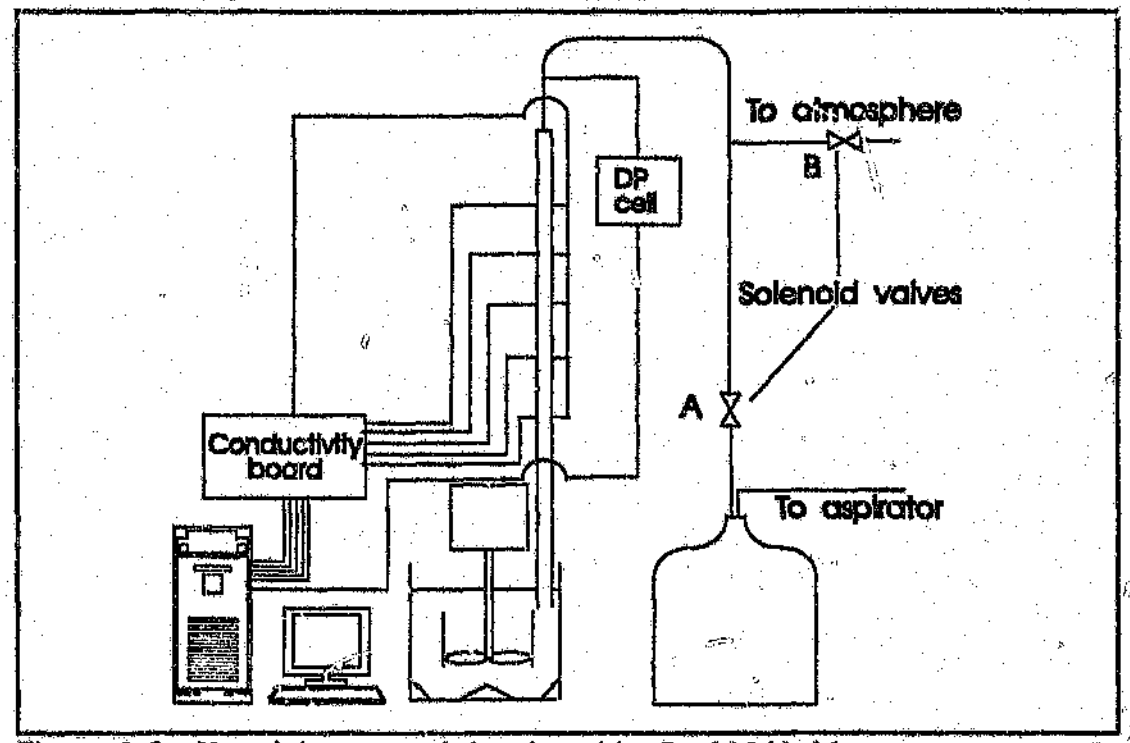


Figure 3.2 - New 'viscometer' developed by Prof M.H. Moys.

The tube itself is a clear PVC tube, about 1.6 meters long. Six different tubes were used, in total. Three smooth tubes of diameters 10mm, 12mm and 16mm, and three roughened tubes of diameters 10mm, 14mm and 18mm. Roughening the tube was accomplished by scoring a groove of about .2 mm in depth relatively evenly in a spiral type fashion inside the tube. The conductivity probes consist of small pieces of 1mm diameter stainless steel wire fitted into holes drilled in the side of the tube and glued in place using PVC cement. (see figure 3.3)

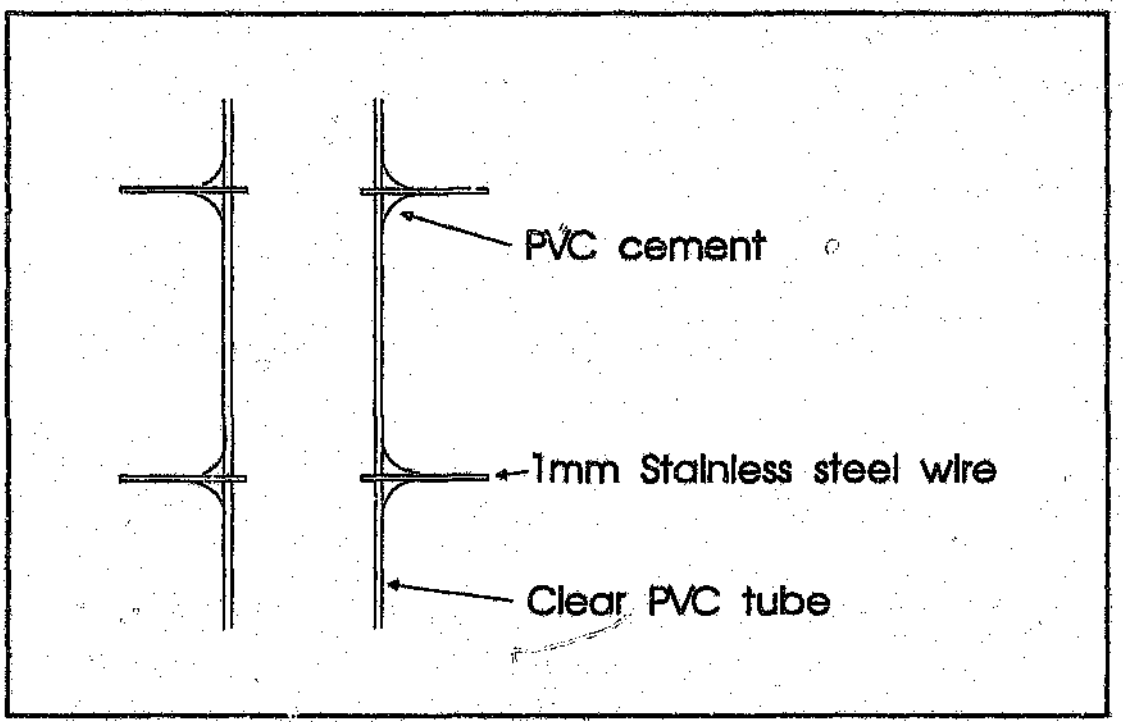


Figure 3.3 - Conductivity probes

The conductivity probes are wired up to a five channel conductivity board which uses a high frequency voltage of 4kHz to excite the probes. The rectified, filtered signals are sent to five analogue inputs of a PC30 data acquisition card. A circuit diagram of one channel on the conductivity board appears in figure 3.4 while the wiring diagram for the whole system appears in figure 3.5.

A brief description of the operation of the conductivity circuitry is as follows. A oscillator (a NE555 integrated circuit) is used to generate a square wave of adjustable frequency of approximately 4 kHz. The mark/space ratio is also variable and was set to unity (to ensure a symmetrical waveform such that the period during which the voltage signal is high is equal to the period when the voltage signal is low). This square wave is chopped and smoothed, to approximate a sine wave and this signal is sent through a reference resistor to

the one probe of the conductivity channel pair. The other probe is earthed. The reference resistor is thus connected in series with the measurement probes, and the voltage is measured across this resistor. If the resistance of the fluid is low, a larger current flows, leading to a higher voltage drop across the reference resistor. This voltage is rectified, using an arrangement of two diodes in conjunction with an operational amplifier. The operational amplifier inverts only the negative signal and the positive signal is added to the negative signal. This signal is then amplified by another operational amplifier and smoothed and filtered using a first order filter.

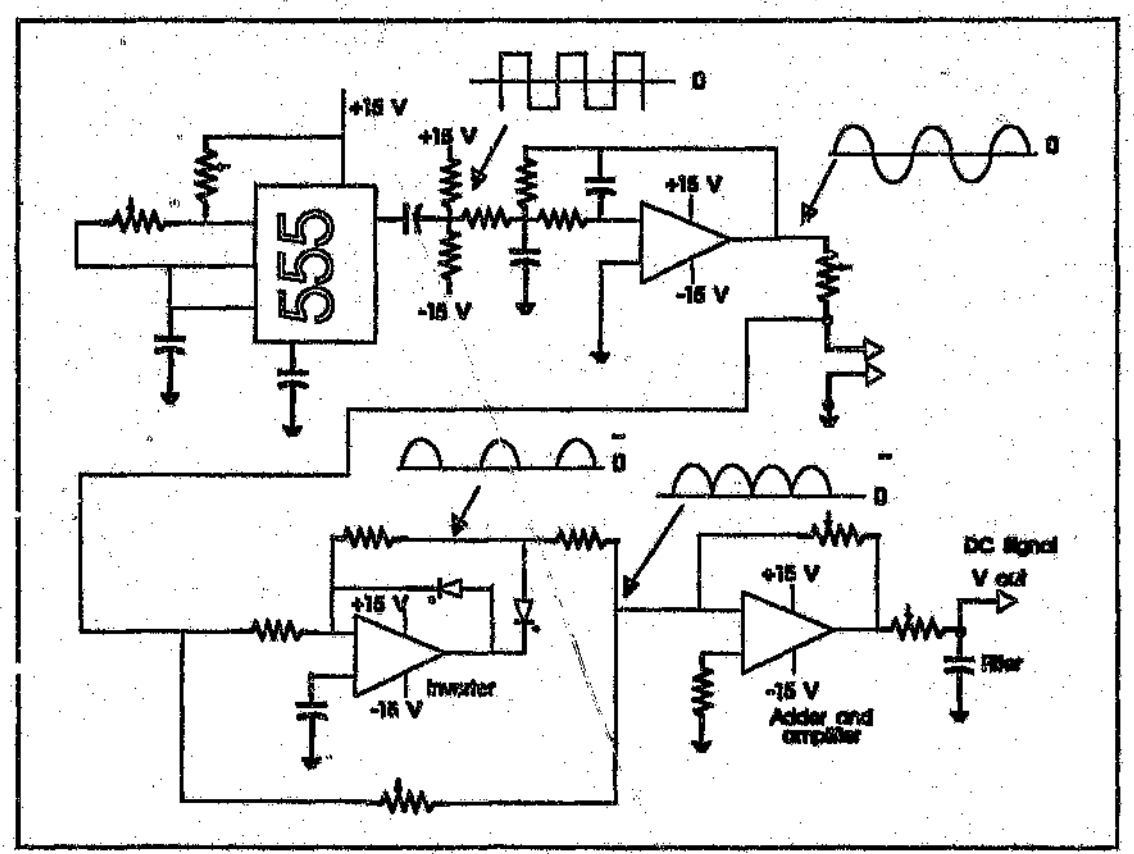


Figure 3.4 - Circuit diagram of one channel of the conductivity circuit

The differential pressure cell has an output signal of 4-20 mA. This signal is converted to a voltage signal as shown in figure 3.5 by connecting a resistor

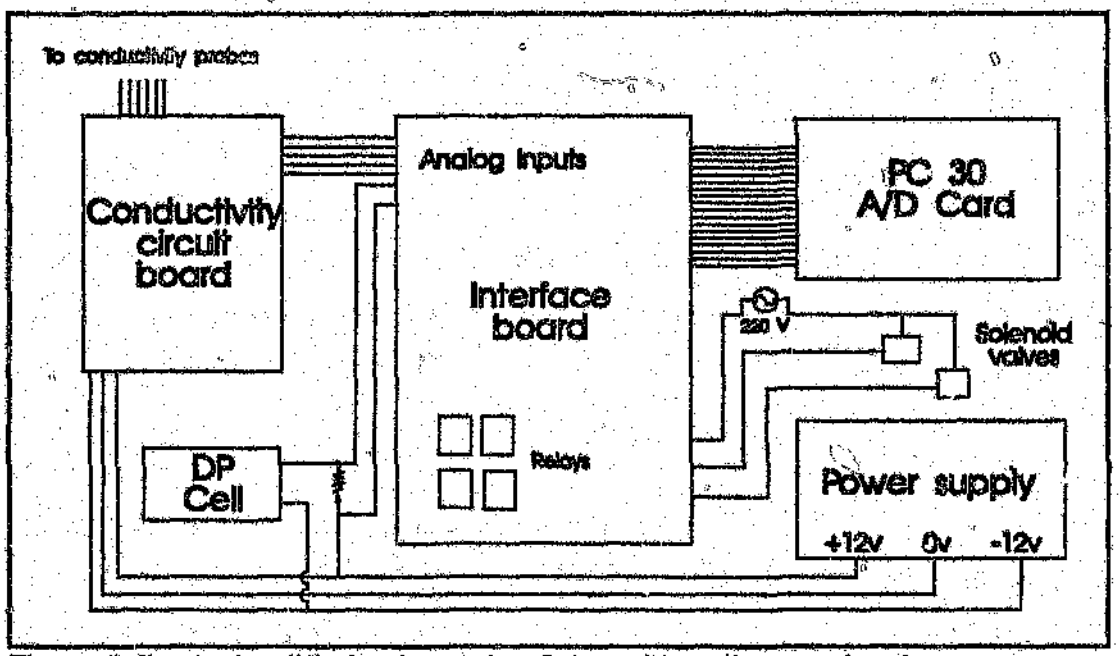


Figure 3.5 - A simplified schematic of the wiring diagram for the system

In the circuit and measuring the voltage drop across it..

The solenoid valves are connected via relays to one of the digital outputs of the PC30 card which is a multi-channel analog to digital card that fits into a free 8 bit slot in the computer. The valves operate on 220 volts AC, actuated by the pc-30 card via two 220 volt relays which are linked to a digital output from the card.

The mixing tank used is a draft tube mixer and is described in more detail in section 3.5.4. A variable speed motor is mounted overhead and is directly coupled via a shaft to a marine impeller.

3.3 Operation of the equipment

The principle of operation of the equipment is as follows (see figure 3.2). Valve A is opened connecting the top of the tube with the low pressure vessel and the slurry is sucked up the tube until the top probe shows a step change in conductivity. At this stage the solenoid valve A is closed, and a reading of the pressure is obtained. The pressure reading thus obtained is used to calculate the density of the fluid using the fact that the static pressure in this case is simply equal to ρgh. The solenoid valve B to atmosphere is opened, thus allowing the slurry in the tube to drain under the influence of gravity. As the slurry drains, the step changes in voltages from the conductivity circuit are recorded and hence the height of the slurry in the tube as a function of time is obtained. From this data the drainage velocity is calculated. The apparent viscosity of the slurry is a function of this velocity.

3.4 Software development

Software was developed which operates the equipment on a continuous basis, opening/closing solenoids to draw the fluid up the tube, allowing the fluid to drain and calculating an apparent viscosity from the drainage data.

The apparent viscosity (as inferred from the drainage velocity) and density (as calculated from the static pressure when the fluid is at a known height) are plotted on the screen in semi real time (there is a slight delay of a few seconds), and thus changes in viscosity can be noted. In the final device the program could be placed onto EPROM on a card, thus possibly eliminating the need for a PC computer to operate the device. The viscometer could then have viscosity and density outputs in the form of two 4-20 mA signals. The algorithm may be roughly summarized as shown in figure 3.6.

At this stage the program also has no control functions built into it. This can be done at a later stage if necessary.

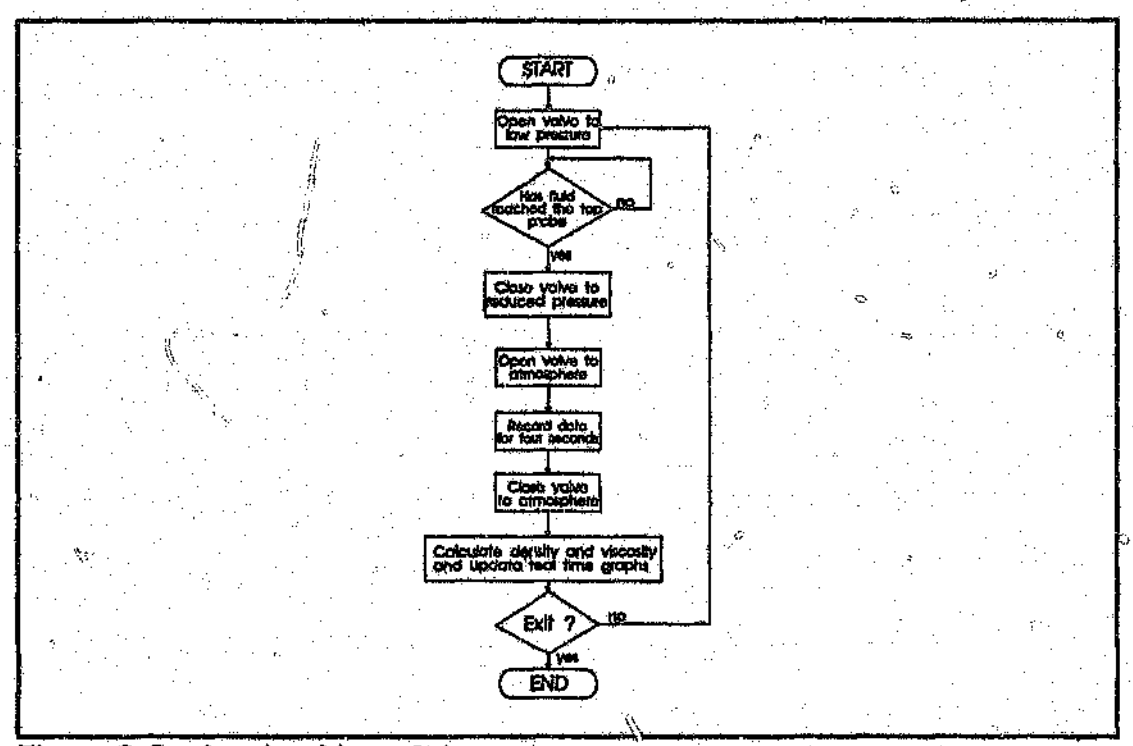


Figure 3.6 - An algorithm of the computer program.

Use is made of digital output channel A to open and close the two solenoids. Procedures were written to open and close solenoids, capture data from the analogue inputs on the card and determine the position of the steps by differentiating the data and checking for a positive change in the derivative.

There are two ways in which the signals from the conductivity board could be handled. The first approach used was to add the signals together and use only one channel of the PC30 card. This has the advantage of being a simpler system from a hardware point of view - only one analogue voltage need be measured (as apposed to five signals). A graph of the signal from the probes using this configuration is shown in figure 3.7. This approach proved

problematic primarily as a result of difficulties in finding the steps in the signals which were of varying size, depending on the conductivity of the fluid and the sensitivity set in the conductivity circuit. Sometimes steps were confused with noise. The second approach used was to feed all five channels into the PC30 card separately. This proved to be more robust and reliable. Even large amounts of noise did not interfere with the step finding routine.

The step finding technique followed initially used an interval halving technique using the number of steps (5) as the known variable. The minium and

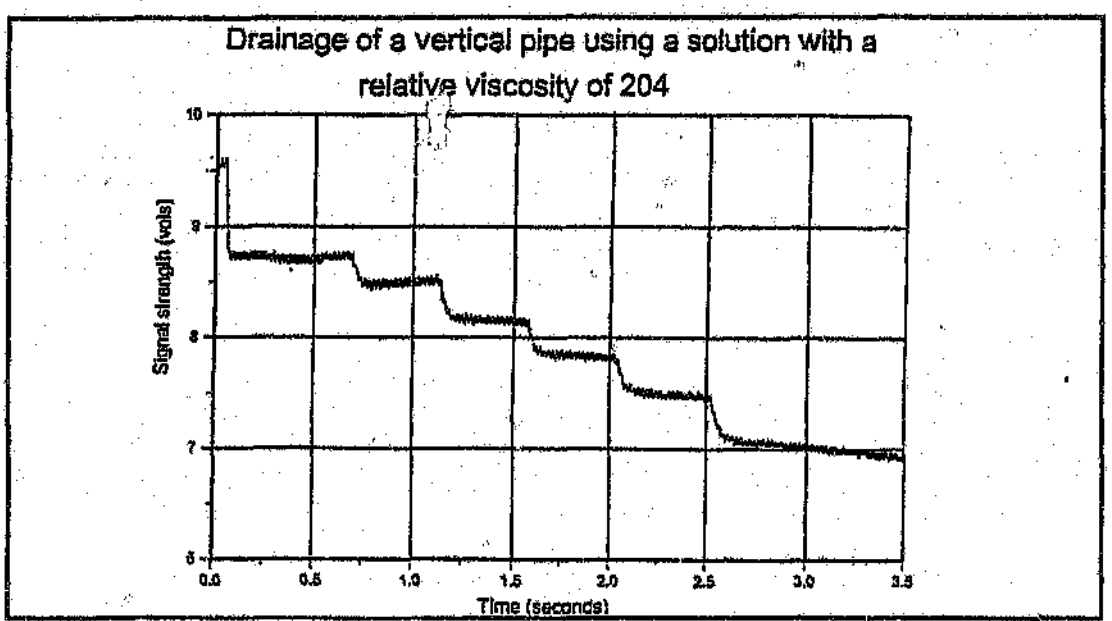


Figure 3.7 - Step changes in voltage with time obtained by adding the 5 voltage signals to get the single voltage shown above.

maximum heights of each step were used as upper and lower bounds. The computer then halves the interval between these two values, and tries this as the next guess for the step size. This gives a number of steps either greater than or less than 5. If there are less than 5 steps the step size is too large and

must be reduced and conversely if there are too many steps, the step height must be increased. This was fairly reliable but did sometimes fail as a result of excessive noise. With the use of five separate channels, for each channel the difference between the voltage at the beginning of the measurement interval (high conductivity) and that at the end of the interval (low conductivity) was halved and a search done to locate the voltage which most closely corresponded to that. The time taken from the beginning of the measurement interval for that step was then calculated.

Elapsed time was simply calculated as follows : the sampling frequency is accurately known since this is set initially and hence the elapsed time can be calculated from the number of samples that have been taken (ie from the position of the voltage value in the data array in the program). It should be noted that the internal clock has a resolution which is far too low for the purposes of time measurement in our case and hence is not used. Some of the important parts of the program are included in appendix 1.

The graphing routines used were based on graphics procedures available in uncompiled form from Quinn Curtis software. Using these procedures a real time scrolling graph showing density and viscosity is displayed.

The data (density and viscosity) is written to a file together with the time taken from the on-board clock in the PC. The file is given a name based on the current date. If this file exists the data is appended, otherwise a new file is created. The operator may exit the program at any stage if desired.

The system can therefore run unattended provided the tube does not get blocked up with slurry.

3.5 Preparation for experiments

The first step in the preparation for experimental work was the choice and calibration of a viscometer which could be used to provide a reference viscosity of any fluids used in the experimental work. Two viscometers were available, both cup and bobbin viscometers, namely a Haake and a Brookfield viscometer. The Haake viscometer was chosen as it can be used to generate the entire shear stress/shear rate diagram, and this could be used to obtain an apparent viscosity. We will now examine the operation and calibration of the Haake viscometer as well as measures used to prevent settling of the slurries used.

3.5.1 Viscosity measurement with the Haake viscometer

Use was made of the MVII P Sensor system with the Haake viscometer. A diagram of the sensor system appears in figure 3.8 while a diagram of the

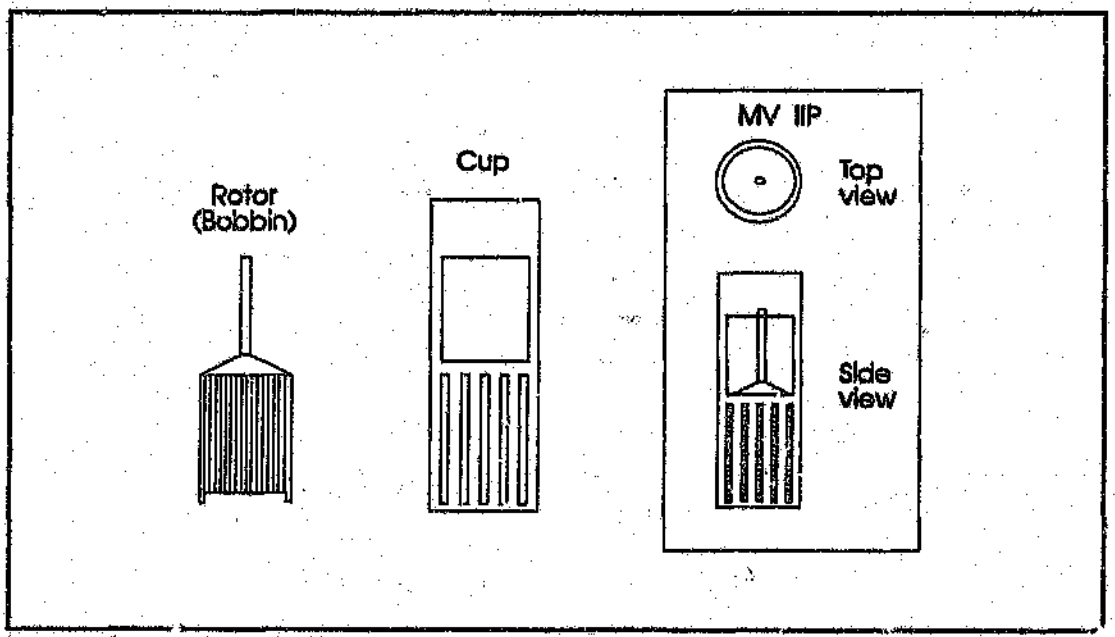


Figure 3.8 - The MV II Sensor system

Haake viscometer used appears in figure 3.9. The shear rate is variable up to a maximum of 512 revolutions per minute. It can be set to sweep in a ramp fashion from 0 to 512 rpm in a period of time set by the user. A sweep time of three minutes was found to be satisfactory. Too low a sweep time yields results which are not very reproducible. The apparent viscosity was chosen to be that at maximum shear as this was quite reproducible.

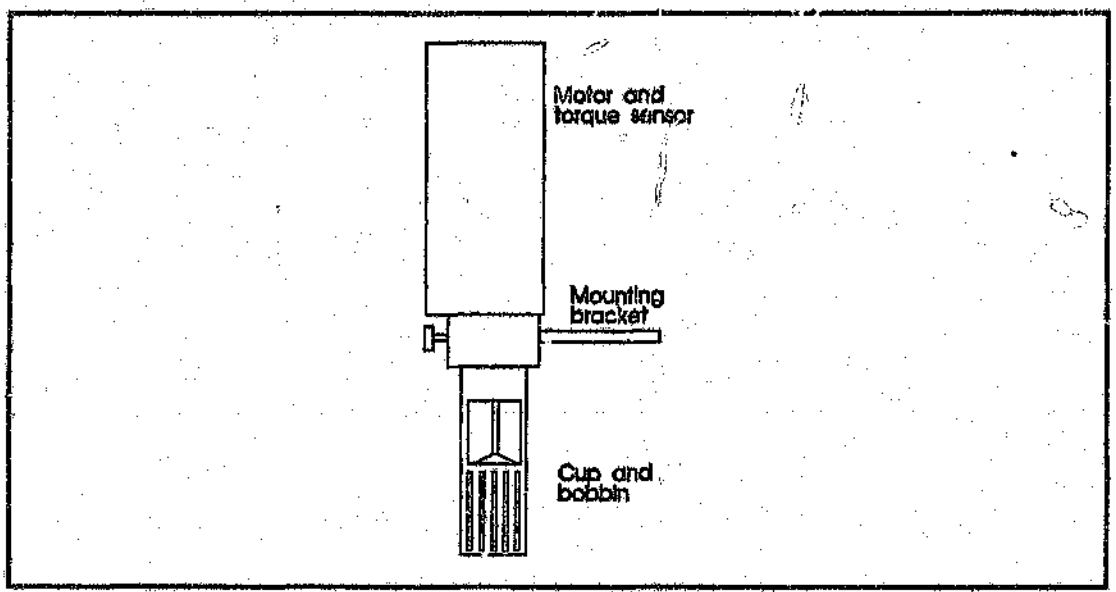


Figure 3.9 - The Haake viscometer

3.5.2 Preparation of standards for calibration

In order to check the calibration of the Haake viscometer, viscosity standards are required. Precision viscosity oils are expensive and have a limited shelf life, hence such oils were not used. Accurate tables are available of the viscosity of glycerol solutions, and a wide range of viscosities are obtainable. Glycerol solutions were chosen as standards. The glycerol standards were prepared from chemically pure glycerol and distilled water. In order to ensure the accuracy of dilution, a pycnometer (a standard 50 ml glass density bottle) was used to check the density of each standard. Data from the CRC handbook was used to obtain the viscosities of the standards. This data was plotted as

shown in chapter 5.2.1. It is clear from these graphs, that the viscosity of glycerol solutions is very sensitive to changes in concentration at higher densities, so an accurate measurement of the density is required to be sure about the viscosity of the standards used.

3.5.3 Preparation of slurries

Various slurries were prepared using solids obtained from different sources. Most experimental work was done using a slurry made from mine dump sand.

The mine dump sand was passed through a 600 micron screen and mixed with water in the draft tube mixing tank. No other special conditioning or preparatory measures were made on this slurry. It was then ready to be used in the experimental work.

Slurry samples from the Western Deep Levels Gold Mine were also used. These samples were treated with 1g lime per kg sample to adjust the pH before the experimental work was performed in order that original conditions in the mineral processing circuit could be more accurately reproduced.

Slurry from the cyclone overflow at the Kinross mine was also used, lime being added to adjust the pH in the ratio of 1g lime per kg sample once again to approximate conditions in the plant more closely.

3.5.4 Techniques used to prevent settling of slurries

Slurries are always difficult to work with due to their settling nature. Steps had to be taken to avoid settling of slurries in any part of the system.

The draft tube mixer was carefully designed to ensure that good mixing would be obtained. The tank was designed in accordance with established design principles for draft tube mixers. Oldshue (1983) examined general mixer design principles with particular emphesis on systems containing suspensions. He

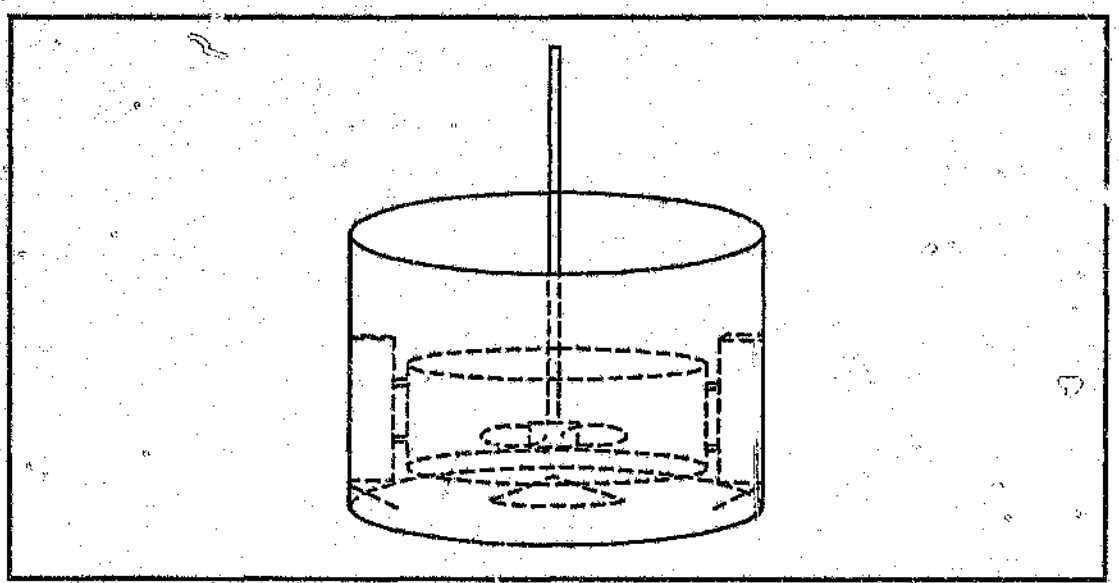


Figure 3.10 - Diagram of a draft tube mixing tank.

recommends the use of a large marine impeller so as to provide maximum mixing conditions for lower speeds of rotation and power input. Oldshue (1983) also stated that the impeller should be located 1/3 of the impeller diameter from the base of the tank. He also recommended the use of fillet around the bottom of the tank, thus reducing the possibility of dead zones. A diagram of the mixer used is shown in figure 3.10. Bourne and Sharma (1974) provide a set of specifications of mixer dimensions as a function of

tank diameter based on a variety of experiments.
These dimensions are shown in table 3.1. Most authors agree that for best results the tank bottom should be contoured in order to prevent dead zones. The ideal type of contouring is shown in figure 3.11, while the fillet and cone approximation is illustrated in figure 3.12.

Parameter	Description	Fraction of tank diameter
T	Tank diameter	1.000
D	Propeller diameter	0.465
D*	Draft tube diameter	0.707
C	Clearance between draft tube bottom and tank bottom and also between liquid level and draft tube top	0.177
L	Length of draft tube	0.336
Z	Liquid level	0.690
B	Baffle width	0.083
B*	Clearance between wall and baffle	0.006
h	Cone height	0.333
d	Cone diameter	0.500
h*	Fillet width = fillet height	0.100

Table 3.1 - Mixer dimension as a function of tank diameter

Even this mixer had problems keeping slurries of more than 70% by mass

solids in suspension, primarily due to the relatively weak stirrer motor used.

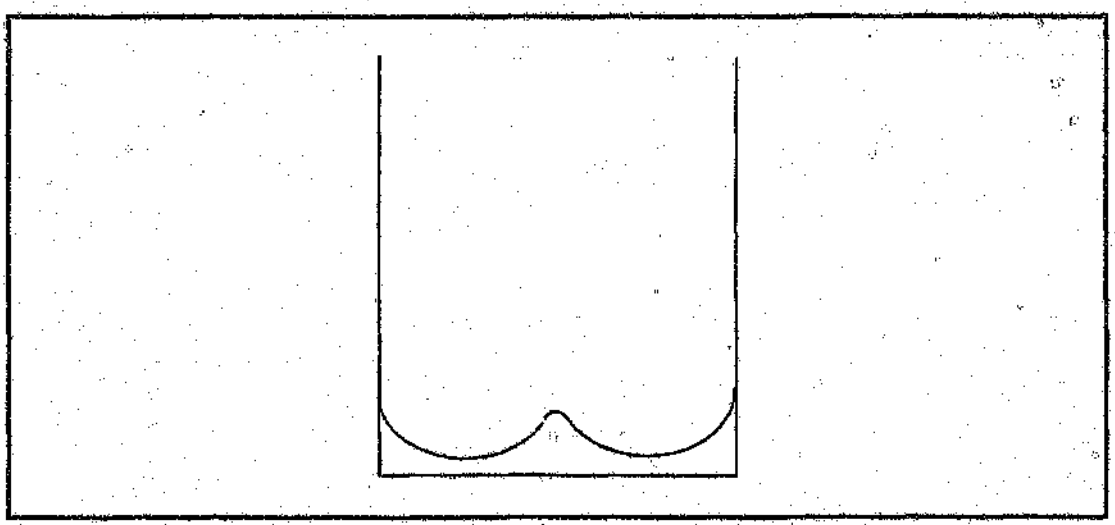


Figure 3.11 - The ideal profile of the base of a draft tube mixer

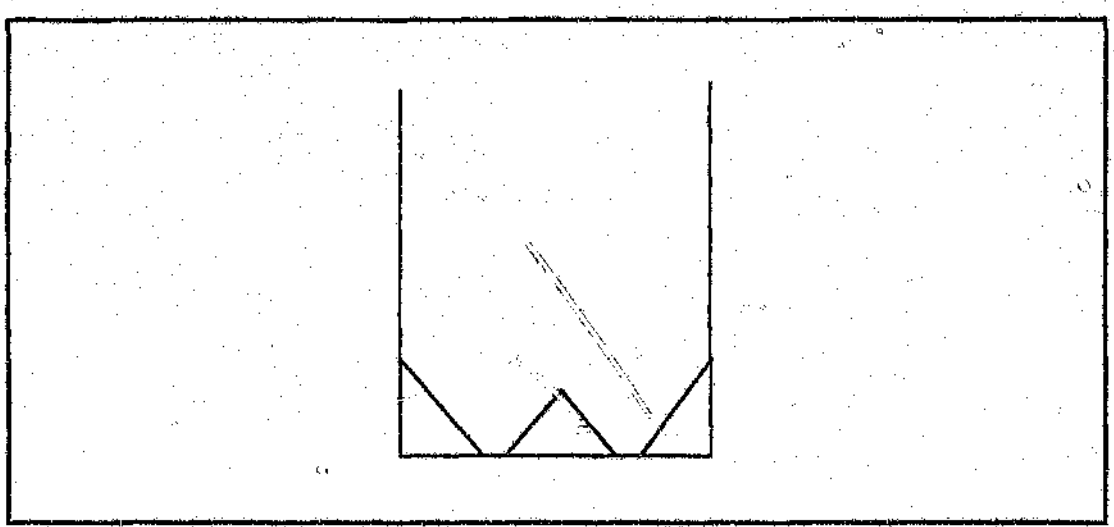


Figure 3.12 - The fillet and cone approximation of the ideal tank bottom

Another problem was related to the positioning of the Haake viscometer in the system. One set up which was tried was to mount the viscometer externally and pump the slurry to the viscometer using a peristaltic pump (see figure 3.13). This did not work well since the slurry blocked up the peristaltic pump

at percent solids above 65 percent by mass. A different set-up was also tried. The viscometer was fitted on the inside of the mixing tank (see figure 3.14). This worked successfully with slurries of up to 71% by mass, when settling occurred.

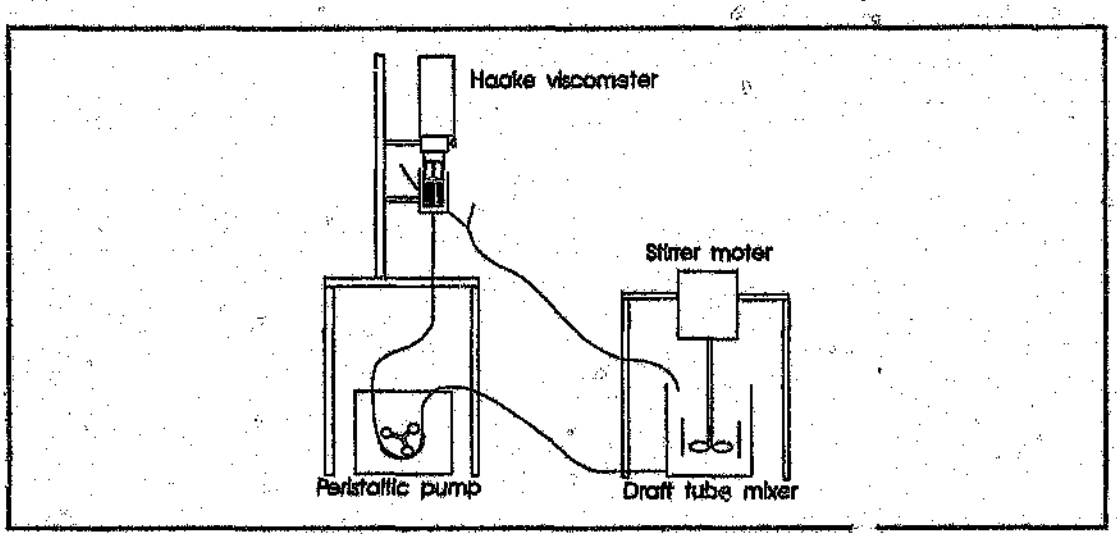


Figure 3.13 - First method of mounting the Haake viscometer

3.6 Experimental procedure

Once the Haake viscometer was calibrated experimental work began with the use of glycerol solutions, followed by carboxy methyl cellulose solutions and then slurries.

The slurry experiments were started by mixing a dilute slurry of known composition and gradually increasing the slurry concentration by adding sand. Rheograms were obtained at each percent solids and about 20 runs on the consistometer under investigation were done on each concentration, before a pre-weighed amount of sand was again added. Results from these experiments can be found in chapter 5.

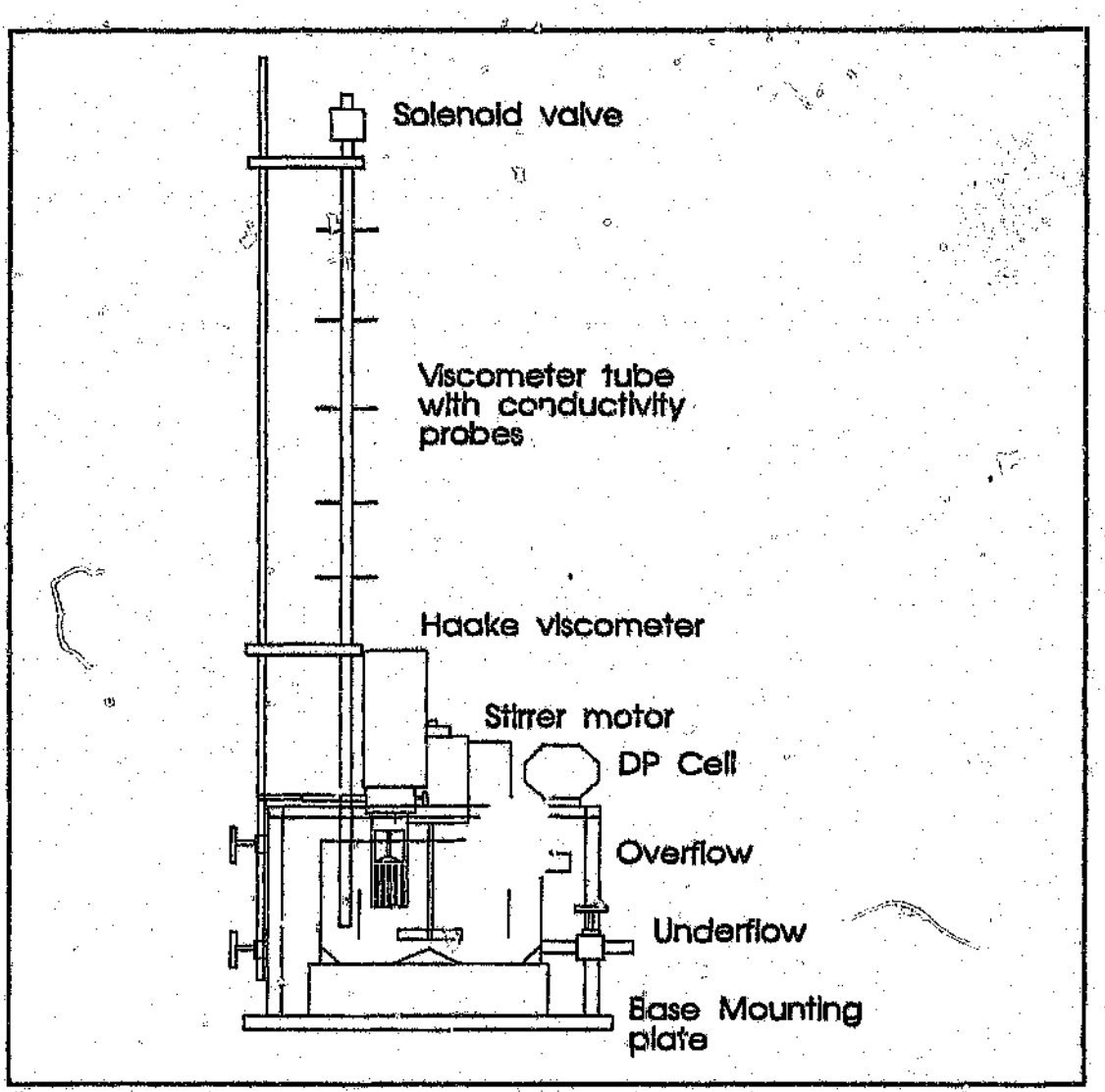


Figure 3.14- Final mounting arrangement of Haake viscometer

3.6.1 Measurement of drainage velocity

The tube was fitted with conductivity probes as detailed in section 3.2. As the air/slurry interface passes a conductivity probe, the conditioned signal voltage from that probe drops. Software was written which could detect that step change and record the time at which this took place. We thus have the times at which the slurry/air interface was at five different heights in the tube. A

least squares fit is done to this data, and the slope of the line gave the average velocity.

3.6.2 Measurement of pressure

The top of the tube is attached to a differential pressure cell. The pressure is measured when the fluid is at the top conductivity probe. Using this pressure, the density of the slurry can be calculated.

3.7 Conclusions

In this chapter we have had a look at the design of an alternative 'viscometer' for the measurement of the apparent viscosities of slurries in particular. We saw that the device could also be used to measure the density of the fluid in question using the static pressure of the fluid when the fluid is at a known height in the tube. The operation of the device was examined and the logic behind the driving software was examined.

CHAPTER 4

THEORETICAL CONSIDERATIONS

The methods used to model the system can be based on two different approaches, namely with the use of a microscopic or macroscopic momentum balance. These two approaches will now be examined and some advantages and disadvantages of each technique will be given.

4.1 Introduction

It is of academic interest that a model be developed which describes the behaviour of the fluid as it drains from the tube. In this chapter a model is developed and solved using acceptable simplifying assumptions.

4.2 The Microscopic momentum balance

4.2.1 The rigorous form of the momentum balance

A small unit element of fluid is examined and a differential generalized momentum balance done on the element, yielding the following equation(see appendix 2 for more details):

$$\rho\frac{\partial}{\partial t}(v_x + v_y + v_z) = -\rho\nabla\cdot\underline{v}\,\underline{v} - \nabla p - \nabla\cdot\underline{\tau} + \rho\underline{g} \qquad (1)$$

where ρ = density of fluid
t = time
v_x = Component of velocity in the x direction
v_y = Component of velocity in the y direction
v_z = Component of velocity in the z direction
τ = Shear stress
g = gravitational acceleration

and

$$\nabla = \left(\frac{\partial}{\partial r} + \frac{\partial}{\partial \theta} + \frac{\partial}{\partial z}\right) \qquad (2)$$

and r, Θ and z are the radial, angular and axial directions in the co-ordinate system.

Using cylindrical co-ordinates for the vectors and assuming the velocity profile and shear stresses are independent of z, that is:

$$\frac{\partial V_z}{\partial z} = 0 \quad \text{and} \quad \frac{\partial \tau_{\theta z}}{\partial z} = 0 \quad \text{and} \quad \frac{\partial \tau_{zz}}{\partial z} = 0 \tag{3}$$

as well as neglecting all angular components reduces this balance to the following differential equation:

$$\frac{\partial V_z}{\partial t} = -\frac{\partial P}{\partial z} \frac{\tau_{rz}}{r} - \frac{\partial \tau_{rz}}{\partial r} + \rho g_z \tag{4}$$

where P is the pressure.

In order to solve this equation information about the shear stress as a function of r would be required. Such information is not available. It is necessary to assume a fluid flow model.

4.2.2 Evaluation of this approach

The microscopic momentum balance therefore has some drawbacks. We have no experimental information about the actual velocity profile, - information necessary to solve for the system using this approach. It would therefore be necessary in any case to assume some sort of velocity profile. We could substitute a model which relates the shear stresses to the velocity gradients, such as the Newtonian model or the power law, and after tedious simplifications get a result, but such simplifications reduce the generality of this approach and negate its advantages. Considering all the other assumptions required the microscopic balance loses a lot of its generality before it becomes solvable, in which case it would be more sensible to start of with a simpler approach which will yield an equally simplified solution.

4.3 The macroscopic momentum balance

Bird (1957) presents an elegant derivation of the macroscopic balances starting with fundamental microscopic relationships. This approach was not used but is of interest.

4.3.1 The generalised form of the macroscopic momentum balance

In this case an unsteady state momentum balance is done on the entire volume of fluid in the tube, as follows (in this case for the drainage of fluid from the pipe) :

$$[\text{accumulation}] = [\text{in}] - [\text{out}] + [\sum \text{forces on system}] \quad (5)$$

the accumulation term can be described mathematically as follows :

$$[\text{accumulation}] = \frac{d(mv)}{dt} \quad (6)$$

also

$$[\text{in}] = 0 \quad (7)$$

$$[\text{out}] = \dot{m}v \quad (8)$$

Forces acting on the system include the pressure force $A\Delta P$, the force resulting from the gravitational acceleration of the fluid, mg, and the friction force. The pressure force should also take into account the pressure drop at the exit of the tube.

The generalised balance can hence be rewritten as shown below:

$$\frac{d(mv)}{dt} = 0 - \dot{m}v + A(P_2 - P_1) + mg + \text{Friction} \qquad (9)$$

The [accumulation] term can be expanded as follows, using the chain rule for differentiation:

$$\frac{d}{dt}(mv) = \frac{d}{dt}\left(\rho A h \frac{dh}{dt}\right) = \rho A\left(\frac{dh}{dt}\right)^2 + \rho A h \frac{d^2h}{dt^2} \qquad (10)$$

and the [momentum out] term is mathematically described as follows:

$$\dot{m}v = \rho A\left(\frac{dh}{dt}\right)^2 \qquad (11)$$

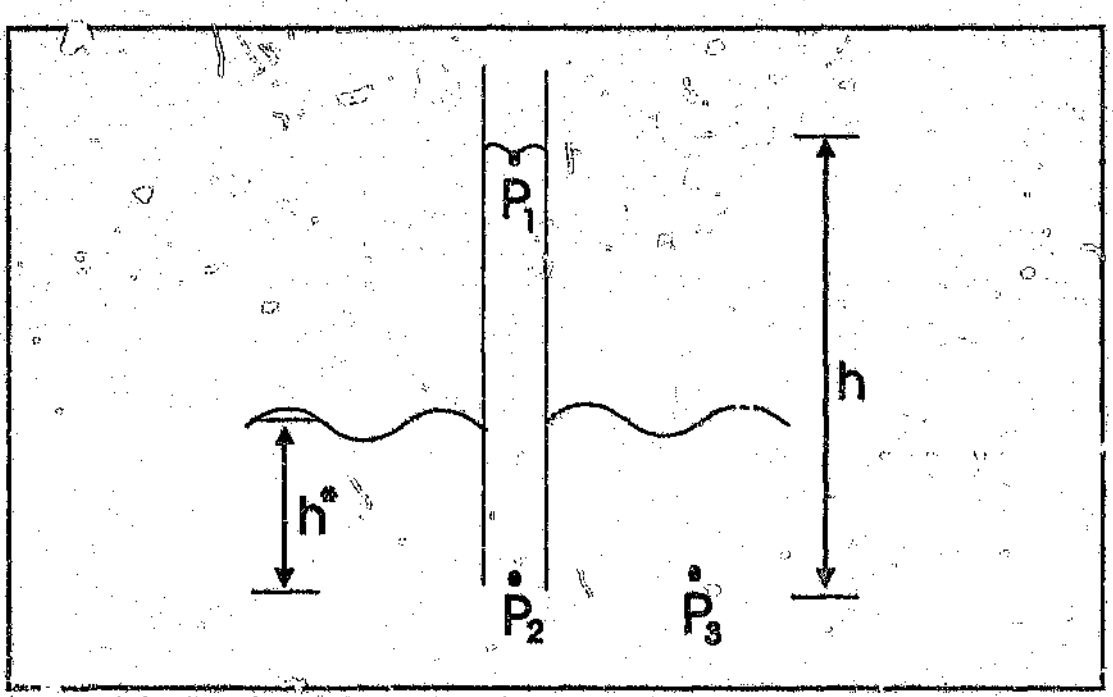


Figure 4.1 - Details of the nomenclature used

The pressure force can be derived as shown below (see figure 4.1 for symbols used):

$$\begin{aligned} \Delta P &= P_2 - P_1 \\ \text{assuming } P_3 - P_2 &= -kv^2 \\ \text{and substituting } P_3 &= \rho g h^* + P_{atm} \\ \text{we get } (P_2 - P_1) &= \rho g h^* + kv^2 = \Delta P \end{aligned} \qquad (12)$$

The friction force is related to the shear stress as follows :

$$\begin{aligned} \text{friction} &= \text{area} * \tau_{rz} \\ &= 2\Pi R h \tau_{rz} \end{aligned} \qquad (13)$$

Substituting all the above terms into the general momentum balance yields the following equation:

$$\rho A\left(\frac{dh}{dt}\right)^2 + \rho A h \frac{d^2h}{dt^2} = 0 + \rho A\left(\frac{dh}{dt}\right)^2 + A\left(\rho g h^* + k\left(\frac{dh}{dt}\right)^2\right) + \rho A h g + 2\Pi R h \tau_{rz}$$

(14)

4.3.2 Using the Newtonian model

The above expression can be much simplified by assuming Newtonian behaviour. This assumption is quite satisfactory for certain slurries (see section 5.4.1)

Assuming Newtonian behaviour allows us to substitute the following into our friction term

$$\tau_{rz} = -\mu \frac{dv_z}{dr} \qquad (15)$$

and hence friction can be expressed as follows :

$$\text{friction} = 2\pi Rh\mu \left.\frac{dV_z}{dr}\right|_{r=R} \qquad (16)$$

But we know that for a Newtonian fluid the velocity profile can be expressed as follows :

$$v_z = 2\bar{v}\left(1 - \left(\frac{r}{R}\right)^2\right) \qquad (17)$$

differentiating v_z with respect to r we get:

$$\frac{dv_z}{dr} = 2\bar{v}\left(\frac{2r}{R^2}\right) = \frac{4\bar{v}r}{R^2} = \frac{4r}{R^2}\frac{dh}{dt} \qquad (18)$$

evaluating this expression at r=R and substituting into the expression for friction we get

$$\text{friction} = -8\pi h\mu \frac{dh}{dt} \qquad (19)$$

Substituting the expression for friction into the original overall balance and simplifying yields the following equation :

$$\frac{d^2h}{dt^2} + \frac{1}{\rho}\frac{dh}{dt}\left(\frac{8\mu}{R} - \frac{k}{h}\frac{dh}{dt}\right) - \frac{gh^*}{h} + g = 0 \qquad (20)$$

where h^* is the height between the bottom of the tube and the surface of the fluid and h is the height of the fluid in the tube from the surface of the fluid in the sampling vessel and μ is the apparent Newtonian viscosity of the fluid. k is a proportionality constant for the pressure drop of the fluid as it exits the tube as defined above.

This equation is difficult to solve analytically since it is neither homogeneous, nor is it linear or exact. No obvious substitution is apparent either which would make it into a standard, solvable form but a number of different but appropriate simplifying assumptions can be made. There are therefore two approaches open to us. We could solve it numerically using some technique such as Runge Kutta or make an appropriate simplifying assumption and solve the slightly simplified form analytically.

4.4 Numerical solution of the differential equation.

In order to solve this differential equation numerically it is necessary to first make an appropriate substitution. We thus substitute v for the rate of change of height with time and this gives us a set of two differential equations to be solved simultaneously:

$$\frac{dh}{dt} = v$$
$$\frac{dv}{dt} + \frac{8\mu v}{\rho R} - \frac{kv^2}{\rho h} - \frac{gh^*}{h} + g = 0 \qquad (21)$$

This may be solved using Runge Kutta. A turbo pascal program was written to solve this using 4th order Runge Kutta. MATLAB was also used to solve this set of differential equations (MATLAB uses a variable step 5th order Runge Kutta algorithm to solve boundary value problems such as this one). The Pascal and Matlab routines can be found in Appendix H. A plot of three typical solutions appears in figure 4.2. It is clear from this plot that the fluid quickly accelerates to its terminal velocity. Finally the fluid oscillates a little, depending on its viscosity. The velocity of the fluid can be calculated from the slopes of the best fit straight line through the data between the heights of 0.8 m and 0.2 m. The values for k used are based on best fits of the simplified analytical solution to experimental data discussed in chapter 5.

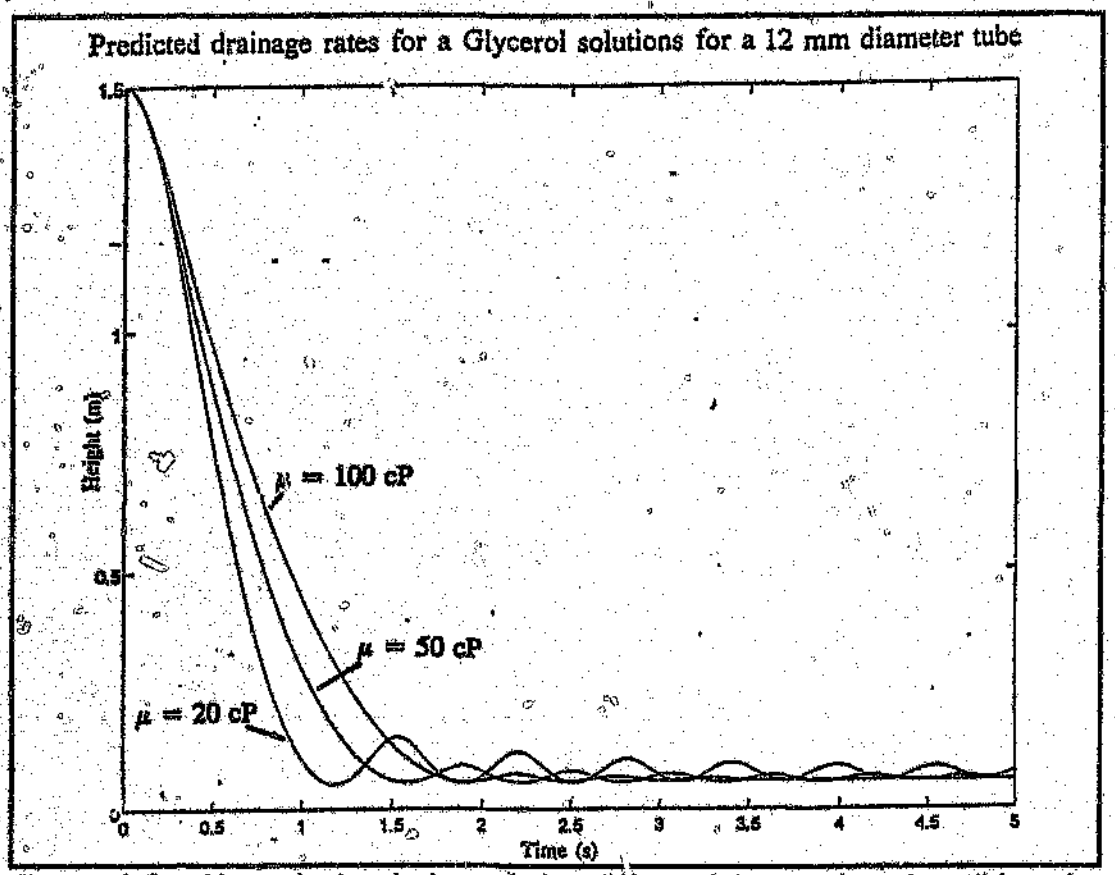


Figure 4.2 - Numerical solution of the differential equation describing the system

4.5 Simplified analytical solution

The most appropriate simplifying assumption is that of neglecting acceleration, since from the experimental results as well as the numerical solution above it is clear that the fluid only accelerates for a very short time period before reaching its terminal velocity - see chapter 5 (we are also not particularly interested in the transient behaviour of the fluid in the tube and this would be a difficult to measure).

Hence neglecting acceleration gives the following differential equation :

$$\frac{k}{ph}\left(\frac{dh}{dt}\right)^2 + \frac{8\mu}{\rho R}\frac{dh}{dt} - \frac{gh^*}{h} + g = 0 \qquad (22)$$

This is a quadratic in dh/dt and can be factorized using the quadratic formula to give dh/dt as a function of h.

$$\frac{dh}{dt} = \frac{-\frac{8\mu}{gR^2} \pm \sqrt{\frac{64\mu^2}{g^2R^4} - \frac{4k}{\rho h}\left(1 - \frac{h^*}{h}\right)}}{\frac{2k}{\rho h}} \qquad (23)$$

In the above equation it seems that the velocity is not constant, but rather that it is a function of height, however from table 4.1 shown below it is clearly a very weak function of h.

Table 4.1 - The effects of changing the height using glycerol solutions of different viscosities as calculated from the analytical solution for a 14 mm tube.

Height (m)	velocity (m/s) $\mu = 50$	veolcity (m/s) $\mu = 150$	velocity (m/s) $\mu = 250$
1.2	1.04162	0.62594	0.33197
1	1.04162	0.62595	0.33197
0.8	1.04163	0.62597	0.33198
0.6	1.04165	0.62601	0.33200
0.4	1.04167	0.62607	0.33201
0.2	1.04190	0.62626	0.33203

Another simplifying assumption which can be made is that of neglecting the end effects - ie neglecting pressure drops as the fluid exits the pipe. In that case the differential equation simplifies down to the following linear DE:

$$\frac{d^2h}{dt^2} - \frac{8\mu}{\rho R}\frac{dh}{dt} + g = 0 \qquad (24)$$

This equation may be simply solved using D operators operators of Laplace transforms to give a solution of the form :

$$h = Ae^{\alpha t} + Be^{\beta t} \qquad (25)$$

Neglecting end effects, as well as acceleration reduces to the simple solution:

$$v = \frac{\rho g R^2}{8\mu} \qquad (26)$$

This is oversimplified, but still shows the underlying variables of importance. It is interesting to note that this is the same expression one would have obtained from the expression of the average velocity in the derivation of the Hagen-Poiseulli law for fluid flowing down a vertical pipe.

All of the equations derived fail to take slippage at the wall into account. It is difficult to quantify this effect and hence this effect is neglected. Roughening the tube walls reduces the slippage and hence this effect should be negligible. The results are presented in the next chapter.

CHAPTER 5

EXPERIMENTAL RESULTS AND DISCUSSION

Experimental work affords us the opportunities to test our ideas and in this sense it is exciting as one is faced with many unexpected results which may require further investigations, or explanations.

5.1 Introduction

In this chapter we examine and discuss the results of batch tests which were conducted using the new viscometer on different fluids, including glycerol solutions, carboxy methyl cellulose solutions and slurries. This chapter does not include tests done on pilot mills (these results and a discussion of pilot mill test work can be found in chapter 6).

5.2 Experiments using glycerol solutions

Glycerol solutions were the first fluids to be used in the experimental work. Glycerol is convenient to work with and the viscosities of glycerol solutions are well documented (CRC Handbook). Data from the CRC Handbook has been plotted in figure 5.1 (see appendix B for a table of viscosity data). The sharp increase in viscosity at higher densities is interesting, as this type of behaviour is also exhibited by slurries.

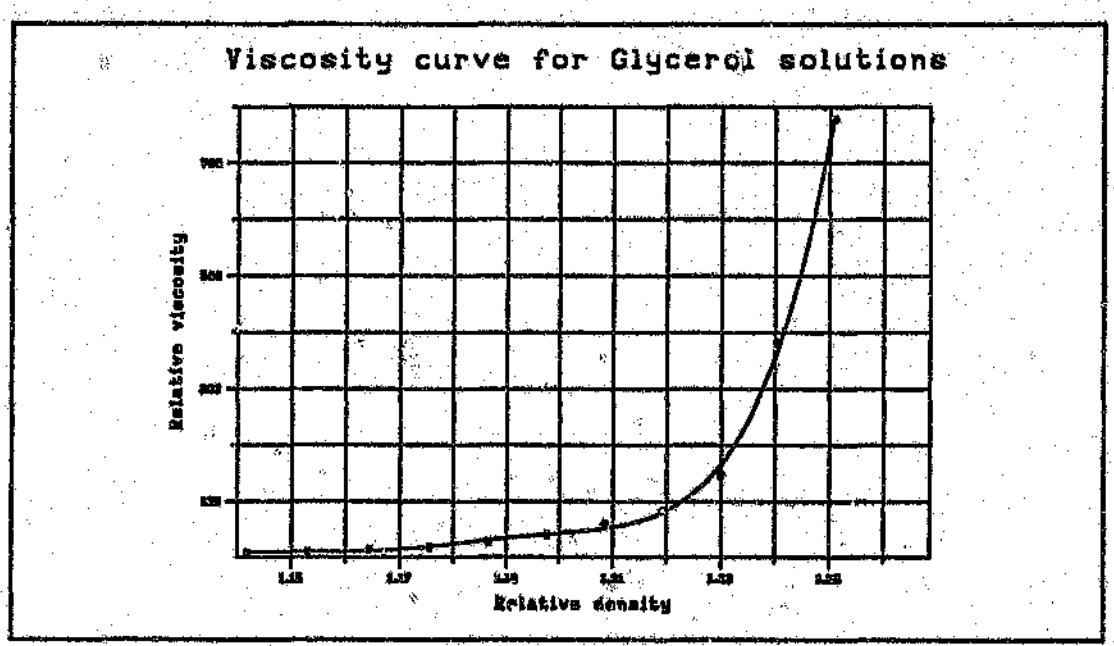


Figure 5.1 - Viscosity of Glycerol solutions (From the CRC Handbook)

5.2.1 The rheology of glycerol solutions

Rheograms were generated using the Haake viscometer with glycerol solutions and some of these are shown in figure 5.2. It is clear from these rheograms that glycerol is a Newtonian fluid, the viscosity of the glycerol being the slope of the lines. The Haake viscometer was also found to be satisfactorily accurate for providing a reference viscosity, against which the experimental results could be compared, since the viscosity of these glycerol solutions was known and these values compared favourably to those based on data from the Haake viscometer.

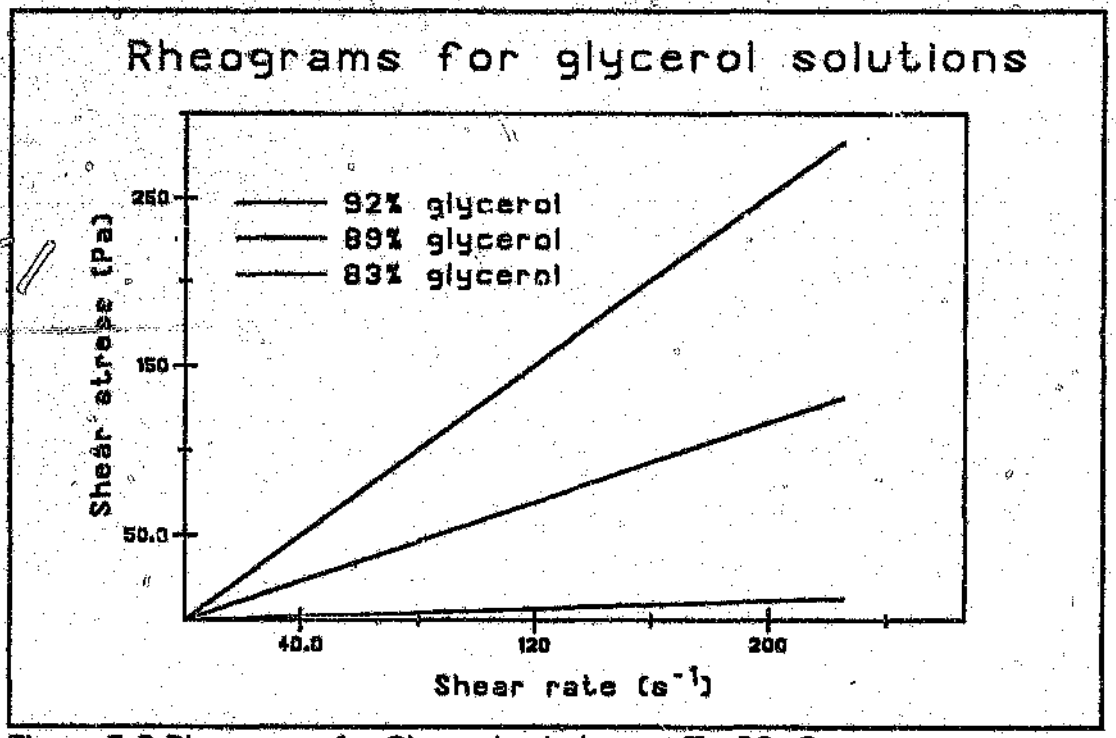


Figure 5.2 Rheograms for Glycerol solutions at T = 22°C

5.2.2 Drainage data using glycerol solutions

Tests were conducted on the glycerol solutions using the vertical tube viscometer and it was found that the velocity of drainage is almost constant during the drainage cycle of the process (the height vs time curves are almost straight lines as can be seen from figure 5.3).

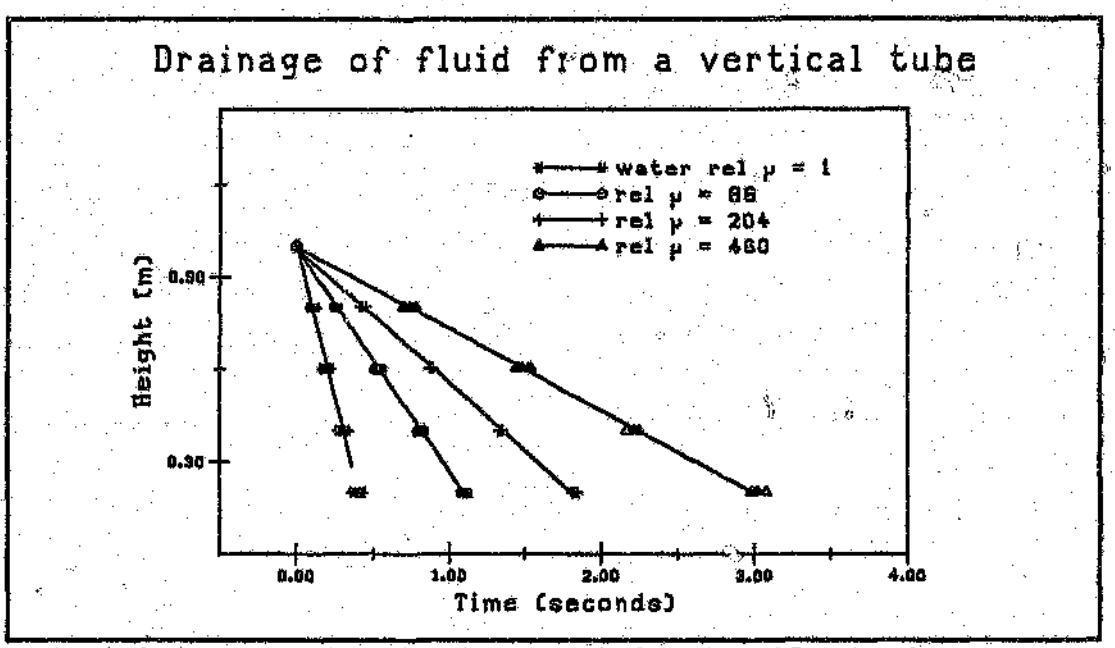


Figure 5.3 - Drainage lines for glycerol solutions in a 12 mm tube

This indicates that the fluid quickly reaches a terminal velocity after a short period of acceleration, and also confirms that the transient response of the fluid is not necessarily of interest in the interpretation of the results. It therefore makes sense to use the average velocity and to plot this data as a function of viscosity. The velocity (as seen from the slopes of the lines) clearly changes quite substantially with changing viscosity. This is more clearly seen in figure 5.4 where data for two different tubes is plotted together with the drainage data predicted from the model.

Experiments were done using glycerol with two different tube diameters at different viscosities. The inverse of the average velocity is plotted as a function of viscosity in figure 5.4. The inverse is plotted as theory indicates that we should expect velocity to be directly proportional to velocity^{-1}, and this is confirmed by the fact that these are virtually straight lines.

The strong relationship between viscosity and velocity is clearly evident from figure 5.4. It is clear that in the 12 mm tube the relationship is stronger. The reproducibility of the results is also evident from the narrow distribution of data. It is therefore clear that the viscometer works satisfactorily well with glycerol solutions. The model was fitted to the experimental data using a least squares fit on the parameter k, (where $\Delta P = kv^2$) in the simplified analytical

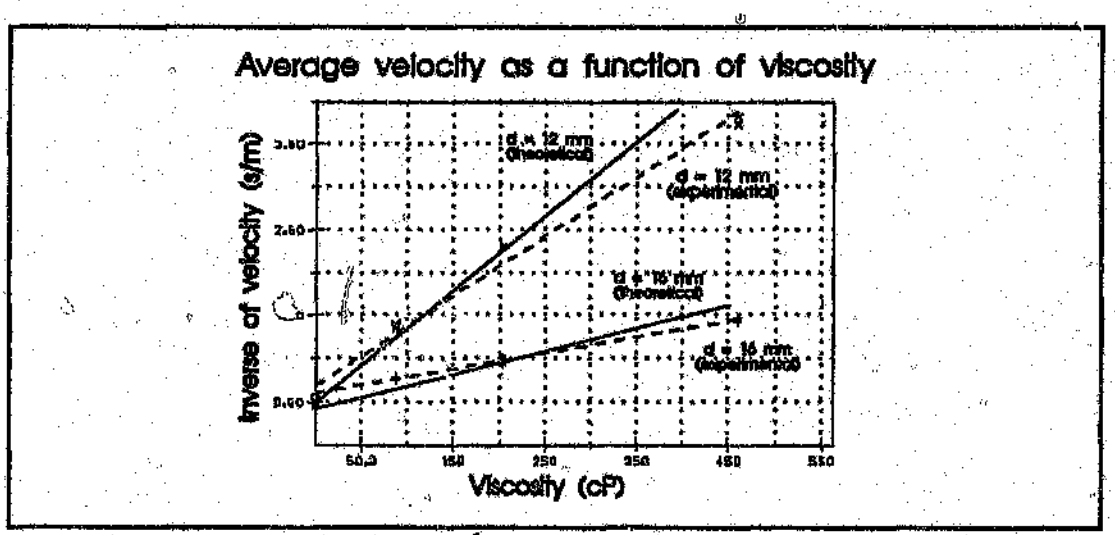


Figure 5.4 - A plot of velocity^{-1} as a function of viscosity using glycerol solutions. The theoretical data comes from the simplified analytical solution.

solution neglecting acceleration. The fit so obtained was a fairly good fit with correlation coefficient of 0.973 and 0.952 for the tube diameters of 16 and 12 mm respectively. This k value was then used in the numerical solution shown in figure 5.4. The Mathcad program used can be found in appendix F.

5.3 Experiments using carboxy-methyl-cellulose solutions

Experiments were conducted on carboxy-methyl-cellulose (CMC) solutions as these solutions are non-Newtonian and we were interested to check if we would still get straight drainage lines as was the case with glycerol.

5.3.1 The rheology of carboxy-methyl-cellulose solutions

CMC solutions are true solutions and are fairly viscous, even in fairly dilute solutions. These solutions are transparent and resemble some form of gel. Using the Haake viscometer, rheograms were generated for some CMC solutions. It was found that very dilute solutions were fairly newtonian but as the concentration of solution increased, marked pseudoplastic behaviour developed. Highly concentrated slurries are also pseudoplastic. The rheograms generated for CMC solutions are shown in figure 5.5.

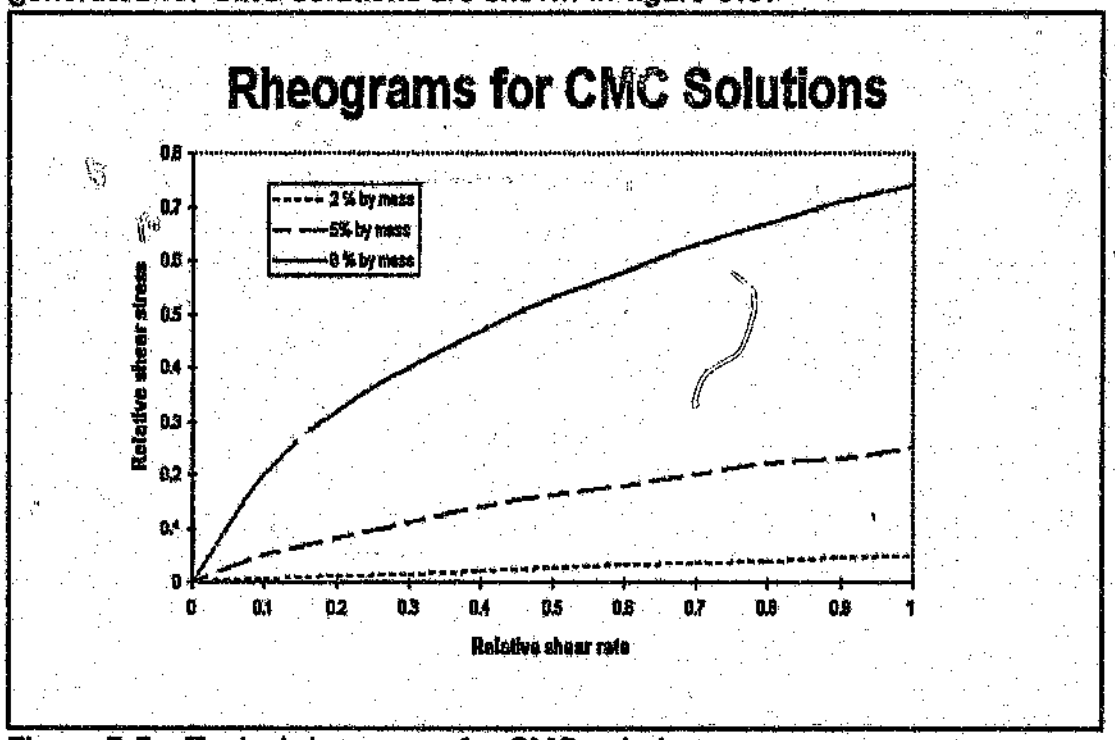


Figure 5.5 - Typical rheograms for CMC solutions

5.3.2 Drainage data from CMC solutions

Experiments were done on CMC solutions and it was found that CMC solutions also have straight drainage lines, with an almost constant drainage velocity, indicating that the rheology of the fluid does little to change the actual, overall shape of the drainage curves, especially under steady state conditions.

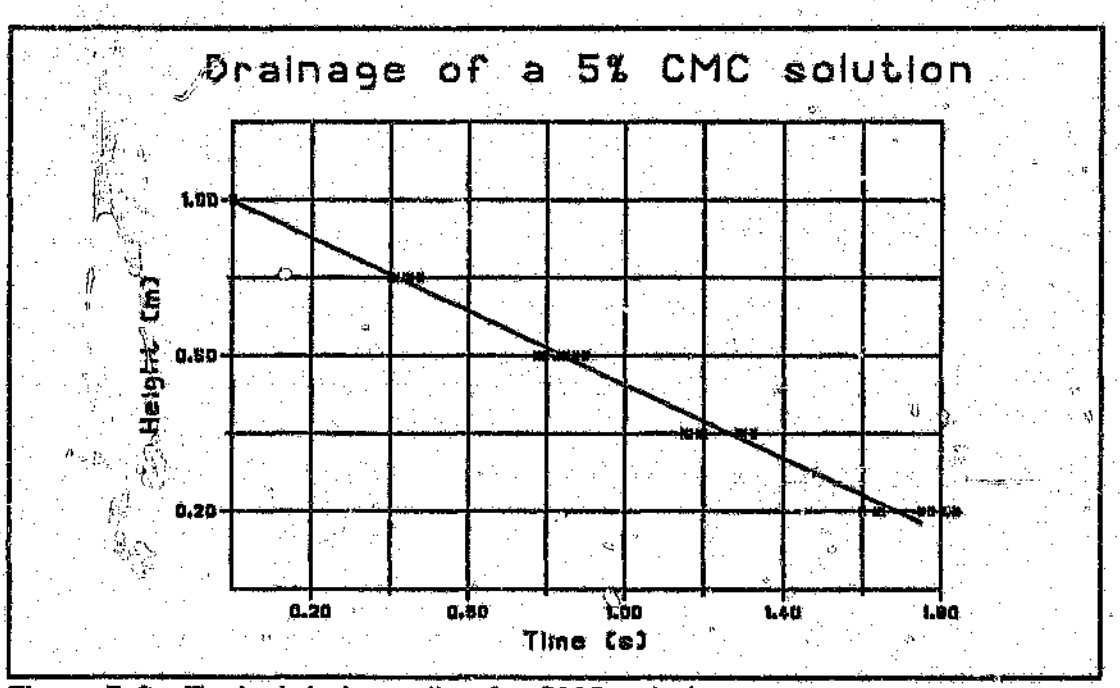


Figure 5.6 - Typical drainage line for CMC solution.

It is possible that during the transient period, where the fluid is accelerating, and hence is subject to changing shear rates, the rheology of the fluid would affect the drainage characteristics, however this time-frame is so small that accurate measurements in this region would be difficult to obtain. Under steady state conditions, however, the fluid is subject to a constant shear rate, hence one would expect similar behaviour to Newtonian fluids. A typical drainage line for a CMC solution is shown in figure 5.6.

The apparent viscosity of the 5% CMC solution used during batch tests was calculated to be 137cP at the maximum shear rate (using the simplified solution to the model neglecting acceleration). However the viscosity predicted from the experimental work using the model and k calculated is 168 cP which corresponds to the apparent viscosity at a relative shear rate of approximately 0.2 (on the rheograms). We can thus see that the shear rate in the tube is lower than the shear rate used as a basis for the calculation of apparent viscosities from the rheograms generated using the Haake viscometer (assuming the calculations and data are correct).

This explains the difference in these two apparent viscosities. We can however see from the rheograms that apparent viscosities are still useful even at lower shear rates. Naturally with Newtonian fluids viscosity is not a function of shear rate and this discrepancy would be smaller. It therefore makes sense, when dealing with non-Newtonian fluids that the apparent viscosity from experimental work should be compared to an apparent viscosity from the Haake viscometer calculated using an appropriate shear rate as a basis.

Shear rate is however not only a function of the tube dimensions, but also depends on the fluid properties, notably the rheology of the fluid. We can estimate the shear rate at the walls of the tube from the velocity of the fluid using a velocity profile calculated from the rheograms and the apparent viscosity calculated.

5.4 Experiments using slurries

Tests were done on a few different slurries, by mixing batches of slurry in a draft tube mixer and sampling directly from the mixer. The results of these experiments are presented in the sections that follow.

5.4.1 The rheology of mineral slurries

Rheograms obtained from mine dump sand, passed through a 600 micron sieve are presented in figure 5.7, while the rheograms from a sample of slurry from the Western Deep Levels gold mine are shown in figure 5.8. The slurry made from mine dump sand has a larger average particle size distribution and it is of interest to compare slurries of different size distributions. Size distribution data can be found in Appendix 2.

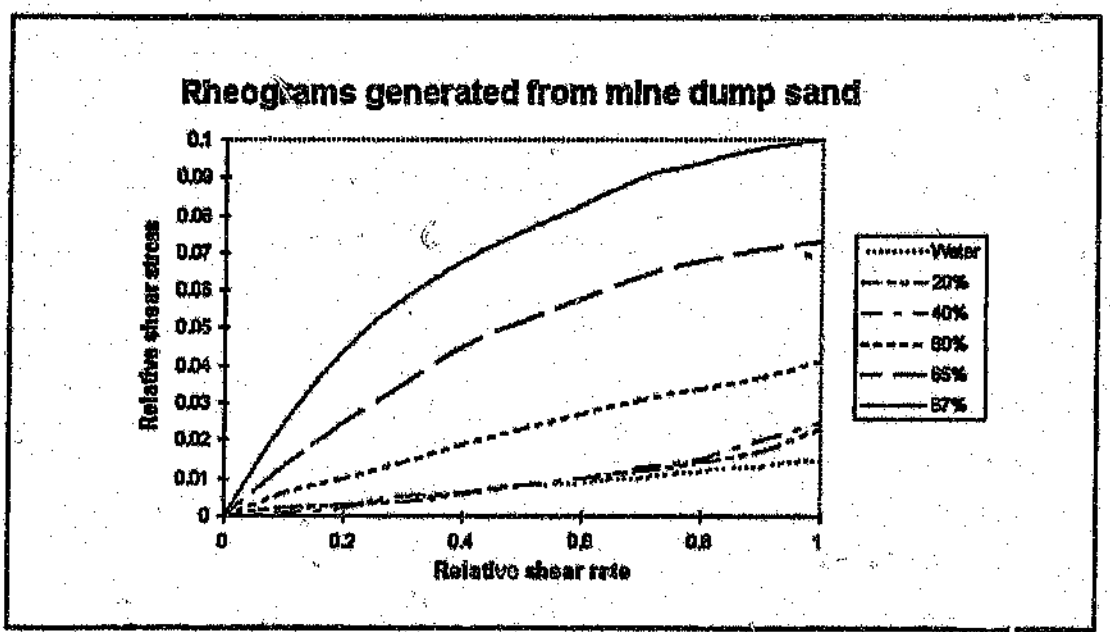


Figure 5.7 - Rheograms from slurry made from mine dump sand

The apparent viscosity (at maximum shear rate) of mineral slurries changes very little in the lower concentration region, and there is in fact only a relatively small change in apparent viscosity in the concentration range 10 to 50 % solids. This is evident from figure 5.8. Figure 5.8 was compiled using the apparent viscosity of mine dump slurries at maximum shear rate (500 rpm) from the rheograms generated using the Haake viscometer.

Viscosity data for this slurry would clearly only be useful in the %solids (by

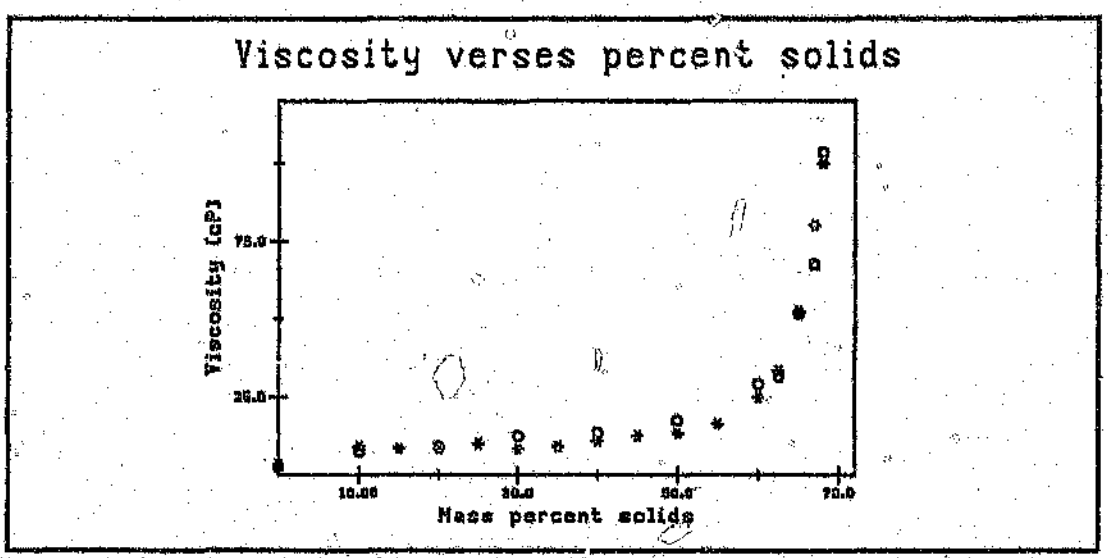


Figure 5.8 - The relationship between %solids and viscosity for mine dump slurry

mass) region of about 60% and higher, since it is only in this region that substantial changes in viscosity occur with increasing % solids - a change in % solids from 60 to 70 % (ie a 17% change) in percent solids, is accompanied by an almost 300% change in viscosity The Mill discharge does exceed 60 % by mass solids, and hence are in this highly sensitive region. This once again serves to illustrate that the accuracy of the viscometer is not critical, and that this measure is clearly potentially more accurate a measure of consistency than % solids, which is in any case difficult to measure accurately on an on-line basis. The Western Deeps sample was treated with lime to adjust the pH of the slurry in order that industrial conditions be more closely approximated, however the effects of pH on slurry rheology were not investigated.

Mineral slurries show different rheological characteristics with changes in concentration. It is clear from the rheograms presented that dilute slurries seem to be slightly dilatant, moderately concentrated slurries are almost

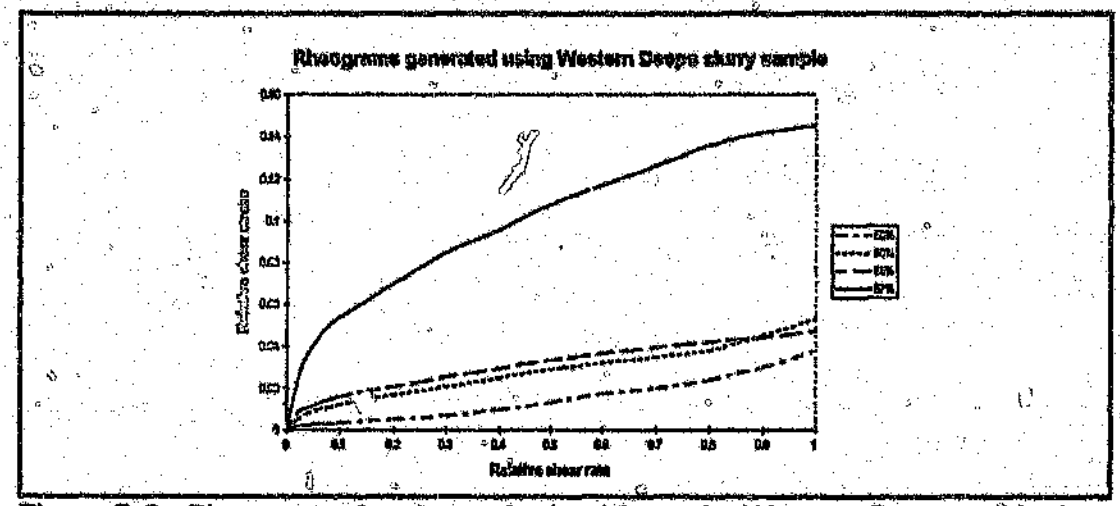


Figure 5.9 - Rheograms for slurry obtained from the Western Deeps gold mine.

Newtonian, while highly concentrated slurries are decidedly pseudoplastic. This is in agreement with the results obtained in previous studies (Kawatra and Eisele 1987). All the rheograms where generated at room temperature, and the temperature was monitored to check if the mixer would cause any significant temperature rise. This however proved not to be a problem.

It is clear that the slurry sample from the Western Deep Levels Gold Mine is more viscous than that made with mine dump sand. This is due to the different size distributions of the slurries as well as possibly different pH's.

5.4.2 Drainage data for mine dump sand

As expected, the drainage velocities were almost constant for most of the slurries examined, and the drainage curves were closely approximated by straight lines. It is more informative to examine how the average velocity changes with pipe diameter and percent solids.

The average drainage velocity as a function of viscosity for mine dump slurry is presented in figure 5.10. The effect of roughening the tube is also clear from these results. It seems essential that the tube be roughened, since this strengthens the dependency of the drainage velocity of the slurry on its viscosity. For the smooth tubes, velocity is clearly only a very weak function of viscosity for the 16 and 20 mm tubes. It is preferable to use larger tubes since they would choke up less frequently.

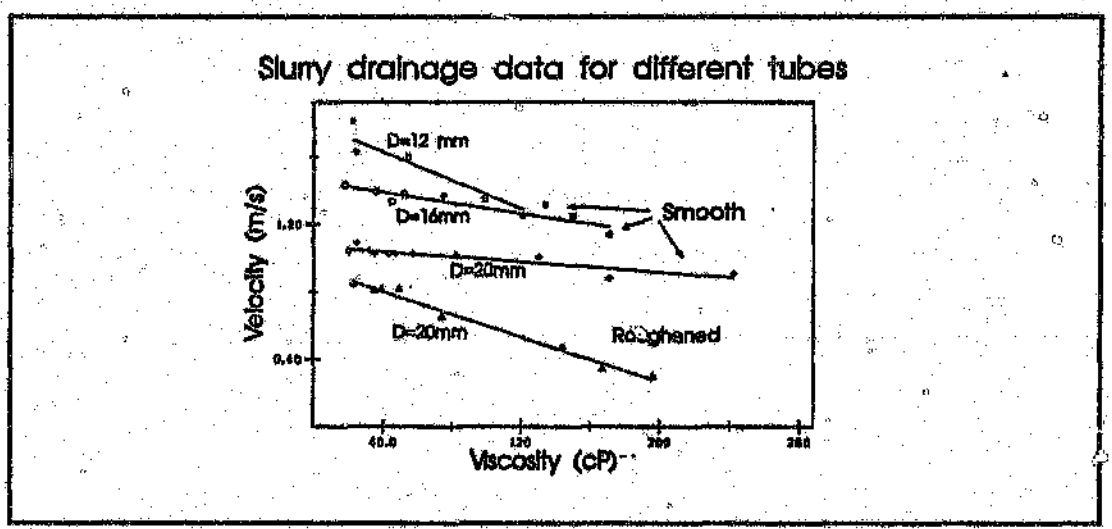


Figure 5.10 - Drainage velocity as a function of percent solids for mine dump slurry

The slurry results are interesting since over much of the viscosity range it was found that drainage velocities in larger tubes were lower than the velocities in small tubes. This was not the case with glycerol. There are a number of factors which may be causing this phenomenon and this deserves further investigation. There are clearly two main effects which are present in this system - namely viscous effects at the walls and the end effect. Based on figures 5.10 (and 5.11 discussed below) it appears that at higher viscosities, the drainage velocity in larger diameter tubes is larger - a result expected over the whole range of viscosities.

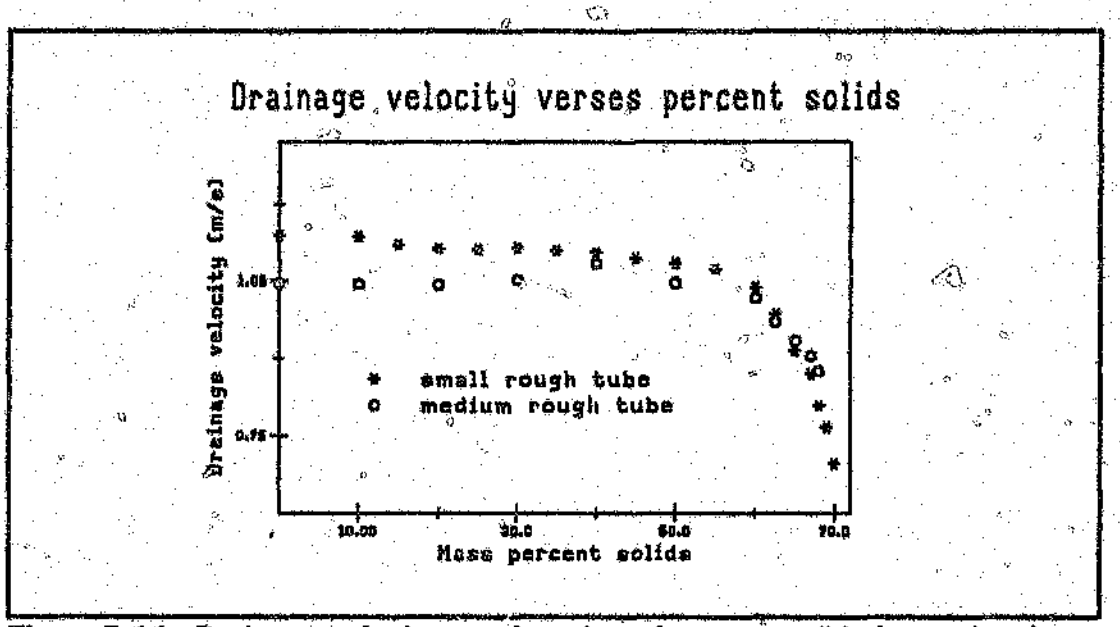


Figure 5.11 - Drainage velocity as a function of percent solids for a mine dump slurry.

There is some cross over point where viscous wall effects dominate over end effects, and this viscosity depends on the tube diameters.

Glycerol did not exhibit this type of behaviour, possibly due to the fact that the glycerol solutions were not subject to mixing during the measurement process. The draft tube mixer generates an upward circulation patten around the sampling tube, possibly magnifying the end effects. Clearly with a larger diameter tube more slurry must be displaced in the fluid below and this effect may be magnified when larger volumes of slurry have to be displaced against this current. It was however found that mixing has very little influence on drainage velocities of water.

The drainage velocity was plotted as a function of percent solids, using mine dump slurry, with some interesting results (as shown in figure 5.11). Two tubes were used with diameters of 12 mm and 16 mm.

The first point to notice is that there is little change in drainage velocities at lower percent solids, despite the fact that the density of the slurry is changing in this region (this is not expected from theory and may result f. We know from figure 5.8 that the viscosity of the slurry is virtually constant over this range so we could postulate that this indicates that the density of the fluid does little to change the drainage velocity. This is good since it is further evidence that there is a simple relationship between viscosity and drainage velocity. It is interesting to compare figure 5.11 to figure 5.8 which was generated using the same slurry. It is clear that the viscosity is related to the inverse of velocity, density being only a minor factor.

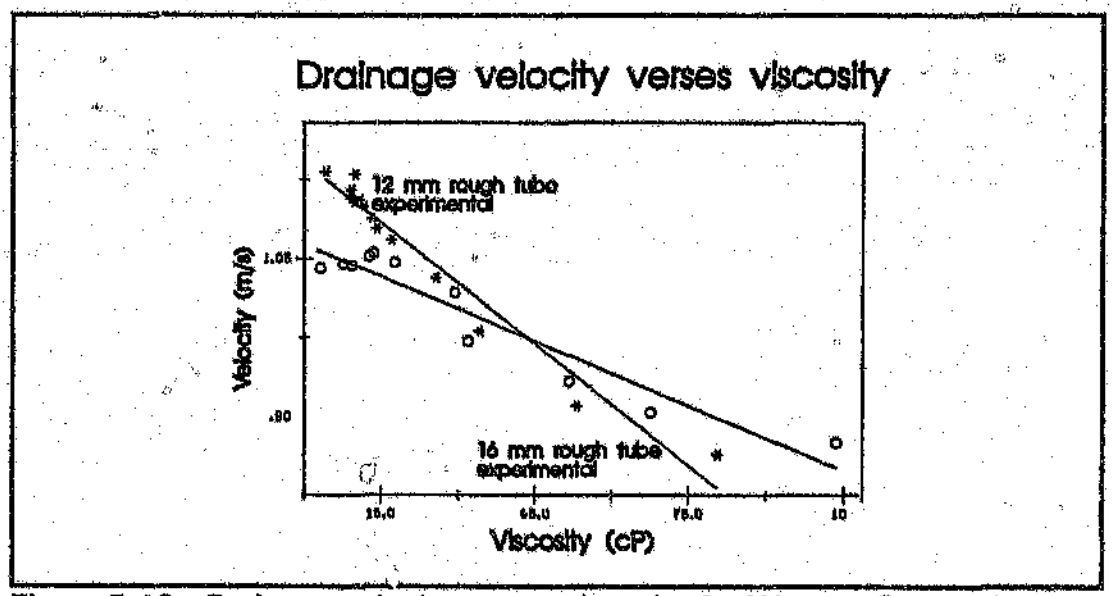


Figure 5.12 - Drainage velocity verses viscosity for Western Deeps slurry

Figure 5.12 shows drainage data from the Western Deeps mine slurry sample. This slurry consists of smaller particles and although there is quite a lot of scatter in the data the trend is clear and this verifies the fact that the lines cross indicating the transition from end effects dominating to viscous wall effects dominating.

5.4.3 Density measurement using the new "viscometer"

As discussed previously, the viscometer was fitted with a differential pressure cell from which the density of the slurry could be obtained. This data is plotted in figure 5.13 (where the theoretical density is plotted based on a solids density of 2650 kg/m^3 and data from two different batches of slurry is used to verify the reproducibility of the data). The results deviate slightly from those predicted using the percent solids, and density of the solids as can be seen from the figure below. This is attributed to the calibration of the differential pressure cell. It may also be an indication that the slurry is not satisfactorily mixed, but based on the clearly visible turbulence at all but the highest percent solids it is believed that this is not the cause of this deviation.

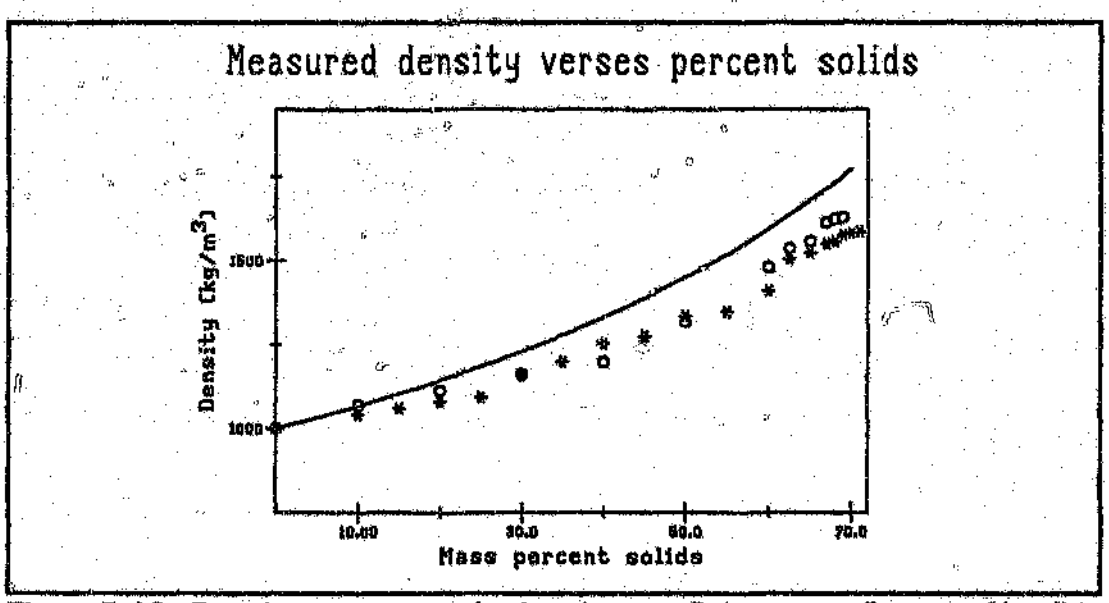


Figure 5.13 - Density as measured using the new "viscometer" verses % solids by mass

5.4.4 Drainage data from Western Deep Levels Gold Mine slurry

In figure 5.14 drainage data from a slurry obtained from the cyclone underflow at the Western Deeps mine is presented. Once again the inverse relationship is clearly noticeable. The average particle size for this slurry is lower than the slurry made up from the mine dump sand.

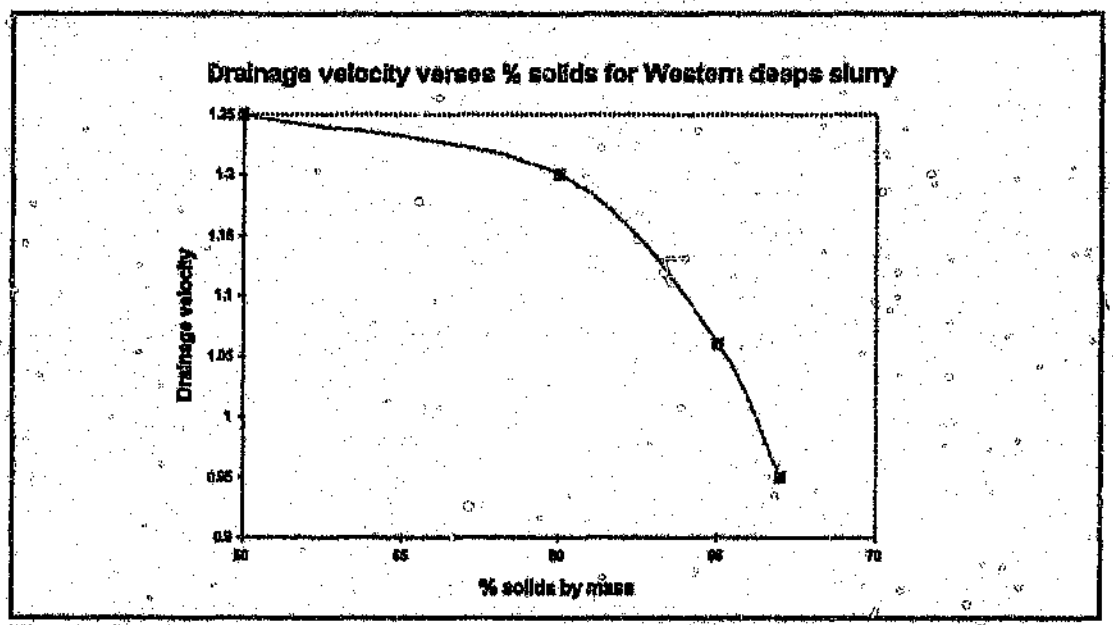


Figure 5.14 - Drainage data from a Western Deeps slurry sample

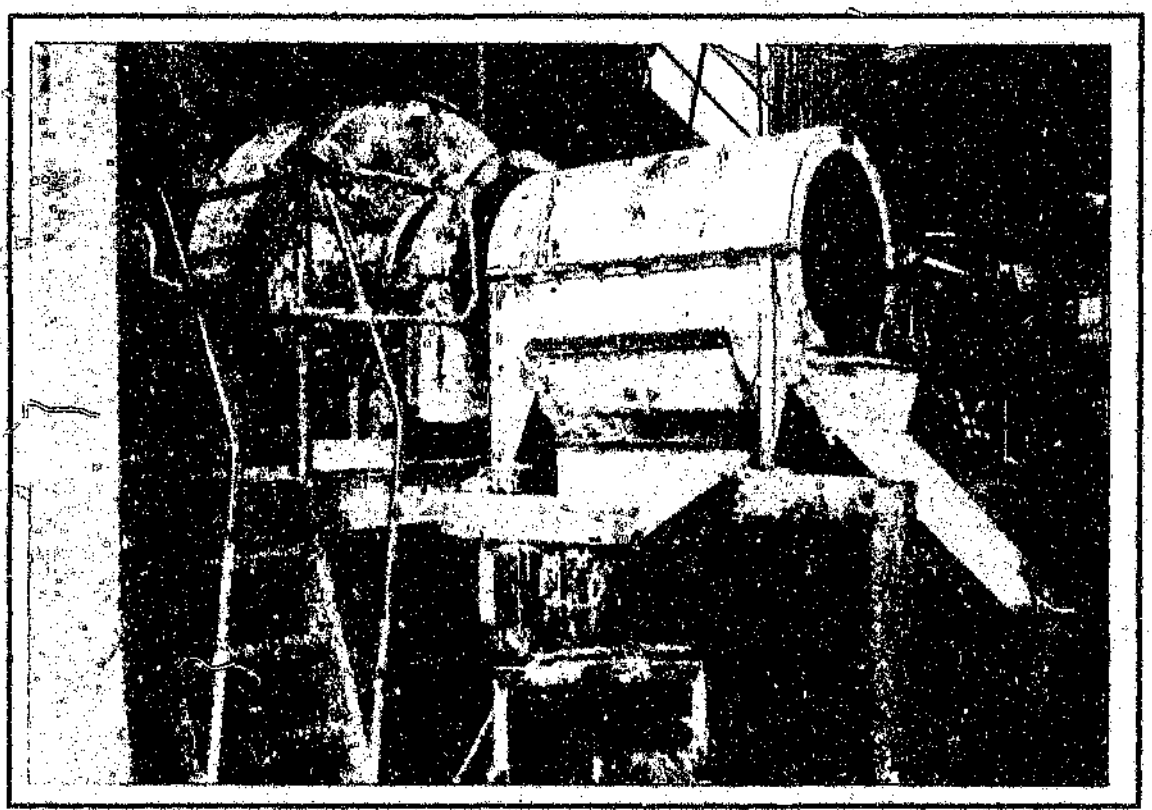
5.5 Conclusions

The viscometer seems to work satisfactorily in batch mode in the laboratory environment and it is possible to correlate viscosity with density and drainage velocities, but how would it perform in the industrial setting, operating in continuous mode? This is a question which will be looked at in chapter 6.

CHAPTER 6

PILOT MILL WORK

The ultimate test is in the field. Although pilot mills are not as demanding as the real thing, they are never-the-less similar in many ways to industrial scale mills and tests on a pilot mill would at least give an indication of the possibility of success.



The mill at Anglo American Research labs

6.1 Introduction

Tests were conducted at two pilot mills, one at the MINTEK research labs in Randburg, and one at Anglo's research labs at Gateway Industrial Park with varied results. The tests at the Anglo research pilot mill have not been completed and are ongoing and so I can only report the latest results on this mill.

6.2 Work conducted at MINTEK

Experimental work was conducted using a pilot scale mill at MINTEK. This work is examined in the following section.

6.2.1 Description of tests conducted on pilot ball mill

The mill used was a screen discharge pilot ball mill and the equipment was set up in such a way that the discharge of the mill flowed into the mixing tank (into which the tube viscometer is lowered) and then into the vertical spindle discharge pump as shown in figure 6.1. The effect that the mixing tank would have on the system would be to dampen the response by introducing a lag and a first order response. This is not ideal since changes in viscosity would not be seen as step changes, but the measurement would still be of value. The feed water to the mill was set at quite a low value (3 l/min), and then a step change was introduced in the feed water flow rate, by increasing the water flow rate to 9 l/min. After a period of time of about 30 minutes the water flow was again reduced to 3 l/min. Data was electronically captured all the time. The results of the test are discussed in th following section.

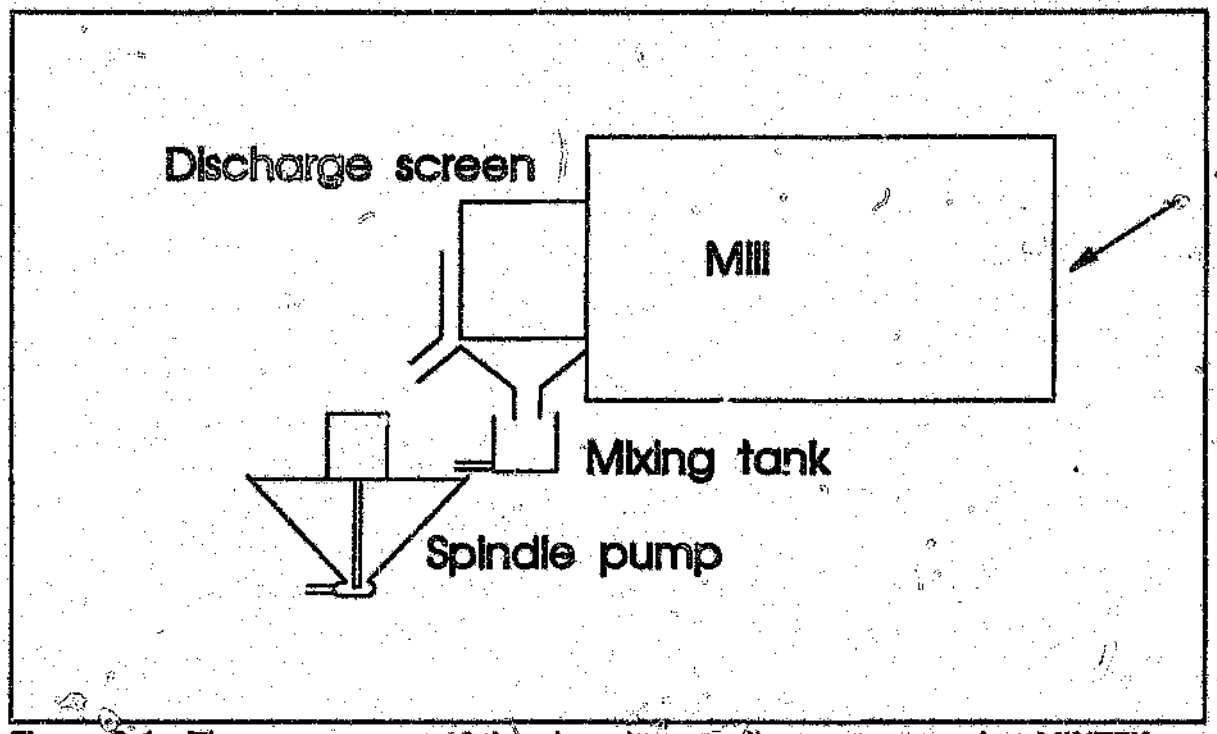


Figure 6.1 - The arrangement of the visco[illegible]pling system used at MINTEK

6.2.2 Discussion of results

The results of this test are presented in figures 6.2 and 6.3. Figure 6.2 Shows how the measured viscosity changed with time, and figure 6.3 shows the response of the measured density (also from our measurement device). It is clear that the measurement device is functioning, at least in that it gives an indication of the density and consistency of the slurry. In this respect the results are encouraging. Everything went well and the experiment was successful. The duration of the test was limited as the feed solids were being depleted fairly rapidly. It is clear from these results that there is a substantial lag in the response which was much larger than expected, since the volume of the mixer was only 5 litres and the flow rate of slurry varied between 5 and 15 l/min.

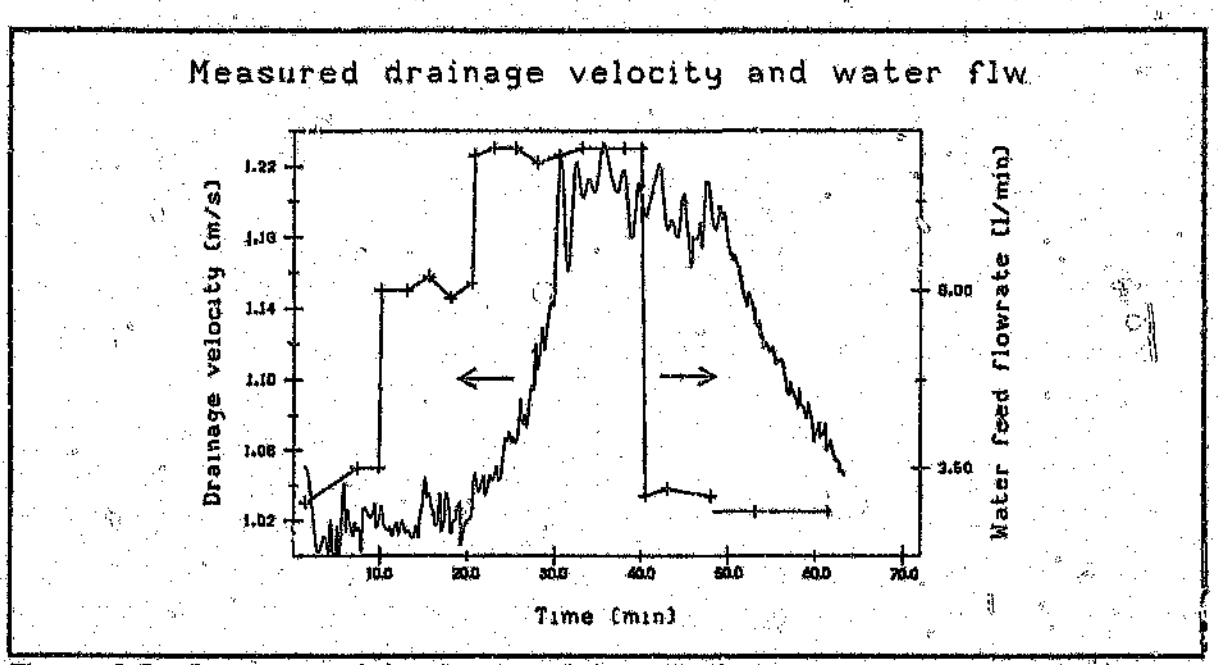


Figure 6.3 - Response of the density of the mill discharge to changes in feed water flow rate

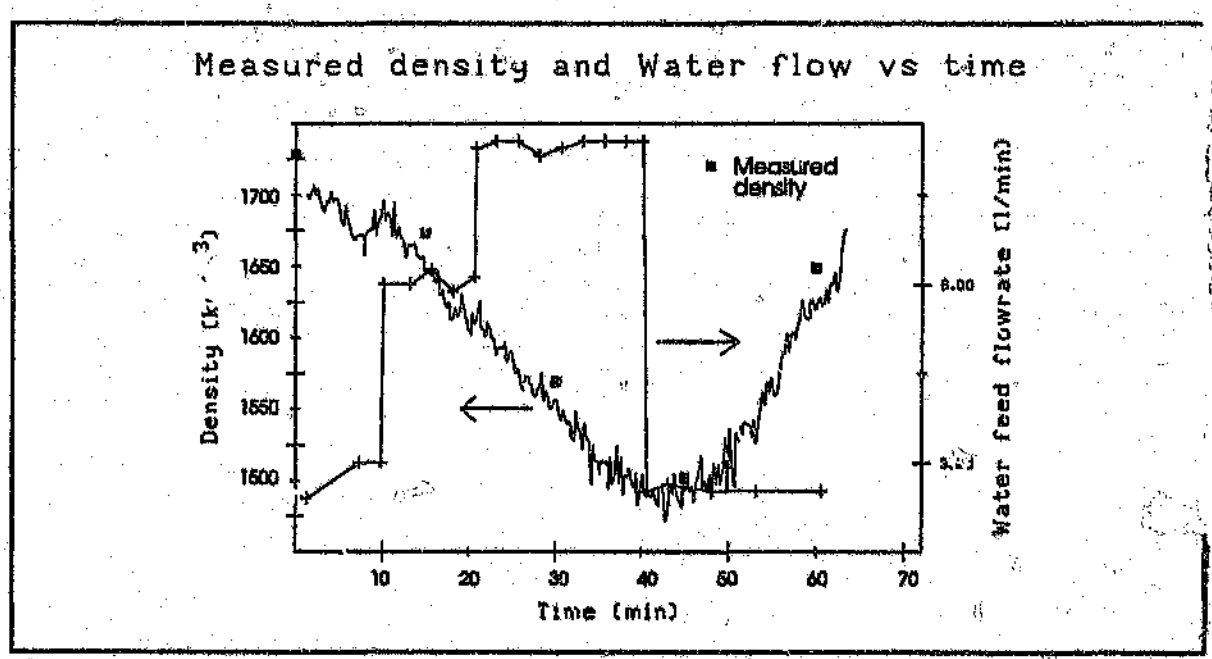


Figure 6.2 - Changes in apparent viscosity of the mill discharge and feed water flow with the progress of time

6.3 Work conducted at the Anglo American research pilot mill

Experimental work was attempted on a pilot scale mill at the Anglo research facilities. These tests are still in progress. There have been problems with the mixing tank. The slurry is very coarse and the motor bearings are effected by sand. Early indications, from attempted experimental work, which did yield a few minutes of data, are that these problems can be overcome. There were however no useful results to report at the time of writing.

6.4 Conclusions

The device shows promise on pilot scale mills. The real test would be on an industrial mill. The main problem is associated with sampling the stream - creating a level of slurry into which the viscometer can be immersed. The viscometer may choke up on large particles (particles larger than 5 mm) but some simple device may be used to prevent such particles entering the tube. The biggest problem to overcome would be that of designing a sampling system for the viscometer which could present the device with a level of slurry from which a representative sample could be drawn which is free of large particles. If this can be done, the device could probably be successfully used in industry.

CHAPTER 7

CONCLUSIONS

In this chapter we summarise the results of the research and discuss the potential of the measurement device. The salient points in this thesis are highlighted.

7.1 Benefits of this research

This research has gone a long way in the development of a potentially very useful concept, a viscometer suitable for use with slurries, and capable of operating in an industrial environment. Further tests remain to be conducted, the main obstacle being the design of a sampling system, to create a level of slurry from which a representative sample may be drawn. This problem is not insurmountable, and no doubt, with further research will also be solved.

The results obtained using this viscometer show that it does work, with slurries of particle size of less than 600 microns. Particles larger than 5 mm in size seem to cause a 16 mm diameter tube to block sporadically (based on experience from the Anglo American reseasrch mill), so with such a system, some sort of separation device will be required on the feed to the viscometer.

7.2 Interesting points to note

The importance of slurry rheology in milling was made clear, and it was confirmed that such a measurement need not be very sensitive, since in the viscosity range of operation of most mill discharge streams, a 1% change in solids content results in about a 30% change in viscosity. This shows how much more sensitive a viscosity measurement is as opposed to a percent solids or density measurement.

The fact that this is only an apparent viscosity at a fixed shear rate does reduce the value of the measurement. If different shear rates were needed they could be obtained by imposing different overall positive pressures across the viscometer during the drainage cycle. This would however complicate the device and the necessity of such information is questionable.

With correct calibration the density measurement on the device will also prove to be

useful. The measurement is reproducible under most conditions, and is not an expensive option.

7.3 Concluding comments

We have achieved all the objectives stated in the introductory chapter, namely by : Gaining a broad understanding of the field, developing the viscometer and density meter almost to prototype stage, producing analytical models to describe its operation and testing the device on a pilot mill.

We have, in principle a simple device which gives an apparent viscosity and density of the slurry being sampled, on an on-line basis. The vis- -ter can sample at a frequency of about once every 6 seconds, which sufficient for the control and monitoring of the discharge stream of . This -ometer could also be used to measure the density and viscosity of slurries in other applications, such as in floatation circuits, classification operations and many other minerals processing operations. The main problem to overcome is devising a mechanism which will produce a level of liquid from which the viscometer could take a representative sample, and this can be achieved with further experimentation.

References

Abbas M. A. and Crowe C. T, Experimental Study of the flow properties of a homogeneous slurry near transitional Reynolds numbers. *Rheologica Acta*, 3 1987. pp 357 - 364.

Baille D. S. and Moys M. H, The measurement and control of the slurry rheology from the discharge of a rotary grinding mill. *Proceedings, 7th National meeting of the South African Institution of Chemical Engineers, Esselen Park, August 1994.* pp 356 - 364.

Baille D. S. and Stewart M, Investigation of the on-line measurement of slurry viscosity. *Unpublished work - WITS University Department of Chemical Engineering 1992.*

Bird R. B, The equations of change and the macroscopic mass, momentum and energy balances. *Chemical Engineering Science*, 6 1957, pp 123 - 131.

Blaszczyk J. and Petela R, Application of a modified rotary rheometer to the investigation of slurries. *Rheologica Acta*, 25 1986. pp521-526.

Bourne, J.R and Sharma, R.N , *Chemical Engineering Journal*, October 1 1984, pp 79 - 83

Boyes J. M, Field testing of on-line slurry measurement technique at Savage river mines. *M.D. Research Company report no. I-MDC16-26*, Oct 1978

Cheng D. C, Further observations on the rheological behaviour of dense suspensions. *Powder Technology*, 37 1984, pp 255-273.

Clarke B, Rheology of course settling suspensions. *Trans. Instn Chem. Engrs*, 45 1967, pp 251-256.

Cohen Y. and Metzner A. B, An analysis of apparent slip flow of polymer solutions. *Rheologica Acta*, 25 1986, pp 28-35.

Dabak T. and Yucel O, Shear viscosity behaviour of highly concentrated suspensions at low and high shear rates. *Rheologica Acta*, 25 1986, pp 527-533.

Dealy J. M, Online measurement of liquid properties. *Chemical Engineering*, Oct 1984, pp 61 - 70.

Downard S., Barley R. W. and Wills B. A, The influence of physical parameters on viscosity measurement in dense media separation. *Dense Medium Operators Conference*, July 1987, pp225-233;

Dutta A, A note on capillary viscometer theory: start-up flow contribution, *Rheologic Acta*, 25 1986, pp 191-194.

Hansford G. S, Levy C. D. and De Kock J. W, Rheological measurements on pulps from South African gold mines. SAIMM Journal, March 1976, pp 363-369.

Hemmings C. E. and Boyes J. M, An On-Line Viscometry Technique for Improved Operating and control of Wet Grinding Circuits. *XIIth International Mineral Processing Congress*, 1977, pp 3-22.

Herbst J. A, The Economic Benefits of Comminution system optimization. *7th European Symposium on Comminution* Part 1, June 1990, pp 37-53.

Jeffery D. J. and Acrivos A, The Rheological Properties of Suspensions of Rigid Particles. AIChE Journal, May 1976, 22, pp 417-432.

Jinescu V. V, The rheology of suspensions. *International Chemical Engineering*, 14 1974, pp 397-420.

Jones R. L. and Chandler H. D, The effect of drag-reducing additives on the rheological properties of silica-water suspensions containing iron(III) oxide and of a typical gold-mine slurry. *SAIMM Journal*, June 1989, pp 187-189.

Kawatra S. K. and Eisele T. C, Rheological Effects in Grinding Circuits. *Mineral processing*, 22 1988, pp 251-259.

Klimpel R. R, Influence of material breakage properties and associated slurry rheology on the breakage rates on wet grinding of coal/ores in tumbling media mills. *Ind. Eng. Chem. Process Des. Dev.*, 18 no.4 1979, pp 265-270.

Laapas H. R ,Viscosity measurement of fast settling mineral suspensions with a modified capillary tube viscometer ,*Proceedings, International Symposium on powder technology*, 81 1982, pp 216-223.

Madersloot W G B and Scott K J, Rheology of particle suspensions. *Technicom Consultancy report*, 1979, p 1-10.

Mcauly M. and Moys M. H, Effect of slurry percent solids on milling efficiency at RM3's Crown mines plant, *Project Report*, pp 1-6.

Marsden D. D, The effect of pH value, temperature and density on the kinematic

viscosity of some South African gold mine slurries. *Journal of the S.A.I.M.M.*, January 1962, pp 391-398.

Montani A. and Moys M. H, The measurement of rheological properties inside a grinding mill. *SAIMM Journal*, 88 no. 6, June 1988, pp 199-206.

Moys M. H, Measurement of slurry properties and load behaviour in grinding mills. *Paper presented at the first IFAC workshop in applied measurements in mineral and metallurgical processing, Sabi-Sabi Game reserve*, October 1988.

Moys M. H, Slurry rheology - the key to further advance in Grinding Mill Control. *SAG Bulletin, Department of Mining and Mineral Process Engineering - University of British Columbia*, 1989, pp 713-727.

Moys M. H, The use of conductivity measurements in the control of grinding mills. *CIM Bulletin*, 80 November 1987, no.907, pp 52-56.

Nguyen Q. D. and Boger D. V, Measuring the flow properties of yield stress fluids. *Annual Review of Fluid Mechanics*, 24, 1992, pp 47-88.

Oldshue, J.Y. *Fluid mixing technology*, McGraw-Hill, 1983.

Reeves, T. J, On-line viscometer for mineral slurries. *Transactions of the Institution of mining and Metallurgy*, 94 December 1985, pp C201-C208.

Skubink M. and Peters D. L, Rheology of Non-Newtonian Fluids - review with a special reference to particle suspensions. *CSIR Review*; June 1992;

Tangsathitkulchai C, Slurry density effects on ball milling in a laboratory ball mill. *Powder Technology*, 59 1989, pp 285-293.

Tangsathitkulchai C. and Austin L. G, Rheology of concentrated Slurries of particles of Natural size distribution Produced by grinding. *Powder Technology*, 56 1988, pp 293-299.

Thomas A D and Cowper T C, Rheology and the CIP process and the Benefits of On-Line Viscosity Monitoring and Control. *RANDOL report, Sacramento 1989*, pp 281-284.

Vermeulen L. A, Ohlson de Fine M J, and Schakowski F, Physical information from the inside of a rotary mill. *SAIMM Journal*, 84, no. 8, August 1984, pp 247-253.

Valentyik L, Continuous measurement of consistency of ferrosilicon/magnetite suspension in a drum type heavy media plant. *National Sand and Gravel Association circular no, 106*, April 1970.

Whitten W, Steffens P and Hitchins J, An Examination of the pulp viscosity in tubes at higher shear rates. *Minerals Engineering*, 6, No. 4, 1993, pp 397-404.

Appendices

Appendix A - Listing of main elements of Pascal program

```
{ $m 3200,0,655360 } { Allocate extra space on the stack }
{$N+,E+}        { 8087 Emulation on, disable software Emulation }
{$S+}           { Stack checking on }
{$I+}           { Error trapping on }
{$G+}           { Generates 80286 instructions - for 80286 only }
{$A+}           { Align vars and constants on word boundaries }

PROGRAM Viscous;
{ Written By     : Darrell Bailie
                   University of the Witwatersrand
                   Johannesburg
  Date (ver 1)   : December 1993
  Current Version : 2.8
  LAST REVISED   : 12/94                                    }

USES printer,rtscreen, rtgraph,graph, rtstdhdr, rtgsubs, rtchart, dos, crt, pc30;

TYPE array1 = ARRAY[1..16] OF INTEGER;
     array2 = ARRAY[0..2550] OF INTEGER;
     array3 = ARRAY[0..500] OF INTEGER;
     array4 = ARRAY[1..20] OF SINGLE;

CONST
  badd          =   $700;
  TotNumSamples =   2500;  {number of samples taken for all chanels}
  NoOfChanels   =   5;

VAR
  Chanels       :   array1;   { list of chanels to monitor }
  all_data      :   array2;   { raw data from all the chanels }
  steps         :   array4;   { time data at each step }
  Position      :   array4;
```

```
  delta_time, vel, viscosity   :    REAL;
  pos,fil,num,density:    INTEGER;
  plot              :    STRING;
  hour,minute,second,sec100 : WORD;

  lc, lf            : rtintarraytype;   {line colors & styles}
  tags              : tagarraytype;     {tag names}
  yvalues           : rtvaluearraytype; {hold current R-T value}
  yvalues1          : rtvaluearraytype; {hold current R-T value}
  ydata             : ARRAY[0..1000] OF RealType; {random data}
  title             : titletype;        {scroll graph title}
  units             : tagtype;          {scroll graph units}
  mtchf             : BOOLEAN;          {staircase method}
  timeint, sampleint, miny, maxy    : RealType;
  rt, lalarm, halarm, stpnt, pinum  : RealType;
  nt, grid, xdecs, ydecs, i         : INTEGER;
  tch                               : string[5];
  index             : LONGINT;

{=============================================================}

PROCEDURE clear_data {fills the data array with zeros};

VAR i : INTEGER;

BEGIN
  FOR i:=1 TO TotNumSamples DO
     all_data[i]:=0;
END;
{=============================================================}
PROCEDURE Get_time(VAR time : REAL ); {gives time in seconds}

VAR  hour,minute,second,sec100 : WORD;
```

```
BEGIN
  GetTime(hour,minute,second,sec100);
  time := (hour*3600 + minute*60 + second + sec100/100)*1000;
END;
{=============================================================}
PROCEDURE ver_chk {checks data aquisition card};

VAR
  r     :  REAL;
  i,k   :  INTEGER;
  quit_f :  BOOLEAN;

BEGIN
   k := diag;
   i := version;
   r := hi(i) + lo(i)/100;
   GotoXY(22, 2);
   WRITELN('PC-30/PC-126 Driver version ', r:4:2);
   quit_f := false;
   if k <> 0 then begin
       writeln;
         writeln('PC-30 dignostics report A/D not installed or other fault.');
       quit_f := true;
   end;
end;
{=============================================================}
PROCEDURE read_data; {reads data from the list in the variable channels...}
                          {taking a fixed number of samples set by TotNumSamples}   {and also calculates
                        the tome increments}

VAR
i,j,m,presclr,nclock  : INTEGER;
time0,time, freq      : REAL;
```

```
BEGIN
    presclr:=20;
    aclock:=60;
    FOR i:=0 TO 15 DO set_gain(i,0);
    ad_prescaler(presclr);
    ad_clock(aclock);
    freq:=2000000/(presclr*aclock);
    rtc_off;
    m := m_chan(Chanels, TotNumSamples, all_data[1]);
    rtc_on;
    delta_time := 1/freq;
END;
{=========================================================}
Procedure OPEN_CLOSE_valve(chnl,value:integer);
{opens or closes the solenoid valves, depending on the integer Value}

BEGIN
  d_mode(0,0,0);
  d_out(chnl,value);
END;
{=========================================================}
PROCEDURE SingleChannelSample(channel_no,no_samp:INTEGER);
{Takes a set number of samples from a single analogue chanel}
VAR i,k, presclr, aclock : INTEGER;

BEGIN
    presclr:=20;
    aclock:=100;
    FOR i:=0 TO 15 DO set_gain(i,0);
    ad_prescaler(presclr);
    ad_clock(aclock);
    FOR i:=0 TO 15 DO set_gain(i,0);
    k:=S_Chan(channel_no,no_samp,all_data[0]);
```

```
END;
{=========================================================================}
PROCEDURE GetDensity(HeightOfFluid {cm}:INTEGER;VAR Density {kg/m3}:INTEGER);
  forward;
{=========================================================================}
PROCEDURE Sample;
{the main sampling routine - operates the viscometer}
  VAR average, new_average : integer;

BEGIN
  open_close_valve(0,0);          {close atmospheric}
  gotoxy(2,12);
  writeln('Valve #2 is closed');
  SingleChannelSample(10,6);
  average:=round((all_data[0]+all_data[1]+all_data[2]+all_data[3])/4);
  open_close_valve(0,8);          {open vaccume}
  gotoxy(2,12);
  writeln('Valve #1 is open   ');
   REPEAT
     gotoxy(20,12);
     writeln('.');
     SingleChannelSample(10,6);
     new_average:=round((all_data[0]+all_data[1]+all_data[2]+all_data[3])/4);
   UNTIL (average>(new_average+50));
  WRITELN;
  open_close_valve(0,0);
  gotoxy(2,12);
  writeln('Valve #1 is closed');  {close vaccume}
  delay(3000);
  GetDensity(87,density);
  open_close_valve(0,16);
  gotoxy(2,12);
  writeln('Valve #2 is open');    {open atmospheric}
```

```
  read_data;
END;

{=========================================================}
PROCEDURE initialise;
{ initialises PC 30 card}
BEGIN
 set_base(badd);
 ver_chk;
 init;
END;

{=========================================================}
PROCEDURE select_channels;
{generates a list of chanels to be sampled}
BEGIN
 chanels[1]:=2;
 chanels[2]:=3;
 chanels[3]:=4;
 chanels[4]:=5;
 chanels[5]:=6;
 chanels[6]:=16;
END;
{=========================================================}
PROCEDURE get_steps;
{Locates where the step changes in each chanel and makes sure there are }
{only 5 steps in total}
VAR
 ChanelNumber,YValue,i,j,counter    : INTEGER;

 BEGIN
  counter:=1;
  FOR ChanelNumber:=1 to NoOfChanels DO
```

```
    BEGIN
      i:=ChanelNumber;
      j:=ToNumSamples+ChanelNumber-100;
      YValue:=round((all_data[i]+all_data[j])/2);
      REPEAT
         counter:=counter+5;
      UNTIL((all_data[counter]>YValue) OR (counter>2500));
      IF Counter>2500 THEN
        BEGIN
          gotoxy(2,14);
          WRITELN('Step # ',ChanelNumber,' not found');
          SOUND(1000);
          DELAY(2000);
          NOSOUND;
        END
      ELSE
        BEGIN
          gotoxy(2,14);
          writeln('Step found on Chanel no.:',ChanelNumber,' at time = ',
              counter*delta_time:5:3,' and position = ',counter);
          Position[ChanelNumber]:=counter;
          Steps[ChanelNumber]:=counter*delta_time;
          counter:=counter+1;
        END;
    END;
  END;
{=========================================================}
PROCEDURE save_steps(k:INTEGER);
{writes the steps to a file}
VAR
 i,j          : INTEGER;
 f            : TEXT;
 filename,no  : STRING;
```

```
BEGIN
  str(k,no);
  filename := 'c:\kinross\S30'+no+'.dta';
  gotoxy(2,12);
  writeln('Saving data to file :',filename);
  ASSIGN(f,filename);
  REWRITE(f);
  WRITELN(f,1);
  WRITELN(f,5);
   FOR i:= 1 to 4 do
    BEGIN
      WRITELN(f,steps[i]:6:3,' ',(1-0.2*(i-1)):4:2);
    END;
   WRITELN(f,'Time = ',hour,':',minute,':',second);
   WRITELN(f,'Density = ',density,' kg/m3');
   WRITELN(f,'Drainage Velocity = ',vel:6:2,' m/s');
   WRITELN(f,'Apparent Viscosity = ',viscosity:6:2,' cP');
  CLOSE(f);
END;
{=========================================================}
PROCEDURE show_steps;
VAR
i           : INTEGER;
BEGIN
    WRITELN(lst,'Run number =',fil);
    WRITELN(lst,'Average Velocity (m/s) = ',vel:4:3);
    WRITELN(lst,'Time (s)      Height(m)');
   FOR i:= 1 to 5 do
    BEGIN
      WRITELN(lst,steps[i]:5:3,'       ',(1-0.2*(i-1)):4:2);
    END;
    WRITELN(lst);
END;
```

```
{=========================================================}
Procedure GetAvgVelocity(VAR velocity : real);
{calculates the average velocity from the slope of the best fit straight line using least squares}
VAR   i  : INTEGER;
      SigmaX,SigmaY,SigmaXY,SigmaXSqr : REAL;
CONST ho=1;
      n=4;
BEGIN
 SigmaX:=0;
 SigmaY:=0;
 SigmaXY:=0;
 SigmaXSqr:=0;
  FOR i:=1 TO n DO
  BEGIN
    SigmaX:=SigmaX+steps[i];
    SigmaY:=SigmaY+ho+(1-i)*0.2;
    SigmaXY:=(SigmaX+steps[i])*(SigmaY+ho+(1-i)*0.2);
    SigmaXSqr:=(SigmaX+steps[i])*(SigmaX+steps[i]);;
  END;
 Velocity:=(n*SigmaXY-SigmaX*SigmaY)/(n*SigmaXsqr-SigmaX*SigmaX);
END;
{=========================================================}
PROCEDURE Getviscosity(velocity:real; Var viscosity:real);
{calculates the viscosity from the velocity}
 BEGIN
  viscosity:=952-1578*velocity+657*velocity*velocity;
  {WRITELN('Viscosity (cP) =',viscosity);}
 END;
{=========================================================}
PROCEDURE GetDensity(HeightOfFluid {cm}:INTEGER;VAR Density
{kg/m3}:INTEGER);
{Calculates the density from the pressure in the tube}
VAR i : INTEGER;
```

```
    Pressure,cmH2O: REAL;
CONST constant1=0.21856;
      constant2=-224.18;
  BEGIN
    Pressure:=0;
    cmH2O:=0;
    SingleChannelSample(13,100);
    FOR i:=0 TO 99 DO
      BEGIN
        cmH2O:=cmH2O+All_Data[i];
      END;
    cmH2O:=(cmH2O/100)*Constant1+Constant2;{Callibration and units}
    cmH2O:=cmH2O+2.5;
    Pressure:=10*9.8*cmH2O;
    writeln('height of water = ',cmH2O:6:2);
    Writeln('Pressure (Pa) = ',Pressure:6:2);
    Density:=ROUND(Pressure*100/(9.8*HeightOfFluid));
    Density:=round(0.68*density+724);}
    Writeln('Density(kg/m3) = ',Density);
    Writeln('Press enter to continue');

  END;
{=========================================================}
PROCEDURE ShowData;
{ displays the data on screen}
 BEGIN
   GOTOXY(2,3);
   WRITELN('Run no = ',fil);
   WRITELN('Time = ',hour,':',minute,':',second);
   WRITELN('Density = ',density:6,' kg/m3');
   WRITELN('Drainage Velocity = ',vel:6:2,' m/s');
   WRITELN('Apparent Viscosity = ',viscosity:6:2,' cP');
END;
```

```
{=========================================================}
Procedure LogToFile(Viscosity : REAL; Density : INTEGER);
{ writes data to a file with the current date in the file name. If that  }
{file exists it appends the file}
 VAR  vis,den                  : TEXT;
     file1,file2,no1,no2       : STRING;
     Year,Month,Day,DayOfWeek,
     Hour,minute,second,sec100  : Word;
 BEGIN
  GetDate(Year,Month,Day,DayOfWeek);
  GetTime(Hour,minute,second,sec100);
  str(month,no1);
  str(day,no2);
  file1 := 'c:\anglo\vis'+no1+'_'+no2+'.dta';
  file2 := 'c:\anglo\den'+no1+'_'+no2+'.dta';
  ASSIGN(vis,file1);
  ASSIGN(den,file2);
    {$I-} APPEND(vis);
          APPEND(den); {$I+}
    IF ioresult<>0 THEN
     BEGIN
       REWRITE(vis);
       REWRITE(den);
     END;
    WRITELN(vis,fil,' ',Hour:2,' ',minute:2,' ',second:2,' ',Viscosity:6:3);
    WRITELN(den,fil,' ',Hour:2,' ',minute:2,' ',second:2,' ',Density);
    CLOSE(vis);

    CLOSE(den);
  END;
{=========================================================}
Procedure SetUpGraph;
{sets up the scrol' graph for real time graphics}
```

```
begin
 { INITIALIZE THE GRAPHICS ADAPTER,
   SET UP 2 REAL TIME WINDOWS}
 rtinitgraphics(defaultbgidir,2,1);

 { RESIZE 2 WINDOWS }
 rtsetpercentwindow(rtstat[0],0.01,0.01,0.99,0.49);
 rtsetpercentwindow(rtstat[1],0.01,0.50,0.99,0.99);
 { VALUES FOR LIMITS }
 timeint := 30.0;  sampleint := 0.2;  miny := 0.0;
 maxy := 500.0;   rt := 0.75;  nt := 1;
 grid := 10;      lalarm := 0;    halarm := 0;
 stpnt := 0;  ratchf := FALSE;
 {tags[0] := 'Viscosity';
 tags[1] := 'Density';}
 lc[0]:=1;
 lf[0]:=0;
  rtinitwindowcolors(rtstat[0],7,0,1,4,15,15,15);
  rtinitwindowcolors(rtstat[1],7,0,1,4,15,15,15);
  { REFER TO EACH OF THE FOLLOWING FUNCTIONS IN THE
   USER DOCUMENTATION FOR A COMPLETE DESCRIPTION OF
   SPECIFIC PARAMETERS }
   rtsetupscrollgraph(rtstat[0],timeint, sampleint, 0, 200, rt,
                      nt, grid, lalarm, halarm, stpnt, 1,1,'Viscosity', 'cP',
                      tags, lc, lf, ratchf); {viscosity}
   rtsetupscrollgraph(rtstat[1],timeint, sampleint, 1000, 1700, rt,
                      nt, grid, lalarm, halarm, stpnt, 1,0,'Density', 'kg/m^3',
                      tags, lc, lf, ratchf);  {density}

  { PUT A BORDER AROUND THE WINDOWS }
   rtborderwindow(rtstat[0],15);
   rtborderwindow(rtstat[1],15);
END;
```

```
{=========================================================}
 Procedure Graph_update;
{updates real time scrol graph}

 begin
   yvalues[0]:=viscosity;
   yvalues1[0]:=density;

 { DISPLAY RANDOM DATA, UPDATE GRAPHS ACCORDING TO PARAMETERS
    SET IN SCROLL SET UP CALLS }
     rtupdatescrollgraph(rtstat[0],yvalues);      {UPDATE EACH WINDOW}
     rtupdatescrollgraph(rtstat[1],yvalues1);     {UPDATE EACH WINDOW}
   INC(index,1);
END;
{=========================================================}
BEGIN {main program body}
  clrscr;
  num:=0;
  fil:=0;
  index:=0;
  SetUpGraph;
  Initialise;
  select_channels;
  clear_data;
 REPEAT
    fil:=fil+1;
    Sample;
    GetTime(hour,minute,second,sec100);
    get_steps;
    GetAvgVelocity(vel);
    GetViscosity(vel,viscosity);
    Graph_update;
    open_close_valve(0,0);
```

```
    LogToFile(Viscosity,Density);
    delay(2000);
  UNTIL ((keypressed));
    rtclosegraphics(1);
END. {main program}
```

Appendix B - Table of viscosities of glycerol solutions

23 GLYCEROL, $CH_2OHCHOHCH_2OH$—(Continued)

A % by wt.	ρ D_4^{20}	D_4^{25}	C_1 g/l	M g-mol-1	C_n g/l	$(C_n - C_1)$ g/l	$(\eta - \eta_0)$ × 10^4	n	λ °C	Q Oslag	S g-mol/l	η_{rel}	η_{sp} cS	ϕ rhe	γ mmho-cm	T g-mol-1
5.00	1.0097	1.0115	50.5	0.348	459.2	39.0	58	1.3368	1.078	0.580	0.315	1.125	1.116	88.71		
6.00	1.0130	1.0138	60.7	0.639	951.3	46.9	70	1.3400	1.316	0.708	0.385	1.155	1.143	86.44		
7.00	1.0144	1.0162	71.0	0.771	943.4	54.9	82	1.3412	1.561	0.829	0.457	1.166	1.171	84.17		
8.00	1.0167	1.0185	81.3	0.88	935.6	62.9	94	1.3424	1.811	0.974	0.530	1.218	1.201	81.90		
9.00	1.0191	1.0209	91.7	0.94	927.8	70.9	106	1.3436	2.064	1.110	0.603	1.253	1.232	79.67		
10.00	1.0215	1.0233	102.1	1.109	919.5	[illegible]	118	1.3448	2.323	1.249	0.678	1.288	1.263	77.48		
12.00	1.0262	1.0281	123.1	1.337	903.1	95.1	142	1.3472	2.880	1.548	0.837	1.362	1.330	73.28		
14.00	1.0311	1.0329	144.4	1.568	886.7	111.5	167	1.3496	3.469	1.865	1.004	1.442	1.401	69.22		
16.00	1.0360	1.0378	165.8	1.800	870.2	128.0	191	1.3521	4.094	2.201	1.177	1.530	1.480	65.22		
18.00	1.0409	1.0428	187.4	2.035	853.6	144.7	217	1.3547	4.756	2.557	1.359	1.627	1.566	61.34		
20.00	1.0459	1.0478	209.2	2.272	836.8	161.5	242	1.3572	5.46	2.93	1.546	1.734	1.661	57.56		
24.00	1.0561	1.0580	255.5	2.752	802.6	195.6	294	1.3624	7.01	3.77	1.944	1.984	1.882	50.31		
28.00	1.0664	1.0683	298.6	3.243	767.8	230.4	347	1.3676	8.77	4.71	2.370	2.274	2.138	43.89		
32.00	1.0770	1.0789	344.8	3.742	732.3	265.9	400	1.3730	10.74	5.78	2.814	2.633	2.449	37.91		
36.00	1.0876	1.0896	391.5	4.252	696.1	302.2	455	1.3785	12.96	6.97	3.276	3.082	2.819	32.36		
40.00	1.0984	1.1003	439.4	4.771	659.0	339.2	511	1.3841	15.50	8.33	3.757	3.646	3.326	27.37		
44.00	1.1092	1.1112	488.1	5.300	621.2	377.1	567	1.3897				4.434	4.003	22.81		
48.00	1.1200	1.1220	537.6	5.838	582.4	415.8	624	1.3954				5.402	4.833	18.47		
52.00	1.1308	1.1328	588.0	6.385	542.8	455.4	681	1.4011				6.653	5.895	15.00		
56.00	1.1419	1.1439	639.4	6.944	502.4	495.8	739	1.4069				8.332	7.311	11.98		
60.00	1.1530	1.1551	691.8	7.513	461.2	537.0	799	1.4129				10.66	9.264	9.36		
64.00	1.1643	1.1663	745.1	8.091	419.1	579.1	859	1.4189				13.63	11.73	7.32		
68.00	1.1755	1.1775	799.3	8.680	376.1	622.1	919	1.4249				18.42	15.70	5.42		
72.00	1.1866	1.1887	854.3	9.277	332.2	666.0	980	1.4310				27.57	23.28	3.62		
76.00	1.1976	1.1997	910.2	9.883	287.4	710.8	1040	1.4370				40.49	33.88	2.46		
80.00	1.2085	1.2106	966.8	10.498	241.7	756.5	1101	1.4431				59.78	49.57	1.67		
84.00	1.2192	1.2214	1024.2	11.121	195.1	803.2	1162	1.4492				84.17	69.18	1.19		
88.00	1.2299	1.2320	1082.3	11.752	147.6	850.7	1223	1.4553				147.2	119.9	0.88		
92.00	1.2404	1.2426	1141.1	12.392	99.2	899.0	1284	1.4613				363.7	310.0	0.36		
96.00	1.2508	1.2530	1200.7	13.039	50.0	948.3	1344	1.4674				778.9	624.0	0.13		
100.00	1.2611	1.2633	1261.1	13.694	0.0	998.2	1405	1.4735				1759.6	1398.1	0.06		

Viscosity data for glycerol solutions (CRC Handbook)

Appendix C - Size distribution data

MALVERN MasterSizer 3.01 Easy Mode Tue 1 Jan 1980 3:10 am

Upper Size	% in	Lower Size	% under	Upper Size	% in	Lower Size	% under
		600	100	31.0	0.3	25.5	4.3
600	1.1	492	98.9	25.5	0.4	20.9	3.9
492	1.3	404	97.6	20.9	0.4	17.1	3.5
404	1.9	332	95.7	17.1	0.4	14.1	3.1
332	3.2	272	92.5	14.1	0.4	11.6	2.7
272	5.8	224	86.7	11.6	0.4	9.48	2.3
224	9.4	183	77.2	9.48	0.4	7.78	1.9
183	13.2	151	64.1	7.78	0.4	6.39	1.6
151	15.2	124	48.8	6.39	0.3	5.24	1.3
124	14.7	101	34.2	5.24	0.3	4.30	1.0
101	11.8	83.3	22.4	4.30	0.2	3.53	0.8
83.3	8.1	68.3	14.3	3.53	0.2	2.90	0.6
68.3	4.8	56.1	9.5	2.90	0.2	2.38	0.4
56.1	2.6	46.0	6.9	2.38	0.1	1.95	0.3
46.0	1.3	37.8	5.6	1.95	0.1	1.60	0.2
37.8	0.8	31.0	4.8	1.60	0.1	1.32	0.1

Result source=Sample
Record No. = 0
Focal length = 300 mm.
Presentation =0903
Volume distribution
Beam length = 2.2 mm.
Obscuration =0.2011
Volume Conc. = 0.1982 %
Residual = 0.245%
Model inup

D(v,0.5) = 125.35 µm
D(v,0.9) = 291.16 µm
D(v,0.1) = 56.51 µm
D(4,3) = 139.45 µm
D(3,2) = 94.47 µm
Span = 1.6
Spec. surf. area
0.1004 sq.m./cc.

Type 'q' to quit, any other key to toggle graph/result display.

Size distribution data for Western Deeps slurry

MALVERN MasterSizer 3.01 Easy Mode Tue 1 Jan 1980 0:26 am

Upper Size	% in	Lower Size	% under	Upper Size	% in	Lower Size	% under
		600	100	31.0	0.2	25.5	2.6
600	6.4	492	93.6	25.5	0.2	20.9	2.4
492	6.6	404	86.9	20.9	0.2	17.1	2.2
404	8.3	332	78.6	17.1	0.2	14.1	2.0
332	11.	272	67.4	14.1	0.2	11.6	1.7
272	14.8	224	52.6	11.6	0.3	9.48	1.5
224	15.6	183	36.9	9.48	0.2	7.78	1.3
183	13.4	151	23.5	7.78	0.2	6.39	1.1
151	8.9	124	14.6	6.39	0.2	5.24	0.8
124	5.2	101	9.3	5.24	0.2	4.30	0.7
101	2.8	83.3	6.6	4.30	0.1	3.53	0.5
83.3	1.6	68.3	5.0	3.53	0.1	2.90	0.4
68.3	0.9	56.1	4.1	2.90	0.1	2.38	0.3
56.1	0.6	46.0	3.5	2.38	0.1	1.95	0.2
46.0	0.4	37.8	3.1	1.95	0.1	1.60	0.1
37.8	0.3	31.0	2.8	1.60	0.1	1.32	0.1

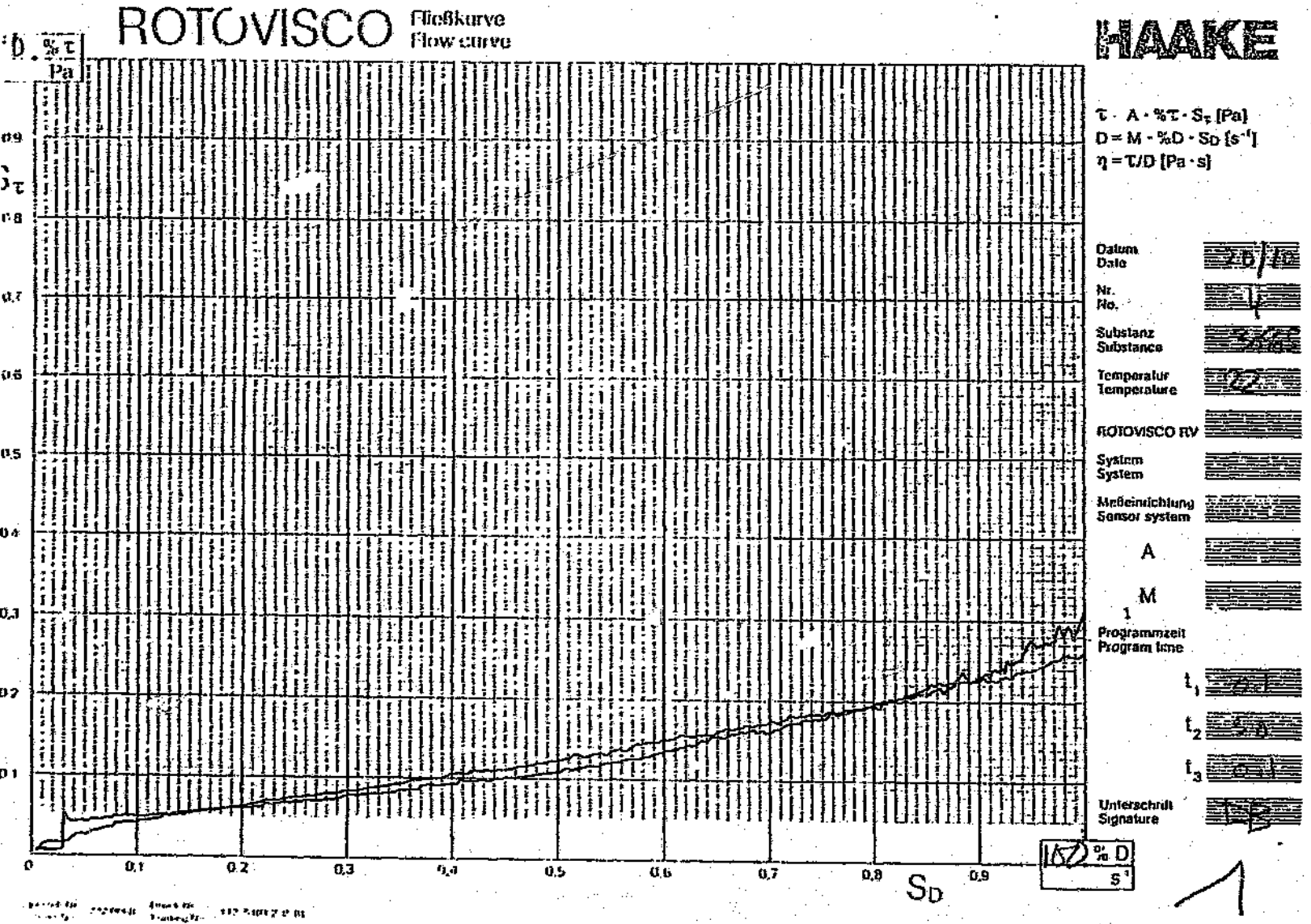
Result source=Sample
Record No. = 0
Focal length = 300 mm.
Presentation =0903
Volume distribution
Beam length = 2.2 mm.
Obscuration =0.2060
Volume Conc. = 0.3040 %
Residual = 0.629%
Model inup

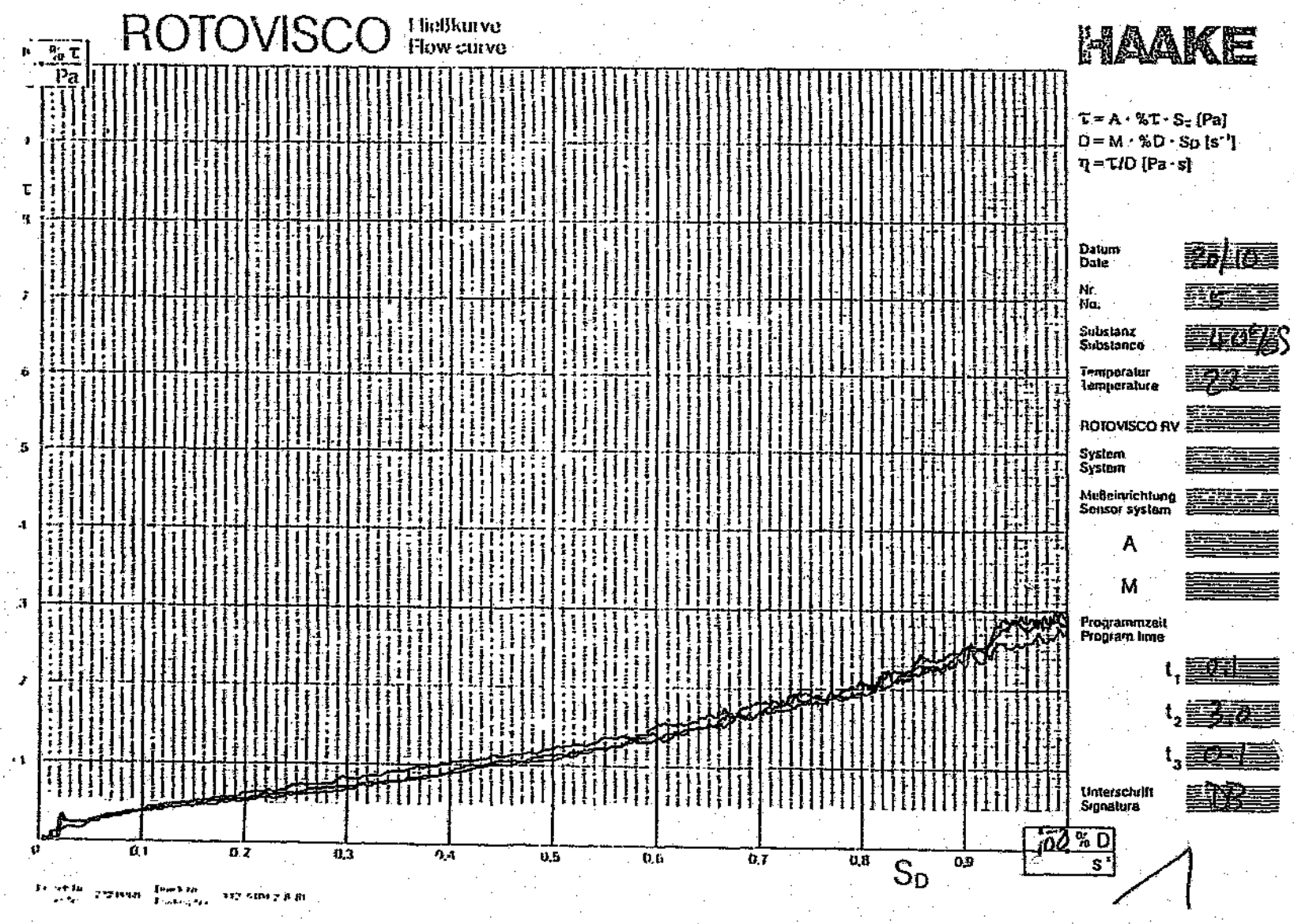
D(v,0.5) = 216.58 µm
D(v,0.9) = 443.59 µm
D(v,0.1) = 102.77 µm
D(4,3) = 240.72 µm
D(3,2) = 172.72 µm
Span = 1.6
Spec. surf. area
0.0635 sq.m./cc.

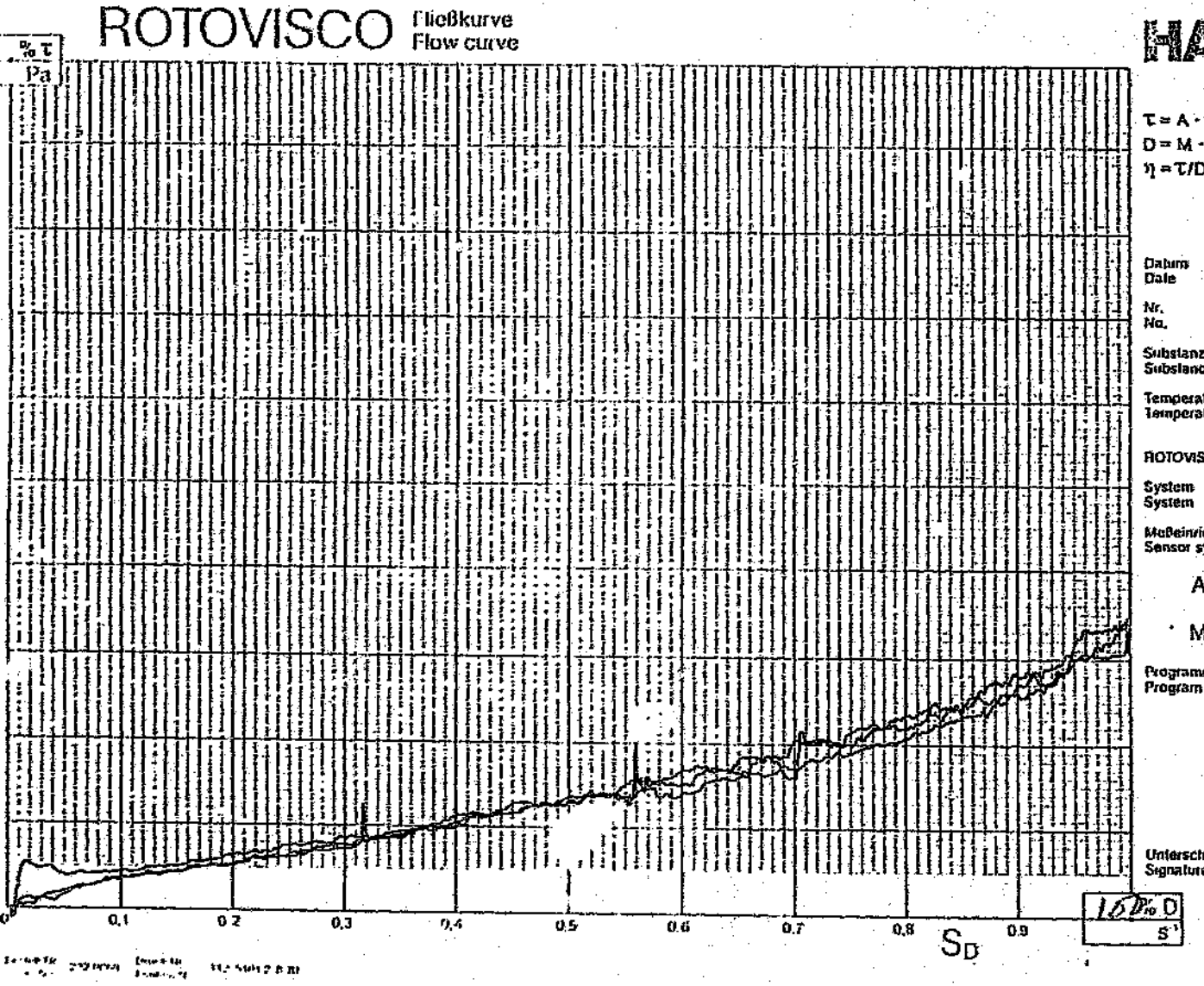
Size distribution data for Kinross sample

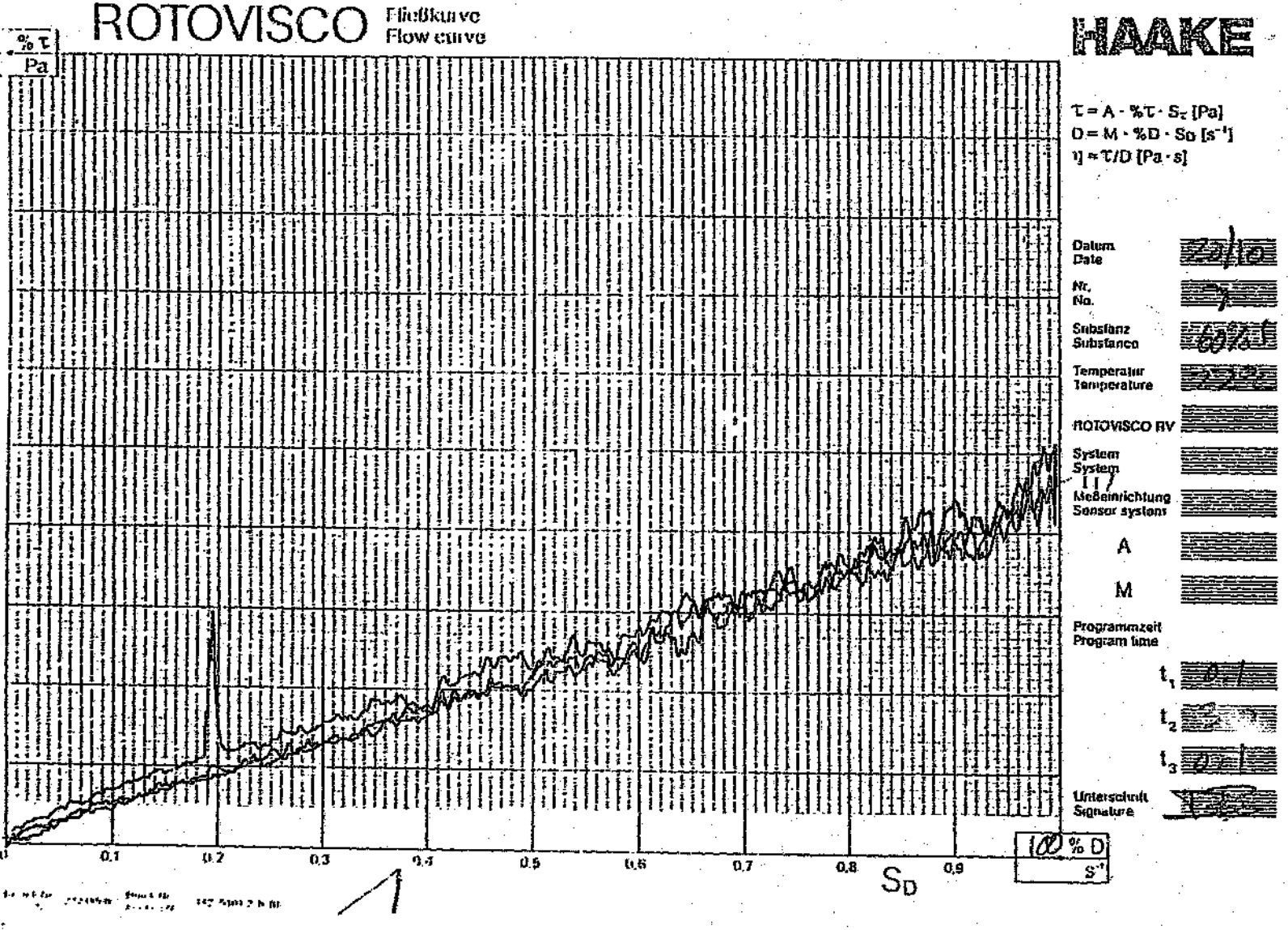
HAAKE
ROTOVISCO Fließkurve
Flow curve
τ = A · %τ · Sτ [Pa]
D = M · %D · SD [s⁻¹]
η = τ/D [Pa · s]
Datum
Date
Nr.
No.
Substanz
Substance
Temperatur
Temperature
ROTOVISCO RV
System
System
Meßeinrichtung
Sensor system
A
M
Programmzeit
Program time
t1
t2
t3
Unterschrift
Signature
%τ
Pa
%D
s⁻¹
SD
0,1
0,2
0,3
0,4
0,5
0,6
0,7
0,8
0,9

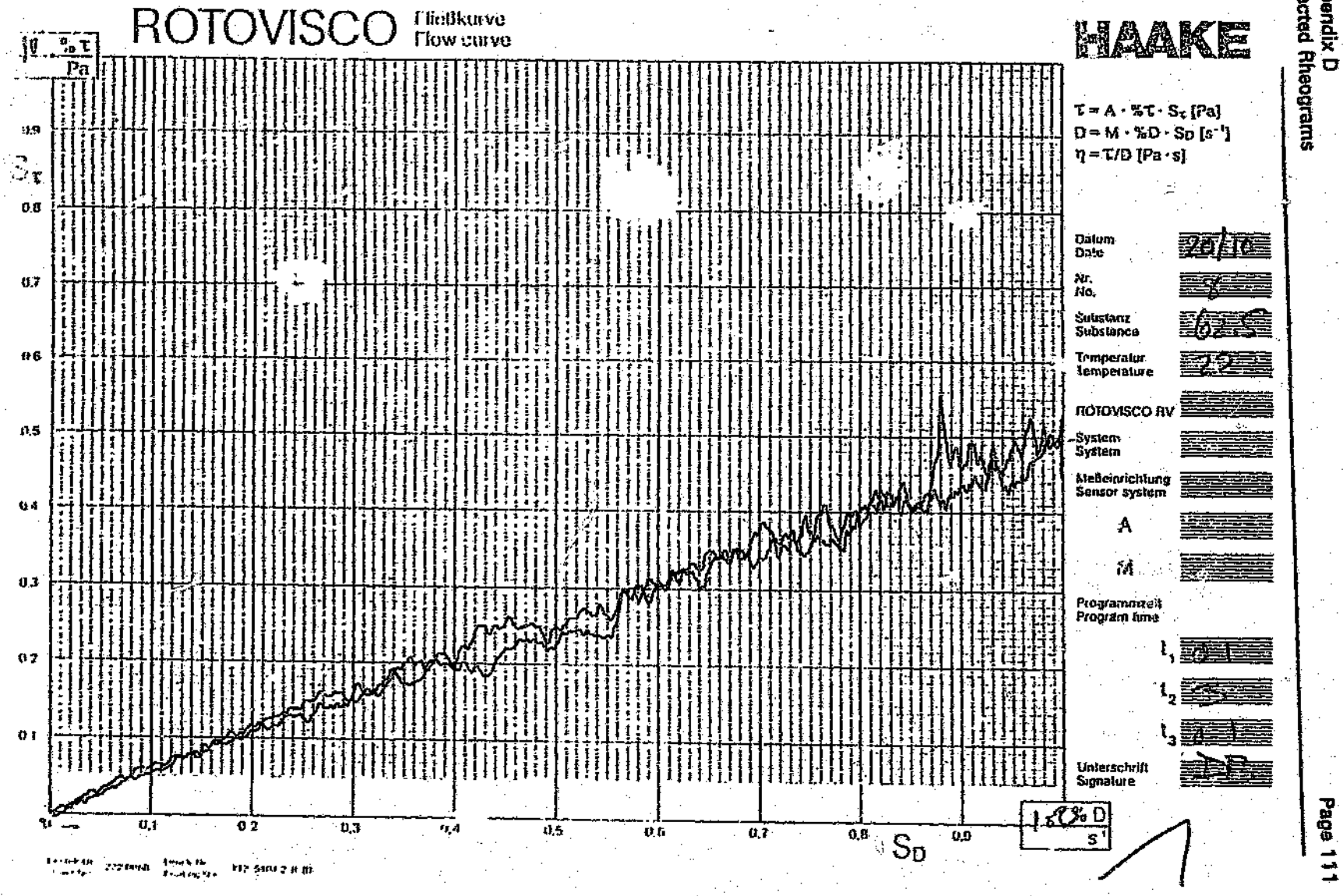
HAAKE
ROTOVISCO
Fließkurve
Flow curve
τ = A · %τ · Sτ [Pa]
D = M · %D · SD [s⁻¹]
η = τ/D [Pa · s]
Datum
Date
Nr.
No.
Substanz
Substance
Temperatur
Temperature
ROTOVISCO RV
System
System
Meßeinrichtung
Sensor system
A
M
Programmzeit
Program time
Unterschrift
Signature
% D
S⁻¹
SD
Pa
τ

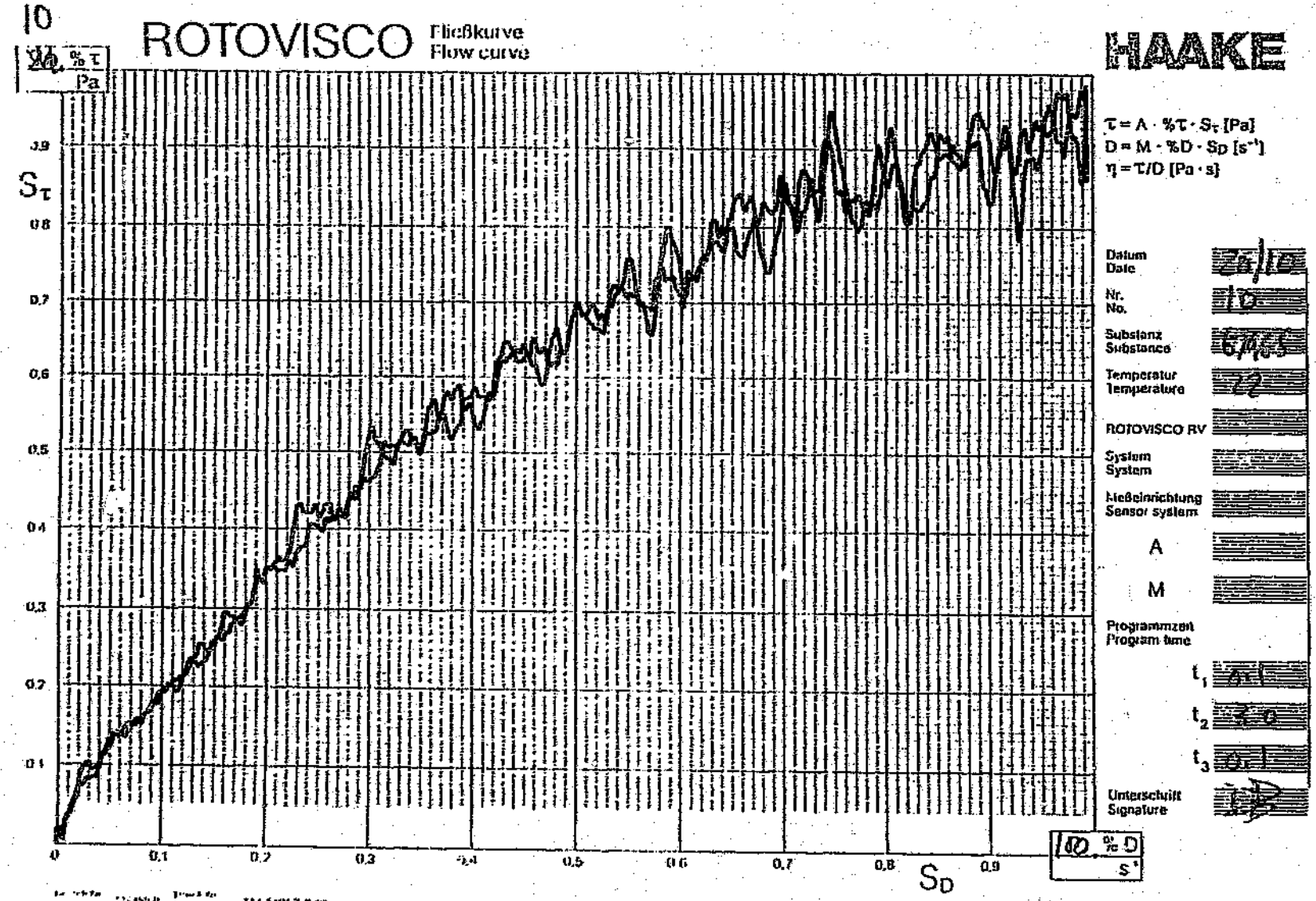

ROTOVISCO
Fließkurve
Flow curve
HAAKE
τ = A + %τ · S_τ [Pa]
D = M + %D · S_D [s⁻¹]
η = τ/D [Pa · s]
Datum
Date
Nr.
No.
Substanz
Substance
Temperatur
Temperature
ROTOVISCO RV
System
System
Meßeinrichtung
Sensor system
A
M
1
Programmzeit
Program time
t1
t2
t3
Unterschrift
Signature
%τ
Pa
%D
s⁻¹
S_D
0
0,1
0,2
0,3
0,4
0,5
0,6
0,7
0,8
0,9

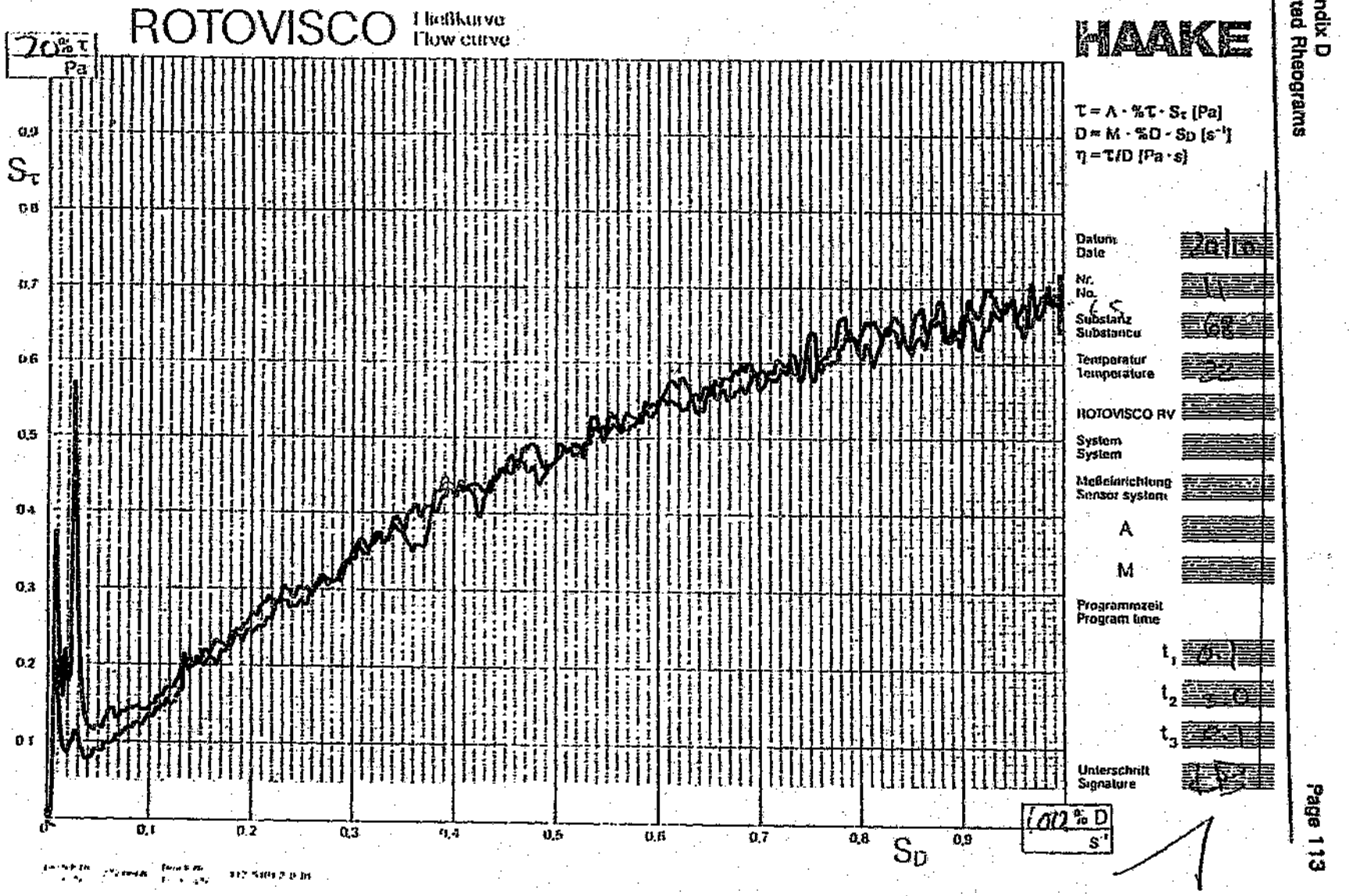

ROTOVISCO
Fließkurve
Flow curve
HAAKE
τ = A · %τ · S_τ [Pa]
D = M · %D · S_D [s⁻¹]
η = τ/D [Pa · s]
Datum
Date
Nr.
No.
Substanz
Substance
Temperatur
Temperature
ROTOVISCO RV
System
System
Meßeinrichtung
Sensor system
A
M
Programmzeit
Program time
t1
t2
t3
Unterschrift
Signature
0
0,1
0,2
0,3
0,4
0,5
0,6
0,7
0,8
0,9
S_D

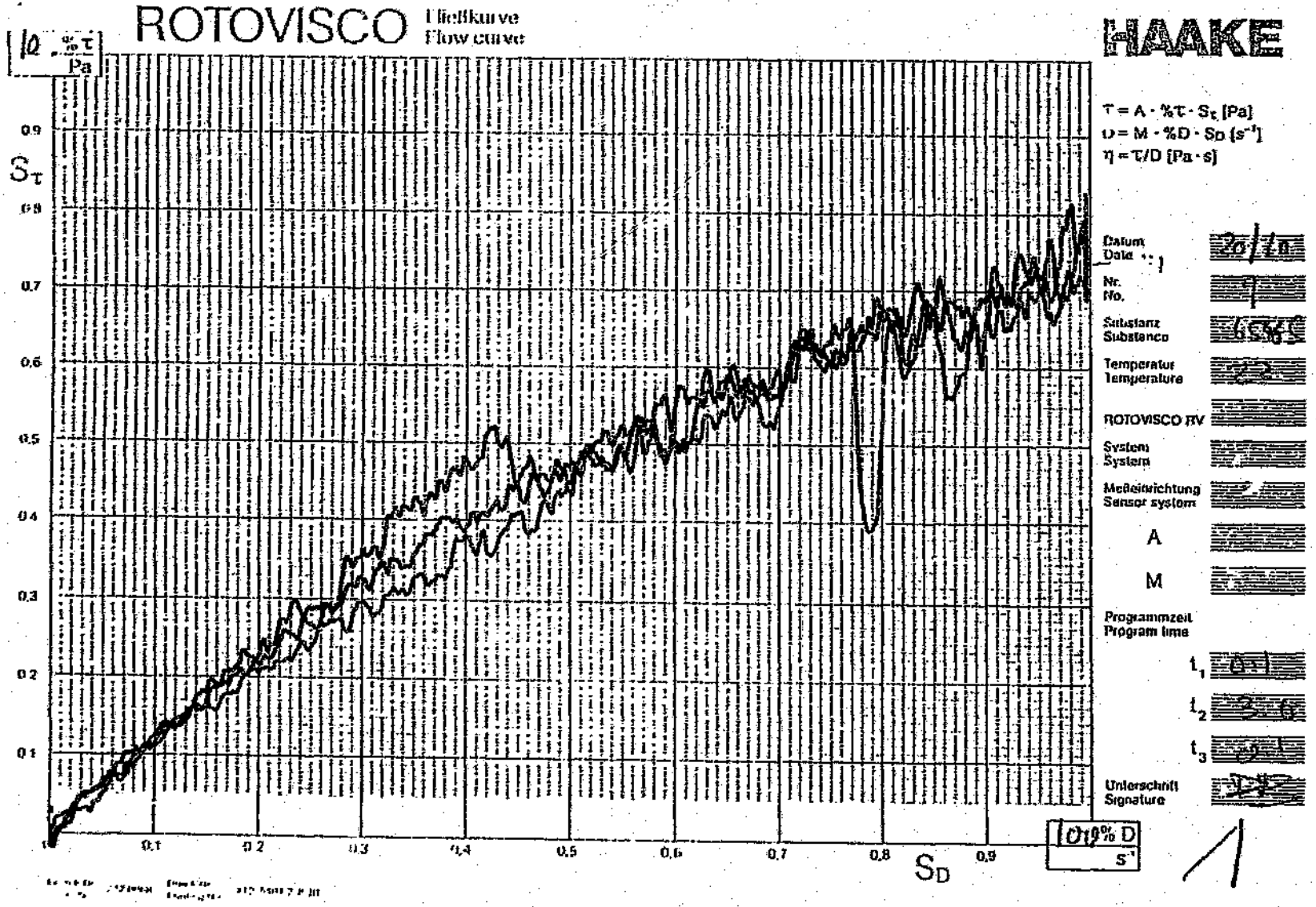

ROTOVISCO
Fließkurve
Flow curve
%τ
Pa
0,1
0,2
0,3
0,4
0,5
0,6
0,7
0,8
0,9
SD
HAAKE
τ = A · %τ · Sτ [Pa]
D = M · %D · SD [s⁻¹]
η = τ/D [Pa · s]
Datum
Date
Nr.
No.
Substanz
Substance
Temperatur
Temperature
ROTOVISCO RV
System
System
Meßeinrichtung
Sensor system
A
M
Programmzeit
Program time
t1
t2
t3
Unterschrift
Signature
%D
s⁻¹


ROTOVISCO Fließkurve
Flow curve
HAAKE
% τ
Pa
τ = A · %τ · Sτ [Pa]
D = M · %D · SD [s⁻¹]
η ≈ τ/D [Pa · s]
Datum
Date
Nr.
No.
Substanz
Substance
Temperatur
Temperature
ROTOVISCO RV
System
System
II
Meßeinrichtung
Sensor system
A
M
Programmzeit
Program time
t1
t2
t3
Unterschrift
Signature
0
0.1
0.2
0.3
0.4
0.5
0.6
0.7
0.8
0.9
SD
100 % D
s⁻¹


ROTOVISCO
Fließkurve
Flow curve
HAAKE
τ = A · %τ · Sτ [Pa]
D = M · %D · SD [s⁻¹]
η = τ/D [Pa · s]
Datum
Date
20/10
Nr.
No.
Substanz
Substance
62
Temperatur
Temperature
22
ROTOVISCO RV
System
System
Meßeinrichtung
Sensor system
A
M
Programmzeit
Program time
t1
t2
t3
Unterschrift
Signature
%τ
Pa
0,9
0,8
0,7
0,6
0,5
0,4
0,3
0,2
0,1
0,1
0,2
0,3
0,4
0,5
0,6
0,7
0,8
0,9
SD
%D
s⁻¹


10
100 % τ
Pa
ROTOVISCO Fließkurve
Flow curve
HAAKE
τ = A · %τ · Sτ [Pa]
D = M · %D · SD [s⁻¹]
η = τ/D [Pa · s]
Datum
Date
Nr.
No.
Substanz
Substance
Temperatur
Temperature
ROTOVISCO RV
System
System
Meßeinrichtung
Sensor system
A
M
Programmzeit
Program time
t1
t2
t3
Unterschrift
Signature
Sτ
SD
0
0,1
0,2
0,3
0,4
0,5
0,6
0,7
0,8
0,9
0,1
0,2
0,3
0,4
0,5
0,6
0,7
0,8
0,9
100 % D
s⁻¹


ROTOVISCO Fließkurve
Flow curve
200 %τ
Pa
S_τ
0,9
0,8
0,7
0,6
0,5
0,4
0,3
0,2
0,1
0
0,1
0,2
0,3
0,4
0,5
0,6
0,7
0,8
0,9
S_D
100 % D
s⁻¹
HAAKE
τ = A · %τ · Sτ [Pa]
D = M · %D · SD [s⁻¹]
η = τ/D [Pa · s]
Datum
Date
Nr.
No.
Substanz
Substance
Temperatur
Temperature
ROTOVISCO RV
System
System
Meßeinrichtung
Sensor system
A
M
Programmzeit
Program time
t_1
t_2
t_3
Unterschrift
Signature


ROTOVISCO
Fließkurve
Flow curve
HAAKE
τ = A · %τ · Sτ [Pa]
D = M · %D · SD [s⁻¹]
η = τ/D [Pa · s]
Datum
Date
Nr.
No.
Substanz
Substance
Temperatur
Temperature
ROTOVISCO RV
System
System
Meßeinrichtung
Sensor system
A
M
Programmzeit
Program time
t1
t2
t3
Unterschrift
Signature
Sτ
SD
0,1
0,2
0,3
0,4
0,5
0,6
0,7
0,8
0,9
1

Appendix E - Unprocessed data

Data for figure 5.3 - Height verses time for the drainage of different glycerol solutions from a 12 mm tube

Height (m)	Time (seconds)			
	$\mu = 1$	$\mu = 88$	$\mu = 204$	$\mu = 460$
1.0	0	0	0	0
0.8	0.09	0.31	0.46	0.75
0.6	0.19	0.53	0.87	1.50
0.4	0.30	0.74	1.34	2.23
0.2	0.42	1.13	1.81	3.02

Data for figure 5.4 - Drainage velocity of glycerol solutions

Viscosity (cP)	Velocity (m/s)	
	d = 12 mm	d = 16 mm
1	1.69	1.96
88	0.72	1.38
204	0.43	1.02
460	0.28	0.69

Data for figure 5.6 - Drainage of a 5% CMC solution from a 12 mm smooth tube.

Time (s)	Height (m)
0	1.0
0.42	0.8
0.84	0.6
1.24	0.4
1.65	0.2

Data for figure 5.8 - The relationship between % solids and apparent viscosity for mine dump slurry as obtained from rheograms generated using the Haake viscometer.

% Solids	Viscosity
0	3.4
10	9.2
15	8.4
20	8.4
25	10
30	9
35	10.9
40	12.3
45	13.4
50	16.3
55	25
59	33.4
63	52.6
65	80.1

Data for figure 5.13 - Drainage velocity from a Western Deeps slurry

% Solids	Velocity (m/s)
50	1.25
60	1.21
65	1.06
67	0.95

Appendix F - MCAD program for simplified analytical solution

$k := 13.7$ delta p = kv^2 at pipe exit fitted using least squares

$g := 9.8$ gravitational acceleration

$i := 1..6$ M = Mass % H = Height $j := 1..6$

$M_i :=$

i
50
55
60
62.5
65
67

$\mu_i :=$

i
13.4
16.3
25
33.4
52.6
80.1

$Vel_i :=$

i
1.084
1.073
1.037
0.986
0.915
0.869

$H_j :=$

j
1.2
1
0.8
0.6
0.4
0.2

$$\rho_i := \frac{2.65 \cdot 10^6}{2650 - 16.5 \cdot M_i}$$

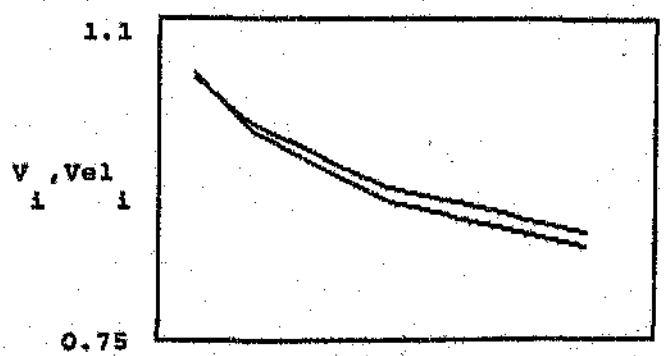
$R := 0.06$ Tube radius

$$V_i := -\left[\left[\frac{-4 \cdot \mu_i}{R^2}\right] + \sqrt{\left[\frac{16 \cdot \mu_i^2}{R^4}\right] - \left[\frac{k \cdot g \cdot \rho_i}{H_j}\right]}\right] \cdot \frac{H_j}{k}$$

V_i

i
1.238404
1.171777
1.0417
0.976195
0.900853
0.854467

$k = 13.7$



Appendix G - Overview of previous work

A brief discussion of selected publications is given in sequential order of publication dates to give the reader a feel for some existing literature relating to the rheology of suspensions and slurries.

Clarke (1967) used a concentric cylinder viscometer with provision for recirculation of solids in his experimental work. (See figure A1). He used quartz, glass and polymethylmethocrylate as solid suspensions in water, using particle diameters of up to 210 μm and volume percent solids of up to 50%. His suspensions were found to be mostly dilatant. He also found that the addition of detergent reduces viscosity while increasing particle diameter, shear rate or density increases the viscosity.

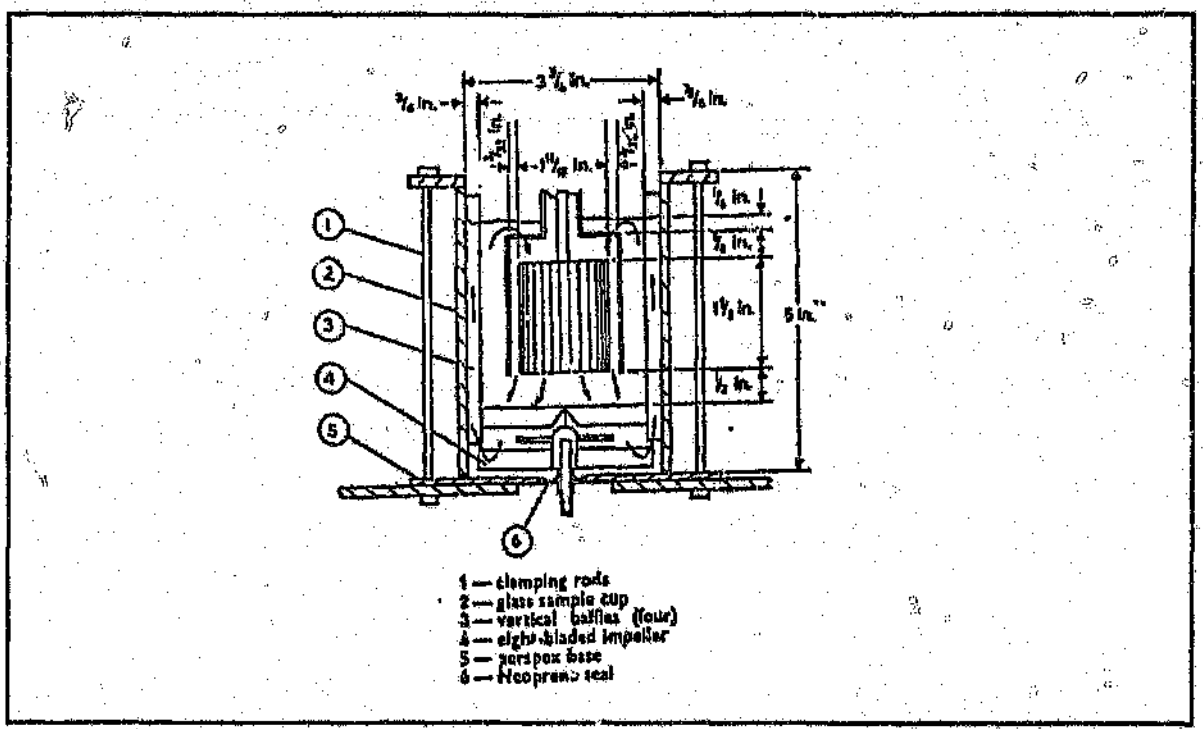


Figure A1 - Sectional view of system used by Clarke (1967)

Valentyik (1970) Investigated the operation of what he describes as a continuous, on-line consistometer. He used a screen to remove the oversize particles from the feed and obtained some encouraging results using a bobbin type rotary viscometer operating at a fixed shear rate. The sampling system he used is pictured in figure A2.

Hansford et al (1976) used a Brookfield viscometer for his experimental work. He also looked at models available from literature and made some comments on the usefulness of capillary viscometers. He also derives the formulas relating the shear stress to the shear rate in the cup and bobbin arrangement. The effect of concentration, temperature and pH on the rheology of slurries is also examined.

Jeffrey and Acrivos (1976) reviewed experimental and theoretical work done on the rheological properties of suspensions, focusing on systems containing rigid, neutrally buoyant particles suspended in Newtonian fluids.

Hemmings and Boyes (1977) described the potential benefits of better control of slurry rheology in milling circuits. They use a rotary cup and bobbin viscometer to obtain an apparent viscosity at a fixed shear rate. The system they used to measure viscosity and density on an on-line basis is specially designed to avoid settling problems and is relatively simple, reliable, compact, robust and sensitive (See figure 2.10 for a schematic of the mounting setup of the viscometer). The mill discharge viscosity was automatically controlled by using the viscometer output signal to regulate the mill water addition using a feedback control loop.

Boyes (1978) performed field tests of an on-line slurry measurement technique at the Savage river mines and describes the main problems encountered which mainly relate to the choking of the measuring device. He used a Brabender 'Consistometer' process viscometer together with an Ohmart density gauge. In his paper it is suggested that an optimum viscosity at

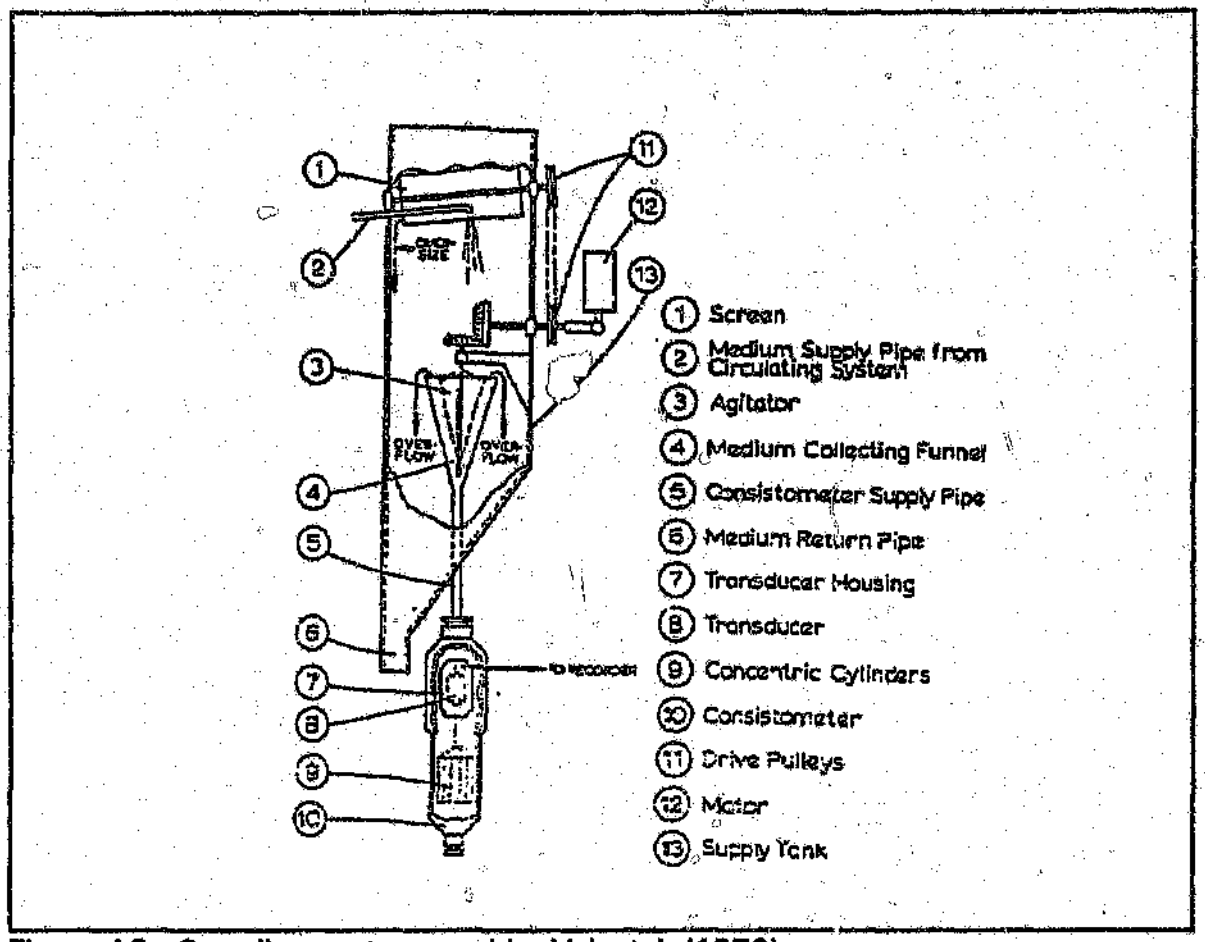


Figure A2 - Sampling system used by Valentyk (1970)

which wet grinding mills should operate is 150 c Poise. It was concluded that the viscometer he tested did work but lacked long term reliability.

Kimpel (1979) Used both a Brookfield and a Haake viscometer in his research and investigated the variation of slurry rheology with fineness of grinding. He also discusses the effects of viscosity on mill performance giving the reader some interesting information.

Cheng (1984) reviewed some 40 items of literature on viscosity measurements with slurries of spherical particles and concluded that the steady shear properties of a dense suspension are

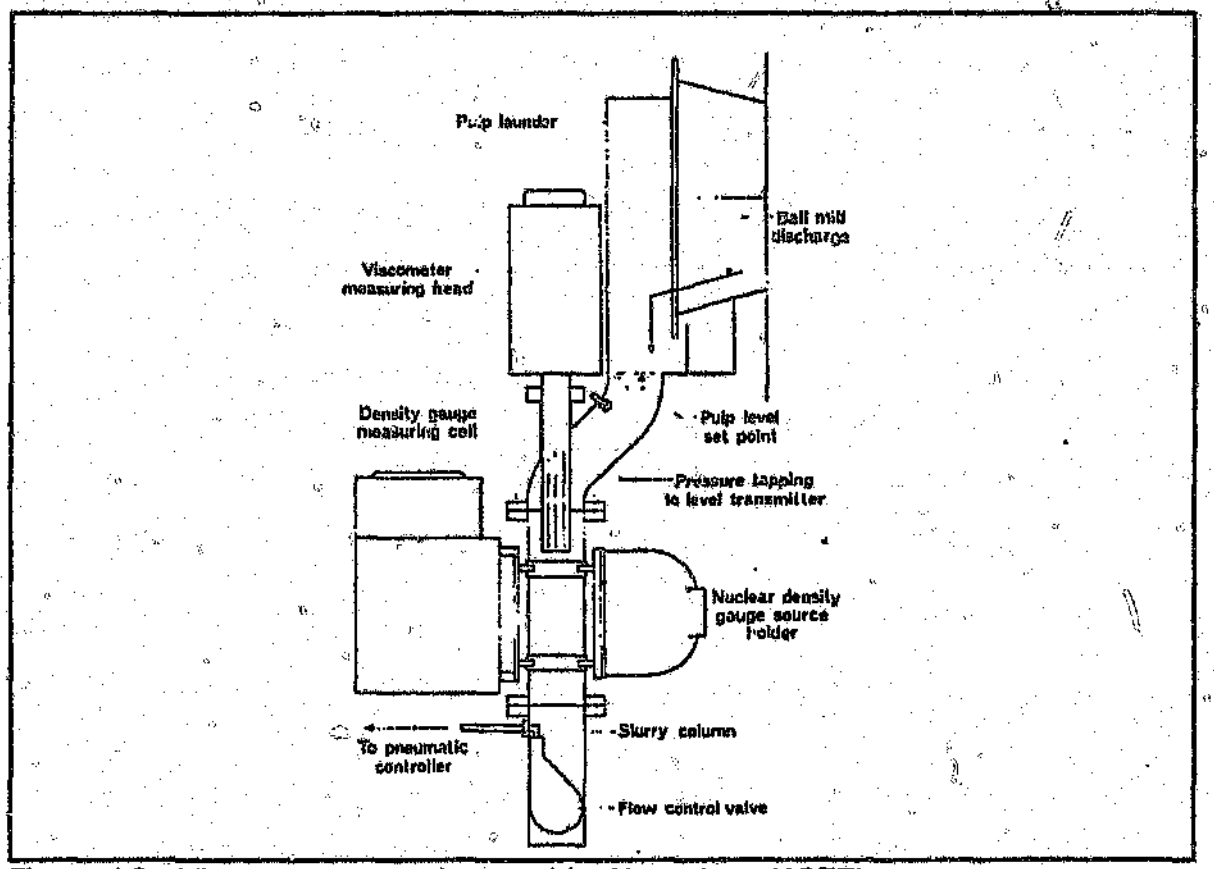


Figure A3 - Viscometer mounting used by Hemmings (1977)

not characterized by a unique viscosity or flow curve but are rather described by a distribution of curves.

Blaszezyk and Petela (1986) used a concentric cylinder viscometer modified so that a continuous co-axial flow could be obtained to eliminate settling. Their work concentrated on coal-oil slurries. Relationships between shear stress, shear rate, temperature, mass fraction of solids and particle size were determined for a coal-oil slurry. The power law coefficients were calculated and their modified viscometer operated satisfactorily with a volume concentration of solids less than 0.4 as well as a maximum particle diameter of less than 0.3 mm and a viscosity of less than 30 PaS.

Dabak and Yucel (1986) used a three parameter model to calculate the shear viscosity at different shear rates for a suspension and obtained results in quite close correlation with experimental data reported in literature.

Abbas and Crowe (1987) performed experimental work on the flow properties of homogeneous slurries using a range of Reynolds numbers from 1200 to 30 000. They worked with a silica gel - chloroform slurry and used 96 μm and 210 μm diameter particles in concentrations up to 30% by volume. They measured the velocity profiles of the slurry flowing in a pipe and the pressure drop across the pipe. One of their goals was to "establish the adequacy of rheological models for slurry flow properties. They found that the presence of larger particles in a slurry delays the onset of turbulent flow. They fitted their profiles using the "law of the wall" model and concluded that neither the Bingham nor the power law were adequate to describe the logarithmic profiles they obtained.

Downward et al (1987) gave some advantages and disadvantages of capillary and rotary viscometers when used with suspensions and examined factors effecting viscosity. He also discussed practical problems he encountered with the use of a modified Stormer viscometer he used in his lab test work. Problems included that of alien particles entering the bearing mechanism. Downward used ferosilicon suspensions.

Kawatra and Elsele (1988) showed that milling efficiency can be improved by better control of slurry rheology and that the rheology of the slurry effects not only the fines production and mill operation but also the separator performance. He used a cup and bobbin viscometer as shown in figure A3.

Montini and Moys (1988) describe a technique for the measurement of slurry consistency inside a grinding mill based on the rate of slurry drainage from a conductivity probe mounted through the mill shell. If successfully applied this measurement would allow for tighter

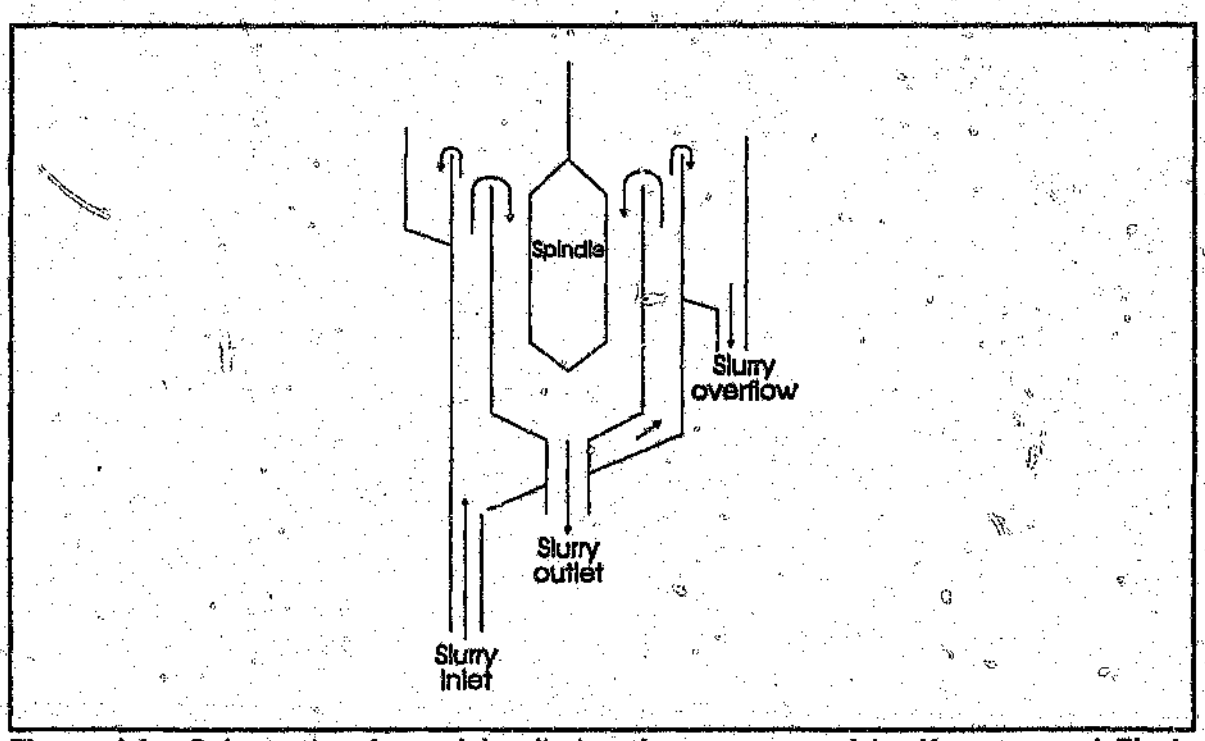


Figure A4 - Schematic of coaxial cylinder viscometer used by Kawatra and Elsele (1988)

control of mill behaviour (see figure 2.7 and 2.9).

Moys (1988) investigates the effect of slurry flow rate and viscosity on the load behaviour and how these variables effect milling efficiency and load behaviour. He also discusses the usefulness of conductivity probes in the shell of the mill and the use of a force probe mounted on the mill shell was also examined (see figure 2.8).

Tangsathitkulchai and Austin (1988) Used a Haake viscometer to investigate the rheology of concentrated slurries of natural size distribution of ground coal and quartz. They found a yield stress at higher concentrations of solids, and also found that percent solids as well and size distribution are the two most important parameters governing slurry rheology.

Herbst (1990) examined the potential benefits of comminution system optimization based on savings achieved at various plants around the world. He also includes some cost/benefit analysis for optimization projects. Sources of savings include improved design (15-40% saving), better control (10-25% saving), use of grinding additives (2-8% saving) and use of better materials (3-14% saving).

Nguyen and Boger (1992) give some interesting information on the different techniques used to measure the viscosity of fluids. The various shear stress formulae are derived for the different systems. They provide a good introduction to the field of rheology of fluids. He provides the reader with interesting information.

Whitten et al (1992) examined the measurement of pulp viscosity using capillary viscometers, in particular in the high shear rate regions for which turbulent or near turbulent conditions exist. He found that slurries have a less marked transition from laminar to turbulent flow and the onset of turbulence is delayed as the percent solids in the slurry is increased.

Appendix H - Matlab and Pascal routines for the numerical solution of the model

DRAW.M

```
[x,v]=ode45('de',0,5,[1.0 0]);
plot(x,v(:,1));
```

DE.M

```
function der = de(x,v)

%parameter x,v;   v=(y,u)

mu=50/1000;
rho=1200;
k=0.001;

k1=8*mu/(rho*0.006);
k2=k*rho;
k3=0.5;
k4=9.8;

der(1)=v(2);
der(2)=-k1*v(2)+k2*v(2).^2./v(1)+k3./v(1)-k4;
```

```
Program RUNGE_KUTTA(Input,output);
VAR t0,h0,v0,h,N,v : real;
    data : text;
Const mu=80;
      rho=1425;
      R=0.006;
      k=8;
      ga=9.8;
      hstar=0.09;

Function f(v:Real):REAL;
Begin
  f:=v;
End;

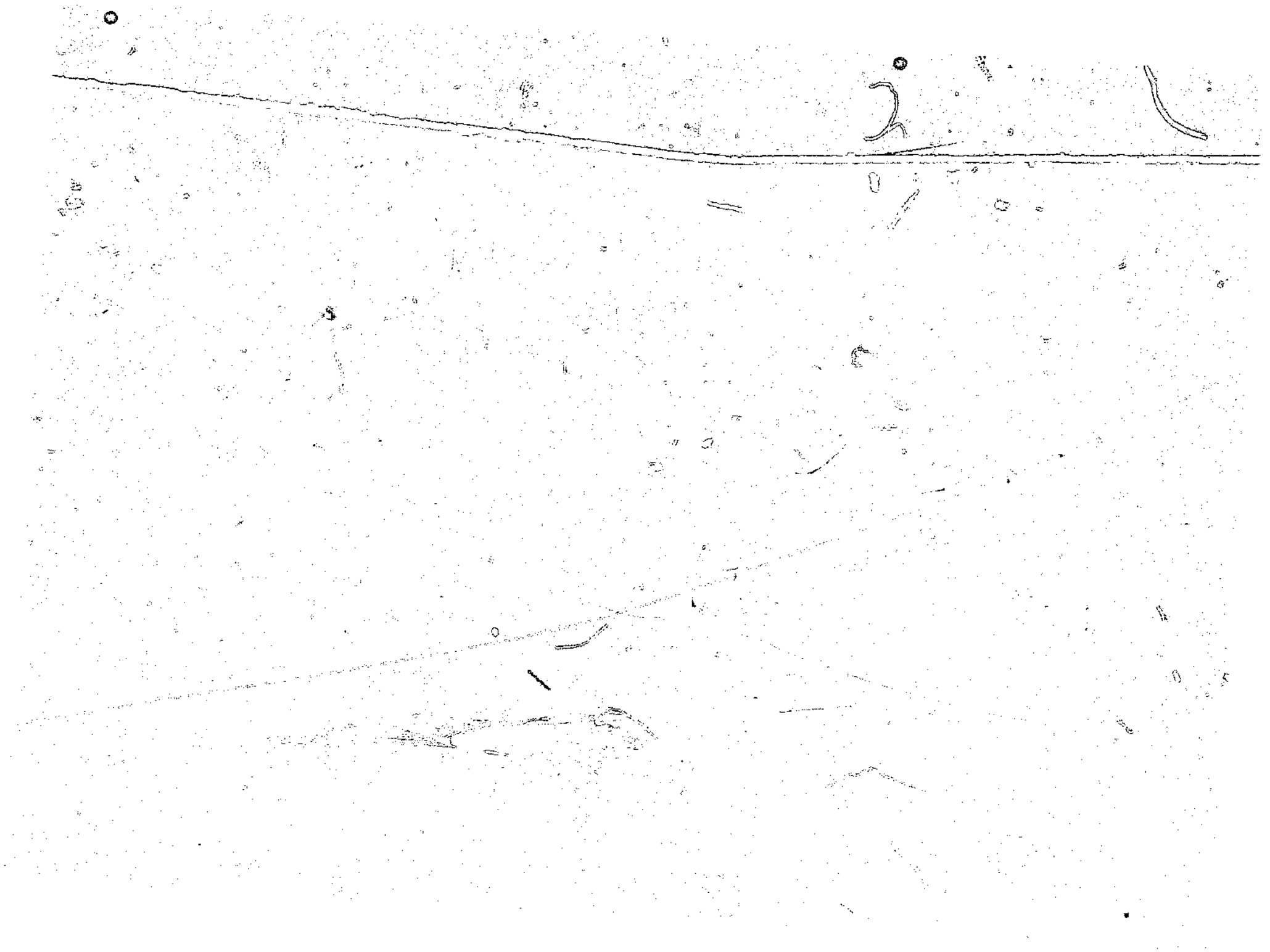
Function g(v,h:Real):REAL;
Begin
  g:=ga+ga*hstar/h+k*v*v/h-8*mu*v/(rho*R);
End;

Procedure R_K(t0,v0,h0,dt:REAL;N:integer);
Var k1,k2,k3,k4,tn,t,
    kk1,kk2,kk3,kk4,XXn:REAL;
    count:Integer;

Begin
  assign(data,'c:\msc\run1.dta');
  rewrite(data);
  writeln(data,1);
  writeln(data,100);
  t:=t0;
```

```
  vn:=v0;
  hn:=h0;
  For count:=0 to N-1 DO
    Begin
      Writeln('h at t= ',t:2,' is: ',hn:10:6,'and v = ',tn:4:2);
      Writeln(data,t:3,' ',h:4:3,v:4:3);
      k1:=dt*f(vn);
      kk1:=dt*g(vn,hn);
      k2:=dt*f(vn+0.5*k1);
      kk2:=dt*g(hn+0.5*h,vn+0.5*k1);
      k3:=dt*f(hn+0.5*h);
      kk3:=dt*g(hn+0.5*h,vn+0.5*k2);
      k4:=dt*f(hn+h);
      kk4:=dt*g(hn+h,vn+k3);
      t:=t+dt;
      hn:=hn+(1/6)*(k1+2*k2+2*k3+k4);
      vn:=vn+(1/6)*(kk1+2*kk2+2*kk3+kk4);
    End;
 close(data);
End;

Begin
  R_K(0,0,1.2,0.01,500);  {t0,v0,h0,delta time,no of intervals}
End.
```



Author: Bailie Darrell Stephen.
Name of thesis: The measurement of the slurry rheology from the discharge of a rotary grinding mill.

PUBLISHER:
University of the Witwatersrand, Johannesburg
©2015

LEGALNOTICES:

Copyright Notice: All materials on the University of the Witwatersrand, Johannesburg Library website are protected by South African copyright law and may not be distributed, transmitted, displayed or otherwise published in any format, without the prior written permission of the copyright owner.

Disclaimer and Terms of Use: Provided that you maintain all copyright and other notices contained therein, you may download material (one machine readable copy and one print copy per page)for your personal and/or educational non-commercial use only.

The University of the Witwatersrand, Johannesburg, is not responsible for any errors or omissions and excludes any and all liability for any errors in or omissions from the information on the Library website.